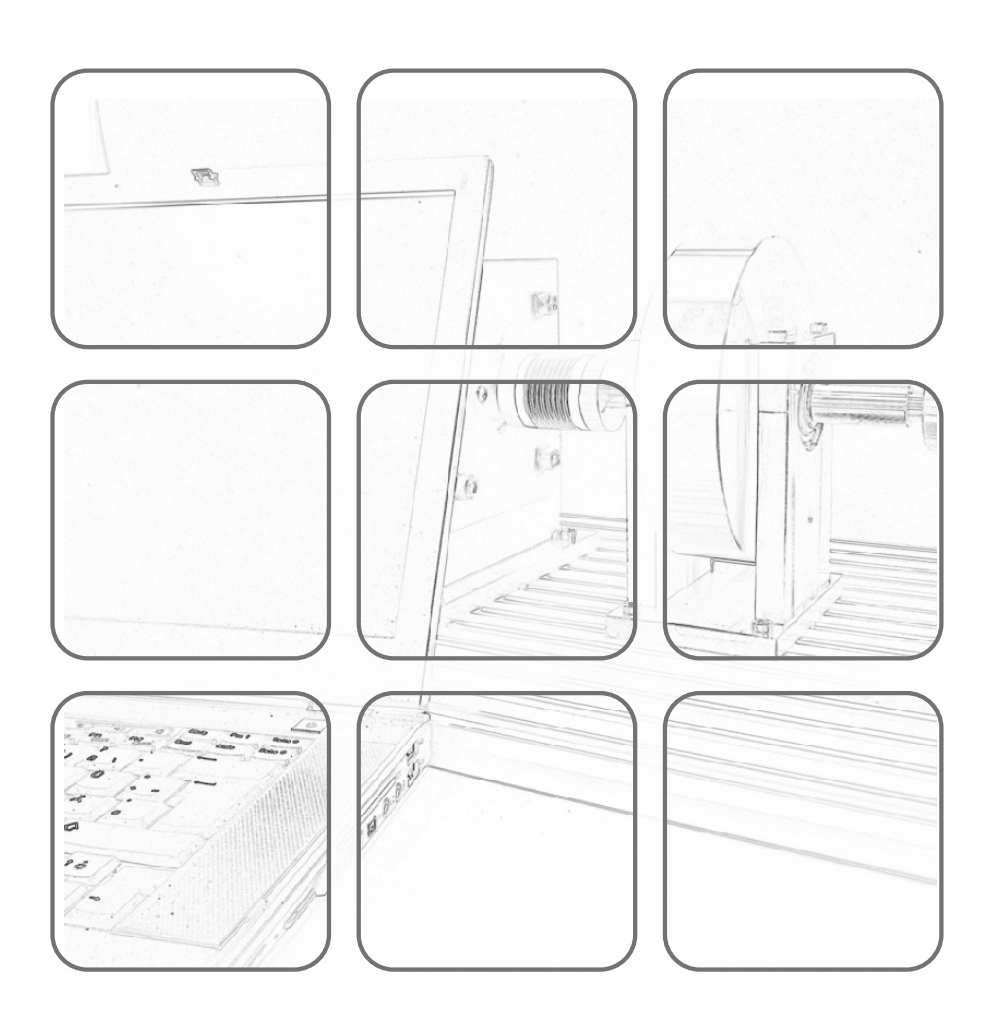




Lecture Winter semester 2025/2026

# A. Deutschmann-Olek, T. Glück, A. Kugi, M.N. Vu

# ADVANCED METHODS IN NONLINEAR CONTROL



## **Advanced Methods in Nonlinear Control**

Lecture Winter semester 2025/2026

A. Deutschmann-Olek, T. Glück, A. Kugi, M.N. Vu

TU Wien Automation and Control Institute Complex Dynamical Systems Group

Gußhausstraße 27–29 1040 Wien

Phone: +43 1 58801 - 37615

Internet: https://www.acin.tuwien.ac.at

© Automation and Control Institute, TU Wien

# **Contents**

1	Diss	pativity and Passivity	1
	1.1	Annealing Simulator	1
	1.2	Solenoid Valve	2
	1.3	System-theoretic Concept	4
		1.3.1 Dissipativity	4
		1.3.2 Passivity	5
		ı v	7
		1.3.4 Passivity and Lyapunov Stability	9
	1.4	Linear Passive Systems	0
	1.5	Positive Realness	3
	1.6	Canonical Form of Passive Systems	5
		1.6.1 Hamiltonian Systems	5
		1.6.2 Port-Hamiltonian Systems	8
	1.7	Passivity-Based Controller Design	
	1.8	References	5
2	Itera	tive learning control 2	6
	2.1	Fixed-point iterations	8
	2.2	Signals, systems, and the frequency domain	1
	2.3	Frequency-domain ILC methods on infinite time horizons	9
		2.3.1 Analysis of ILC laws	0
		2.3.2 Deterministic design methods	2
		2.3.3 Stochastically optimal learning laws	5
		2.3.4 Q-filtering and robustness	8
		$2.3.5  \text{Implementation aspects}  \dots  \dots  \dots  \dots  5$	1
	2.4	Discrete-time systems on finite time horizons	6
		2.4.1 Lifted system respresentation	7
		2.4.2 ILC as an online optimization strategy	1
		2.4.3 Norm-optimal ILC strategies $\dots \dots \dots$	2
	2.5	References	4

# 1 Dissipativity and Passivity

In simple terms, the concept of dissipativity and passivity is the system-theoretic generalization of the principle of conservation of energy, which states that in a closed system energy is neither created nor destroyed. A closer look at the system-theoretic concept of dissipativity will show, however, that this is a priori not related to the principle of conservation of energy and only allows analogous statements for certain physical systems. This analogy to physical systems certainly contributes to the understanding of these concepts, which is why two physical systems, a heat transfer system and an electromechanical system, are discussed below.

# 1.1 Annealing Simulator

Figure 1.1 shows the schematic representation of a so-called annealing simulator, which is used to generate predefined temperature profiles for metal samples by ohmic heating and free or forced convection (compressed air or fan). It is obvious for this system to neglect

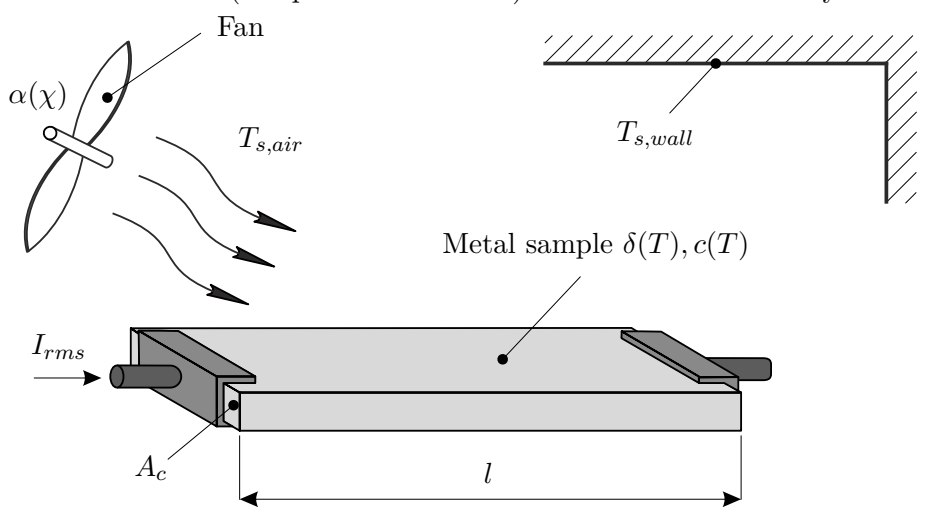


Figure 1.1: Annealing simulator.

the electromechanical effects and to capture the change in the energy stored in the system solely by the change in the thermally stored energy. The principle of conservation of energy then states that the change in the thermally stored energy V satisfies the relationship

$$\frac{\mathrm{d}}{\mathrm{d}t}V = p_{in} - p_{out} \tag{1.1}$$

where  $p_{in}$  and  $p_{out}$  describe the energy flows into the system and out of the system. It is assumed that the temperature T in the metal sample is uniformly distributed at any time

1.2 Solenoid Valve Page 2

t, that the surface of the sample is very small compared to the surrounding walls and that heat conduction can be neglected. The thermal energy stored in the sample V is given by

$$V(T) = c(T)mT (1.2)$$

with the constant sample mass m and the specific heat capacity c(T). Using Ohm's law, the energy flow into the sample is calculated as

$$p_{in} = I_{rms}^2 \delta(T) \frac{l}{A_c} \tag{1.3}$$

with the RMS value of the current flowing through the sample  $I_{rms}$ , the specific resistance  $\delta(T)$ , the length of the sample l and the cross-sectional area of the sample  $A_c$ . The energy flows from the sample to the environment are caused on the one hand by free and forced convection

$$p_{out,1} = \alpha(\chi)A_s(T - T_{s,air}) \tag{1.4}$$

and on the other hand by thermal radiation

$$p_{out,2} = \varepsilon \sigma A_s \left( T^4 - T_{s,wall}^4 \right) \tag{1.5}$$

caused.  $A_s$  denotes the surface of the metal sample,  $T_{s,air}$  and  $T_{s,wall}$  are the temperatures of the surrounding air and walls,  $\varepsilon$  is the emissivity,  $\sigma = 5.67 \cdot 10^{-8} \; \mathrm{Wm^{-2}K^{-4}}$  is the Stefan-Boltzmann constant and  $\alpha(\chi)$  is the convection coefficient, where  $\chi$  stands for the rotational speed of the fan in the case of a fan and for the pressure in the case of compressed air. For free convection,  $\alpha(\chi)$  is constant and lies in the range of  $2-25 \; \mathrm{Wm^{-2}K^{-1}}$ . The mathematical model of the annealing simulator is obtained simply by inserting (1.2) - (1.5) into (1.1) with the state variable T and the input variables  $\mathbf{u}^{\mathrm{T}} = [I_{rms}, \chi, T_{s,air}, T_{s,wall}]$ . Integrating (1.1) along a solution curve from time  $t_0 = 0$  to time t for given input variables  $\mathbf{u}(\tau)$ ,  $0 \le \tau \le t$ , then we obtain

$$V(T(t)) - V(T(0)) = \int_0^t s(I_{rms}, \chi, T_{s,air}, T_{s,wall}, T) d\tau$$
 (1.6)

with

$$s(I_{rms}, \chi, T_{s,air}, T_{s,wall}, T) = I_{rms}^2 \delta(T) \frac{l}{A_c} - \alpha(\chi) A_s(T - T_{s,air}) - \varepsilon \sigma A_s \left(T^4 - T_{s,wall}^4\right).$$

$$(1.7)$$

Equation (1.6) states that the thermal energy V stored in the system at time t is equal to the energy stored at time  $t_0 = 0$  plus or minus the energy added to or removed from the system during this time with the so-called supply rate  $s(I_{rms}, \chi, T_{s,air}, T_{s,wall}, T)$ .

### 1.2 Solenoid Valve

Figure 1.2 shows the solenoid valve with a cylindrical housing and a cylindrical plunger with mass m and diameter D. The coil consisting of N windings with a total internal resistance R is supplied with a voltage  $U_0$ . It is assumed that the magnetic resistance of

1.2 Solenoid Valve Page 3

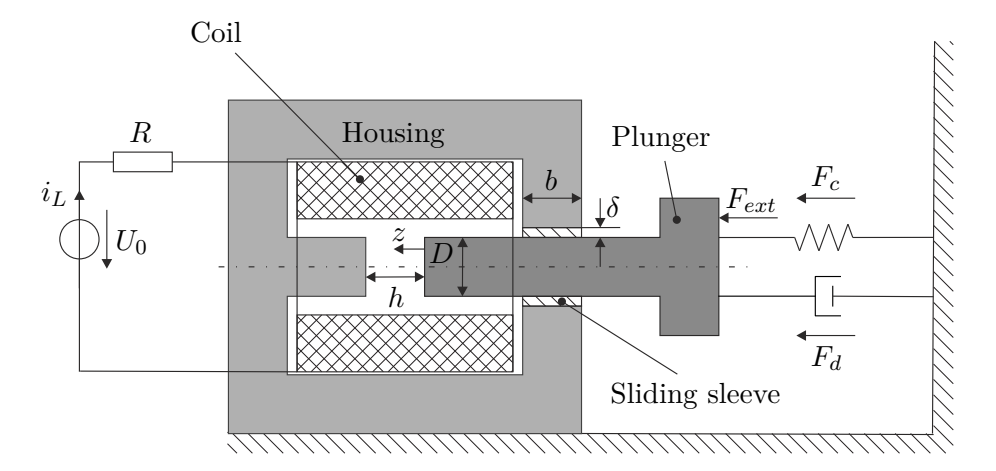


Figure 1.2: Simple solenoid valve.

the housing and the plunger is zero, that the sliding sleeve has the same permeability as air, and that the geometric dimensions satisfy  $h \ll D$  and  $\delta \ll b$  (no stray flux). Analogously to (1.1), the change in the energy stored in the system V is given by the relationship

$$\frac{\mathrm{d}}{\mathrm{d}t}V = p_{in} - p_{out} - p_{diss} \tag{1.8}$$

with the energy flows  $p_{in}$  and  $p_{out}$ , which flow across the system boundaries into the system or out of the system, and with the power dissipated  $p_{diss}$ . Under the above assumptions, the co-energy stored in the magnetic circuit is calculated in the form

$$\check{w}_L = \frac{1}{2}L(z)i_L^2$$
(1.9)

with the equivalent inductance of the magnetic circuit

$$L(z) = \frac{\mu_0 N^2 D^2 \pi (D + \delta) \pi b}{4(h - z)(D + \delta) \pi b + \delta D^2 \pi}$$
(1.10)

and the permeability of air  $\mu_0 = 4\pi \times 10^{-7} \, \mathrm{V \, s/(A \, m)}$ .

Exercise 1.1. Calculate the relationship for the inductance L(z) from (1.10).

Since the considered solenoid valve is magnetically linear, the expressions for energy  $\hat{w}_L$  and co-energy  $\check{w}_L$  are identical. The magnetic force acting on the plunger is calculated as

$$F_{mag} = \frac{\partial}{\partial z} \check{w}_L = \frac{1}{2} \frac{\partial L(z)}{\partial z} i_L^2 . \tag{1.11}$$

As depicted in Figure 1.2, the plunger acts against a linear spring-damper system with the damping force  $F_d = dv$ ,  $v = \dot{z}$ , d > 0, the spring force  $F_c = cz(t)$ , c > 0, and an external

force  $F_{ext}$ . The mathematical model of the solenoid valve is then

$$\frac{\mathrm{d}}{\mathrm{d}t}z = v\tag{1.12}$$

$$\frac{\mathrm{d}}{\mathrm{d}t}v = \frac{1}{m} \left( \frac{1}{2} \frac{\partial L(z)}{\partial z} i_L^2 - cz - dv + F_{ext} \right)$$
(1.13)

$$\frac{\mathrm{d}}{\mathrm{d}t}i_L = \frac{1}{L(z)} \left( U_0 - Ri_L - \frac{\partial L(z)}{\partial z} i_L v \right) \tag{1.14}$$

with the state variables  $\mathbf{x}^{\mathrm{T}} = [z, v, i_L]$  and the input variables  $\mathbf{u}^{\mathrm{T}} = [U_0, F_{ext}]$ . The energy stored in the system now consists of the magnetic energy (1.9), the kinetic energy of the plunger, and the potential energy of the spring

$$V = \frac{1}{2} \left( L(z)i_L^2 + mv^2 + cz^2 \right). \tag{1.15}$$

The change in stored energy V along a solution curve is obtained in the form

$$\frac{\mathrm{d}}{\mathrm{d}t}V = \underbrace{U_0 i_L + F_{ext} v}_{p_{in} - p_{out}} - \underbrace{\left(dv^2 + Ri_L^2\right)}_{p_{diss}} . \tag{1.16}$$

Integrating (1.16) along a solution curve from time  $t_0 = 0$  to time t for given input variables  $\mathbf{u}(\tau)$ ,  $0 \le \tau \le t$ , we obtain

$$V(\mathbf{x}(t)) - V(\mathbf{x}(t_0)) \le \int_{t_0}^t s(U_0, F_{ext}, i_L, v) d\tau$$
 (1.17)

because  $p_{diss} \geq 0$  and using the supply rate

$$s(U_0, F_{ext}, i_L, v) = U_0 i_L + F_{ext} v$$
 (1.18)

# 1.3 System-theoretic Concept

### 1.3.1 Dissipativity

The following considerations are based on a nonlinear dynamic system of the form

$$\frac{\mathrm{d}}{\mathrm{d}t}\mathbf{x} = \mathbf{f}(\mathbf{x}, \mathbf{u})$$

$$\mathbf{y} = \mathbf{h}(\mathbf{x}, \mathbf{u})$$
(1.19)

with the state  $\mathbf{x} \in \mathcal{X} \subset \mathbb{R}^n$ , the input  $\mathbf{u} \in \mathcal{U} \subset \mathbb{R}^m$  and the output  $\mathbf{y} \in \mathcal{Y} \subset \mathbb{R}^p$ . It is assumed that the state  $\mathbf{x}(t)$  at any time t is uniquely determined by the choice of the input  $\mathbf{u}(t)$  and the initial state  $\mathbf{x}(0) = \mathbf{x}_0$ . This allows to define the so-called supply rate  $s(\mathbf{u}, \mathbf{y}) : \mathcal{U} \times \mathcal{Y} \to \mathbb{R}$ , a real-valued function that for all initial values  $\mathbf{x}_0 \in \mathcal{X}$  and all input variables  $\mathbf{u}$  satisfies the condition

$$\int_0^t |s(\mathbf{u}, \mathbf{y})| d\tau < \infty \tag{1.20}$$

for all times  $t \geq 0$ .

**Definition 1.1.** The system (1.19) is called dissipative with respect to the supply rate s if a non-negative function  $V(\mathbf{x}): \mathcal{X} \to \mathbb{R}$  exists such that the so-called integral dissipativity inequality

$$V(\mathbf{x}(t)) - V(\mathbf{x}(0)) \le \int_0^t s(\mathbf{u}(\tau), \mathbf{y}(\tau)) d\tau$$
 (1.21)

for all initial values  $\mathbf{x}(0) \in \mathcal{X}$  and all input variables  $\mathbf{u}(t)$  for all times  $t \geq 0$  is fulfilled. The function  $V(\mathbf{x})$  is called *storage function*. If the equality sign holds in (1.21), the system (1.19) is called *lossless with respect to the supply rate s*.

In the sense of this definition, the annealing simulator of Figure 1.1 is lossless with respect to the supply rate (1.7) and the solenoid valve of Figure 1.2 is dissipative with respect to the supply rate (1.18). If the storage function  $V(\mathbf{x})$  is continuously differentiable with respect to  $\mathbf{x}$ , then one can calculate the change of  $V(\mathbf{x})$  along a solution curve of (1.19) and one obtains the so-called differential dissipativity inequality

$$\frac{\mathrm{d}}{\mathrm{d}t}V(\mathbf{x}) \le s(\mathbf{u}(t), \mathbf{y}(t)) \tag{1.22}$$

for all times  $t \geq 0$ .

### 1.3.2 Passivity

Passivity can be viewed as a special case of dissipativity. For the definition, consider again the system (1.19), where now the dimension of the system input m is equal to the dimension of the output p.

**Definition 1.2.** The system (1.19) with m = p is called *passive*, if a constant  $\delta$  exists such that the inequality

$$\int_{0}^{t} \mathbf{y}^{\mathrm{T}} \mathbf{u} \mathrm{d}\tau \ge \delta \tag{1.23}$$

for all admissible input variables  $\mathbf{u}(t)$  and all  $t \geq 0$  is fulfilled. If in addition for suitable real constants  $\alpha$ ,  $\beta$  the inequality

$$\int_0^t \mathbf{y}^{\mathrm{T}} \mathbf{u} \mathrm{d}\tau \ge \delta + \alpha \int_0^t \mathbf{u}^{\mathrm{T}} \mathbf{u} \mathrm{d}\tau \quad \text{bzw.} \quad \int_0^t \mathbf{y}^{\mathrm{T}} \mathbf{u} \mathrm{d}\tau \ge \delta + \beta \int_0^t \mathbf{y}^{\mathrm{T}} \mathbf{y} \mathrm{d}\tau \qquad (1.24)$$

for all admissible input variables  $\mathbf{u}(t)$  and all  $t \geq 0$  is fulfilled, then the system is called  $\alpha$ -input passive or  $\beta$ -output passive.

Obviously,  $\delta \leq 0$  because the inequality (1.23) must also hold for the input variable  $\mathbf{u}(t) = \mathbf{0}$ .

**Theorem 1.1** (Connection Passivity and Dissipativity). For the system (1.19) with m = p, a non-negative function  $V(\mathbf{x}) : \mathcal{X} \to \mathbb{R}$  exists such that (integral passivity inequality)

$$V(\mathbf{x}(t)) - V(\mathbf{x}(0)) \le \int_0^t \mathbf{y}^{\mathrm{T}} \mathbf{u} d\tau$$
 (1.25)

for all admissible input variables  $\mathbf{u}(t)$ , all  $\mathbf{x}(0)$  and all  $t \geq 0$ , then the system (1.19) is passive from the input  $\mathbf{u}$  to the output  $\mathbf{y}$ . Obviously, according to Definition 1.1 this is equivalent to the fact that the system (1.19) with respect to the special bilinear supply rate  $s(\mathbf{u}, \mathbf{y}) = \langle \mathbf{y}, \mathbf{u} \rangle = \mathbf{y}^T \mathbf{u}$  is dissipative. If in addition the system (1.19) is dissipative with respect to the supply rate  $s(\mathbf{u}, \mathbf{y}) = \mathbf{y}^T \mathbf{u} - \alpha \|\mathbf{u}\|^2$  or  $s(\mathbf{u}, \mathbf{y}) = \mathbf{y}^T \mathbf{u} - \beta \|\mathbf{y}\|^2$  for suitable real constants  $\alpha$ ,  $\beta$ , then (1.19) is  $\alpha$ -input passive or  $\beta$ -output passive. A lossless passive system is also called a conservative system in this context.

*Proof.* The proof of the theorem is trivial, since due to  $V(\mathbf{x}) \geq 0$  from (1.25) it immediately follows

$$\int_0^t \mathbf{y}^{\mathrm{T}} \mathbf{u} \mathrm{d}\tau \ge -V(\mathbf{x}(0)) = \delta . \tag{1.26}$$

With this definition, the solenoid valve of Figure 1.2 with the input  $\mathbf{u}^{\mathrm{T}} = [U_0, F_{ext}]$  and the output  $\mathbf{y}^{\mathrm{T}} = [i_L, v]$  is passive, indeed even  $\beta$ -output passive with  $0 < \beta < \min(d, R)$ , since for the dissipated power from (1.16) we have  $p_{diss} = dv^2 + Ri_L^2 \ge \beta \|\mathbf{y}\|^2$ . The physical interpretation of the passivity inequality (1.25) is now as follows: If the expression  $\mathbf{y}^{\mathrm{T}}\mathbf{u}$  represents power (e.g., suitable pairs of currents and voltages in electrical systems or collocated velocities and forces in mechanical systems) and  $V(\mathbf{x})$  is the energy stored in the system, then the passivity inequality (1.25) states that the increase in the energy stored in the system is less than or equal to the energy supplied to the system.

Exercise 1.2. Show that the integrator with the state-space representation

$$\frac{\mathrm{d}}{\mathrm{d}t}x = u \tag{1.27}$$

$$y = x$$

is passive.

Exercise 1.3. Under what conditions on the parameters  $\sigma_0$ ,  $\sigma_1$ ,  $\sigma_2$ ,  $r_C$ ,  $r_H$ , and  $v_0$  does the LuGre friction model (see lecture notes for the VO Nonlinear Dynamic Systems and Control [1.1]) describe a passive system from the input  $\Delta v$  to the output  $F_R$ . The LuGre friction model can be written in the form

$$\frac{\mathrm{d}}{\mathrm{d}t}z = \Delta v - \frac{\mathrm{abs}(\Delta v)}{\chi(\Delta v)}\sigma_0 z$$

$$F_R = \sigma_0 z + \sigma_1 \frac{\mathrm{d}}{\mathrm{d}t}z + \sigma_2 \Delta v$$
(1.28)

with

$$\chi(\Delta v) = r_C + (r_H - r_C) \exp\left(-\left(\frac{\Delta v}{v_0}\right)^2\right). \tag{1.29}$$

Exercise 1.4. Show that a nonlinear characteristic  $y = \psi(u)$  that satisfies the sector condition  $k_1 u^2 \le \psi(u) u \le k_2 u^2$  is  $k_1$ -input passive and  $\left(\frac{1}{k_2}\right)$ -output passive according to Definition 1.2.

### 1.3.3 Properties of Passive Systems

Passive systems now have the remarkable property that the parallel connection and the feedback of passive systems, as shown in Figure 1.3, are again passive.

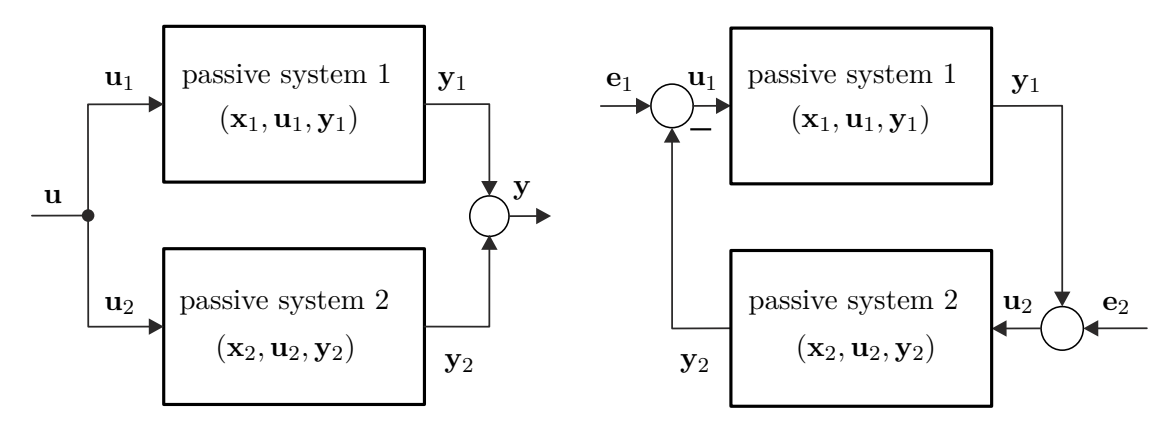


Figure 1.3: Parallel connection and feedback of two passive systems.

*Proof.* To show this, we assume two passive systems of the form (1.19) with m = p. There are two non-negative storage functions  $V_1(\mathbf{x}_1)$  and  $V_2(\mathbf{x}_2)$  that satisfy the

passivity inequalities

$$V_1(\mathbf{x}_1(t)) - V_1(\mathbf{x}_1(0)) \le \int_0^t \mathbf{y}_1^{\mathrm{T}} \mathbf{u}_1 \, \mathrm{d}\tau$$

$$V_2(\mathbf{x}_2(t)) - V_2(\mathbf{x}_2(0)) \le \int_0^t \mathbf{y}_2^{\mathrm{T}} \mathbf{u}_2 \, \mathrm{d}\tau.$$

$$(1.30)$$

For the parallel connection according to Figure 1.3 we have  $\mathbf{u}_1 = \mathbf{u}_2 = \mathbf{u}$ ,  $\mathbf{y} = \mathbf{y}_1 + \mathbf{y}_2$ , and thus

$$V_1(\mathbf{x}_1(t)) + V_2(\mathbf{x}_2(t)) - V_1(\mathbf{x}_1(0)) - V_2(\mathbf{x}_2(0)) \le \int_0^t (\mathbf{y}_1^{\mathrm{T}} + \mathbf{y}_2^{\mathrm{T}}) \mathbf{u} d\tau$$
 (1.31)

or

$$V(\mathbf{x}(t)) - V(\mathbf{x}(0)) \le \int_0^t \mathbf{y}^{\mathrm{T}} \mathbf{u} d\tau$$
 (1.32)

with the non-negative storage function  $V(\mathbf{x}) = V_1(\mathbf{x}_1) + V_2(\mathbf{x}_2)$  and the state  $\mathbf{x}^T = [\mathbf{x}_1^T, \mathbf{x}_2^T]$ .

*Exercise* 1.5. Show that the closed loop of the feedback of two passive systems (see Figure 1.3, right picture) from the input  $(\mathbf{e}_1, \mathbf{e}_2)$  to the output  $(\mathbf{y}_1, \mathbf{y}_2)$  is passive.

Furthermore, the cascade connection of two passive systems according to Figure 1.4 is passive, provided the connecting system is energy-conserving, i.e., the following interconnection condition

$$\int_0^t \left( \mathbf{y}_1^{\mathrm{T}} \mathbf{u}_I + \mathbf{y}_2^{\mathrm{T}} \mathbf{y}_I \right) \mathrm{d}\tau = 0 \tag{1.33}$$

is fulfilled. It is easily verified that this is the case, since the following passivity inequality

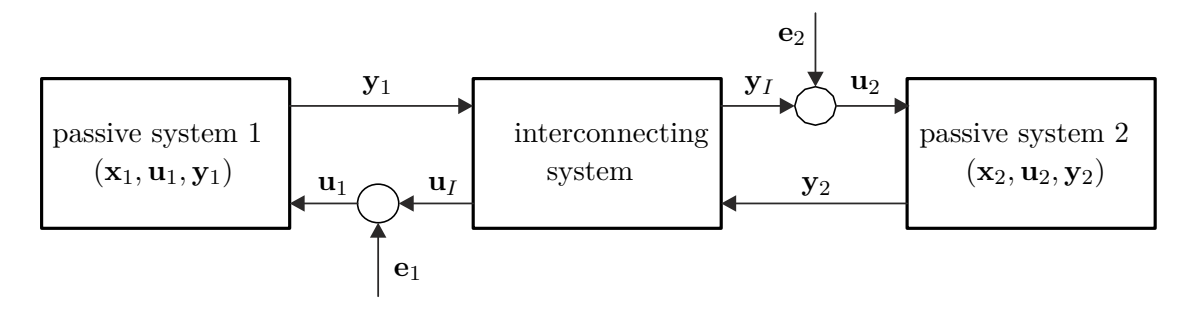


Figure 1.4: Cascade connection of passive systems.

$$V(\mathbf{x}(t)) - V(\mathbf{x}(0)) \le \int_0^t (\mathbf{y}_1^{\mathrm{T}} \mathbf{e}_1 + \mathbf{y}_2^{\mathrm{T}} \mathbf{e}_2) d\tau$$
 (1.34)

with  $V(\mathbf{x}) = V_1(\mathbf{x}_1) + V_2(\mathbf{x}_2)$  and  $\mathbf{x}^T = [\mathbf{x}_1^T, \mathbf{x}_2^T]$  holds. It is precisely this property that is used in certain passivity-based controller design methods, where system 1 corresponds to a passive plant and system 2 to a passive controller. For the interconnected system, a

system of the form

$$\begin{bmatrix} \mathbf{u}_I \\ \mathbf{y}_I \end{bmatrix} = \begin{bmatrix} \mathbf{0} & \mathbf{U}_I(\mathbf{x}) \\ -\mathbf{U}_I^{\mathrm{T}}(\mathbf{x}) & \mathbf{0} \end{bmatrix} \begin{bmatrix} \mathbf{y}_1 \\ \mathbf{y}_2 \end{bmatrix}$$
(1.35)

with an arbitrary quadratic matrix  $\mathbf{U}_I(\mathbf{x})$  is chosen.

Exercise 1.6. Show that (1.35) satisfies the interconnection condition (1.33).

### 1.3.4 Passivity and Lyapunov Stability

It is assumed that the system (1.19) is passive with a continuously differentiable, positive definite storage function  $V(\mathbf{x})$ . Then it follows immediately from the passivity inequality (1.25) in its differential form

$$\frac{\mathrm{d}}{\mathrm{d}t}V(\mathbf{x}) \le \mathbf{y}^{\mathrm{T}}\mathbf{u} \tag{1.36}$$

that the equilibrium  $\mathbf{x} = \mathbf{0}$  of the free system (1.19), i.e., for  $\mathbf{u} = \mathbf{0}$ , is stable in the sense of Lyapunov with the Lyapunov function  $V(\mathbf{x})$ . Whether the equilibrium is asymptotically stable must be investigated on a case-by-case basis using the invariance principle of Krassovskii-LaSalle. For the feedback of two passive systems, as shown in the right part of Figure 1.3, the asymptotic stability of the equilibrium of the free closed-loop system, i.e., for  $\mathbf{e}_1 = \mathbf{e}_2 = \mathbf{0}$ , can be traced back to properties of the subsystems.

**Theorem 1.2.** Assume that the equilibrium  $\mathbf{x}_1 = \mathbf{0}$  of subsystem 1 is asymptotically stable and  $\alpha$ -input passive according to Definition 1.2 with a continuously differentiable, positive definite storage function  $V_1(\mathbf{x}_1)$ . Furthermore, let subsystem 2 be zero-state detectable and  $\beta$ -output passive according to Definition 1.2 with a continuously differentiable, positive definite storage function  $V_2(\mathbf{x}_2)$ . Then the equilibrium of the closed-loop system  $(\mathbf{x}_1, \mathbf{x}_2) = (\mathbf{0}, \mathbf{0})$  is asymptotically stable if  $\alpha + \beta > 0$  holds.

Before this theorem is shown, the concepts of zero-state detectability and zero-state observability should be defined.

**Definition 1.3.** The system (1.19) is called zero-state detectable (zero-state observable) if from  $\mathbf{u}(t) = \mathbf{0}$  and  $\mathbf{y}(t) = \mathbf{0}$  for all times  $t \geq 0$  it follows  $\lim_{t \to \infty} \mathbf{x}(t) = \mathbf{0}$  ( $\mathbf{x}(t) = \mathbf{0}$  for all times  $t \geq 0$ ).

*Proof.* To prove Theorem 1.2, choose a Lyapunov function  $V(\mathbf{x}) = V_1(\mathbf{x}_1) + V_2(\mathbf{x}_2)$  and calculate its time derivative

$$\frac{\mathrm{d}}{\mathrm{d}t}V(\mathbf{x}) \le -(\alpha + \beta)\|\mathbf{y}_2\|^2 \ . \tag{1.37}$$

However, according to Theorem 1.2,  $\alpha + \beta > 0$ , so it follows immediately that the equilibrium of the closed-loop system  $(\mathbf{x}_1, \mathbf{x}_2) = (\mathbf{0}, \mathbf{0})$  is stable in the sense of Lyapunov. Due to the zero-state detectability of subsystem 2 and the asymptotic stability of the equilibrium  $\mathbf{x}_1 = \mathbf{0}$  of subsystem 1, one can show that the largest positive invariant set contained in  $\mathcal{H} = \left\{ \mathbf{x} \in \mathcal{X} | \frac{\mathrm{d}}{\mathrm{d}t} V(\mathbf{x}) = 0 \right\}$  is the origin  $(\mathbf{x}_1, \mathbf{x}_2) = (\mathbf{0}, \mathbf{0})$ . However, according to the invariance principle of Krassovskii-LaSalle, the

equilibrium of the closed-loop system  $(\mathbf{x}_1, \mathbf{x}_2) = (\mathbf{0}, \mathbf{0})$  is asymptotically stable.

Theorem 1.2 is needed in connection with the concept of absolute stability, in particular for the derivation of the circle and Popov criterion.

# 1.4 Linear Passive Systems

For a linear time-invariant system of the form

$$\frac{\mathrm{d}}{\mathrm{d}t}\mathbf{x} = \mathbf{A}\mathbf{x} + \mathbf{b}u$$

$$y = \mathbf{c}^{\mathrm{T}}\mathbf{x} + du,$$
(1.38)

the property of passivity can also be determined from the associated transfer function

$$G(s) = \frac{\hat{y}(s)}{\hat{u}(s)} = \mathbf{c}^{\mathrm{T}}(s\mathbf{E} - \mathbf{A})^{-1}\mathbf{b} + d.$$
 (1.39)

Without loss of generality, only single-input systems are considered here, for multi-input systems, see the literature cited at the end. According to Definition 1.2, the system (1.38) is passive if and only if the following inequality

$$\int_0^t yu\mathrm{d}\tau \ge 0 \tag{1.40}$$

is fulfilled. Thus, the following theorem for the passivity of linear time-invariant single-input systems can be given:

**Theorem 1.3.** The linear time-invariant system (1.38) with the transfer function G(s) from (1.39) is

(1) passive if and only if

$$\operatorname{Re}(G(I\omega)) \ge 0 \quad \text{for all } \omega,$$
 (1.41)

(2)  $\alpha$ -input passive with  $\alpha > 0$  if and only if

$$\operatorname{Re}(G(I\omega)) \ge \alpha > 0 \quad \text{for all } \omega$$
 (1.42)

(3) and  $\beta$ -output passive with  $\beta > 0$  if and only if

$$\operatorname{Re}(G(I\omega)) \ge \beta |G(I\omega)|^2 > 0 \quad \text{for all } \omega .$$
 (1.43)

Note that verifying the conditions (1.41) - (1.43) is simple by using the Nyquist locus of G(s).

*Proof.* To prove this theorem, one needs the so-called *Parseval theorem*. Let x(t) and y(t) denote two square-integrable time functions, i.e. x(t),  $y(t) \in L_2(-\infty, \infty)$ , and

$$\hat{x}(\omega) = \int_{-\infty}^{\infty} x(t) \exp(-\mathrm{I}\omega t) dt \quad \text{and} \quad \hat{y}(\omega) = \int_{-\infty}^{\infty} y(t) \exp(-\mathrm{I}\omega t) dt$$
 (1.44)

are the corresponding Fourier transforms, then we have for the inner product

$$\int_{-\infty}^{\infty} x(t)y(t)dt = \langle x, y \rangle = \langle \hat{x}, \hat{y} \rangle = \frac{1}{2\pi} \int_{-\infty}^{\infty} \hat{x}(\omega)\hat{y}^*(\omega)d\omega . \qquad (1.45)$$

From (1.45), we get

$$||x||_2 = ||\hat{x}||_2 \ . \tag{1.46}$$

To apply the Parseval theorem for the proof of Theorem 1.3, the cut-off operator ( ) $_T$  in the form

$$u_T(t) = \begin{cases} u(t) & \text{für } t \le T \\ 0 & \text{für } t > T \end{cases}$$
 (1.47)

is introduced. Furthermore, it is assumed that the time functions u(t) and y(t) are causal, i.e., u(t) = 0 and y(t) = 0 for t < 0. This yields

$$\int_0^T u(t)y(t)dt = \int_{-\infty}^\infty u_T(t)y_T(t)dt = \frac{1}{2\pi} \int_{-\infty}^\infty \hat{u}_T(\omega)\hat{y}_T^*(\omega)d\omega$$
 (1.48)

and with  $\hat{y}(\omega) = G(I\omega)\hat{u}_T(\omega)$ , we obtain

$$\int_{0}^{T} u(t)y(t) dt = \frac{1}{2\pi} \int_{-\infty}^{\infty} G^{*}(I\omega)\hat{u}_{T}(\omega)\hat{u}_{T}^{*}(\omega) d\omega$$

$$= \frac{1}{2\pi} \int_{-\infty}^{\infty} (\operatorname{Re}(G(I\omega)) - \operatorname{I}\operatorname{Im}(G(I\omega)))|\hat{u}_{T}(\omega)|^{2} d\omega .$$
(1.49)

Since the left-hand side of (1.49) is purely real, the imaginary part on the right-hand side must vanish, and we have

$$\int_0^{\mathrm{T}} u(t)y(t)\mathrm{d}t = \frac{1}{2\pi} \int_{-\infty}^{\infty} \mathrm{Re}(G(\mathrm{I}\omega))|\hat{u}_T(\omega)|^2 \mathrm{d}\omega \ . \tag{1.50}$$

" $\Leftarrow$ ": Now assume that (1.42) holds, then it follows

$$\int_0^T u(t)y(t)dt \ge \frac{\alpha}{2\pi} \int_{-\infty}^\infty |\hat{u}_T(\omega)|^2 d\omega = \alpha \int_0^T u^2(t)dt$$
 (1.51)

and thus, according to Definition 1.2, the  $\alpha$ -input passivity of (1.38).

" $\Rightarrow$ ": Conversely, if the system (1.38) is  $\alpha$ -input passive, then there exists an  $\alpha > 0$  such that the inequality

$$\int_{0}^{T} u(t)y(t)dt \ge \alpha \int_{0}^{T} u^{2}(t)dt \tag{1.52}$$

is fulfilled, or using the Parseval theorem, we obtain

$$\frac{1}{2\pi} \int_{-\infty}^{\infty} (\operatorname{Re}(G(I\omega)) - \alpha) |\hat{u}_T(\omega)|^2 d\omega \ge 0.$$
 (1.53)

The inequality (1.53) is only valid for all input variables u(t) if for all  $\omega$  we have  $\text{Re}(G(I\omega)) \geq \alpha$ . Assume that there exists an  $\omega_0$  such that  $\text{Re}(G(I\omega_0)) < \alpha$ , then one sees that for the input variable  $u(t) = U\sin(\omega_0 t)$  and sufficiently large T the inequality (1.53) is not fulfilled. Thus, point (2) and for  $\alpha = 0$  also point (1) of Theorem 1.3 is proven.

Exercise 1.7. Prove point (3) of Theorem 1.3.

As a simple application example, it will be shown that the PID controller

$$R(s) = V \frac{1 + T_I s}{s} \frac{1 + T_D s}{1 + \alpha T_D s}$$
 (1.54)

with the positive parameters V,  $T_I$ ,  $T_D$ , and  $0 < \alpha < 1$  is passive. To do this, simply calculate

$$Re(R(I\omega)) = \frac{V(T_I + T_D(1 - \alpha) + \alpha T_D^2 T_I w^2)}{1 + \alpha^2 T_D^2 w^2} > 0.$$
 (1.55)

Exercise 1.8. Show that a PI controller is passive.

*Exercise* 1.9. Show that the linear time-invariant system (1.38) with the transfer function G(s) from (1.39) is passive if

$$|\arg(G(\mathrm{I}\omega))| \le \frac{\pi}{2}$$
 (1.56)

Exercise 1.10. Consider a standard control loop with a passive plant G(s) and an  $\alpha$ -input passive controller R(s) with  $\alpha > 0$ . Show that the closed-loop system is BIBO-stable.

Remark: Use the Nyquist criterion for this purpose.

Exercise 1.11. The relationship between current  $\hat{i}(x,s)$  and voltage  $\hat{u}(x,s)$  at the location x=0 and at the location x=l of a long electrical line with the capacitance per unit length c, the inductance per unit length l, the resistance per unit length r, and the conductance per unit length q is

$$\begin{bmatrix} \hat{u}(0,s) \\ \hat{\imath}(0,s) \end{bmatrix} = \begin{bmatrix} \cosh(\gamma(s)l) & Z_0(s)\sinh(\gamma(s)l) \\ \frac{1}{Z_0(s)}\sinh(\gamma(s)l) & \cosh(\gamma(s)l) \end{bmatrix} \begin{bmatrix} \hat{u}(l,s) \\ \hat{\imath}(l,s) \end{bmatrix}, \tag{1.57}$$

where  $Z_0(s)$  denotes the characteristic impedance and  $\gamma(s)$  the propagation coefficient

$$Z_0(s) = \sqrt{\frac{r+sl}{g+sc}} \quad \text{and} \quad \gamma(s) = \sqrt{(r+sl)(g+sc)}.$$
 (1.58)

1.5 Positive Realness Page 13

Check for different load impedances  $Z_L(s)$  with

$$\hat{u}(l,s) = Z_L(s)\hat{\imath}(l,s) \tag{1.59}$$

the passivity of the transfer function  $G(s) = \frac{\hat{u}(0,s)}{\hat{\imath}(0,s)}$ .

### 1.5 Positive Realness

For linear time-invariant systems (1.38), the term positive realness of the associated transfer function (1.39) is very often used instead of passivity. Without proof, it should be noted that the system (1.38) is passive if and only if (1.39) is positive real.

**Theorem 1.4.** A transfer function G(s) is positive real if and only if

- (1) G(s) has no poles in the right open s-half plane,
- (2)  $\operatorname{Re}(G(I\omega)) \geq 0$  for all  $\omega$ , for which  $I\omega$  is not a pole of G(s), and
- (3) if  $s = I\omega_0$  is a pole of G(s), then this pole is simple and for finite  $\omega_0$  the residual

$$\lim_{s \to I\omega_0} (s - I\omega_0)G(s) \tag{1.60}$$

must be positive and real. If  $\omega_0$  is infinite, then the limit

$$\lim_{\omega \to \infty} \frac{G(I\omega)}{I_{\omega}} \tag{1.61}$$

must be positive and real.

We call G(s) strictly positive real if  $G(s-\delta)$  for a suitable  $\delta > 0$  is positive real.

### Exercise 1.12. Show that the conditions

- (1) the degree difference between the numerator and denominator polynomial of G(s) is -1,0 or 1, and
- (2) G(s) has no zeros in the right open s-half plane

are necessary for G(s) to be positive real.

Exercise 1.13. Are the following transfer functions

$$G_1(s) = -(s-3), G_2(s) = \frac{1}{s^2 + 2s + 1}, G_3(s) = \frac{s+1}{s^2 + 1}, G_4(s) = \frac{s+10}{(s+1)(s+2)}$$

$$(1.62)$$

positive real?

1.5 Positive Realness Page 14

As shown in the following theorem, the positive realness of a transfer function G(s) is closely related to the solvability of a system of equations. For the proof of this theorem, see the literature cited at the end.

Theorem 1.5 (Kalman-Yakubovich-Popov (KYP)-Lemma). Given is the system (1.38), where it is assumed that the pair  $(\mathbf{A}, \mathbf{b})$  is reachable and the pair  $(\mathbf{c}^T, \mathbf{A})$ is observable. The transfer function (1.39) is positive real (passive) if and only if a scalar w, a vector m, and a positive definite matrix P exist such that the following conditions

$$\mathbf{P}\mathbf{A} + \mathbf{A}^{\mathrm{T}}\mathbf{P} = -\mathbf{m}\,\mathbf{m}^{\mathrm{T}}$$

$$\mathbf{P}\mathbf{b} = \mathbf{c} - \mathbf{m}w$$

$$w^{2} = 2d$$
(1.63)

are fulfilled. The transfer function (1.39) is strictly positive real according to Theorem 1.4 if and only if scalars w and  $\varepsilon > 0$ , a vector **m**, and a positive definite matrix **P** exist such that the following conditions

$$\mathbf{P}\mathbf{A} + \mathbf{A}^{\mathrm{T}}\mathbf{P} = -\mathbf{m}\,\mathbf{m}^{\mathrm{T}} - \varepsilon\mathbf{P}$$

$$\mathbf{P}\mathbf{b} = \mathbf{c} - \mathbf{m}w$$

$$w^{2} = 2d$$
(1.64)

are fulfilled.

Exercise 1.14. Assume w,  $\mathbf{m}$ ,  $\mathbf{P} > \mathbf{0}$ , and  $\varepsilon > 0$  are solutions of (1.64). Show that in the case  $d \neq 0$  the Riccati equation

$$\mathbf{P}\left(\frac{\varepsilon}{2}\mathbf{E} + \mathbf{A}\right) + \left(\frac{\varepsilon}{2}\mathbf{E} + \mathbf{A}^{\mathrm{T}}\right)\mathbf{P} + (\mathbf{c} - \mathbf{P}\mathbf{b})\frac{1}{2d}(\mathbf{c}^{\mathrm{T}} - \mathbf{b}^{\mathrm{T}}\mathbf{P}) = \mathbf{0}$$
(1.65)

is fulfilled.

As an application of the KYP lemma, consider the closed-loop control system of Figure 1.5 with the nonlinear passive plant in the forward path and the strictly positive real controller in the feedback path. Assume the passive nonlinear system has a continuously differentiable, positive definite storage function  $V_1(\mathbf{x}_1)$ , which satisfies the differential passivity inequality (see (1.36))

$$\frac{\mathrm{d}}{\mathrm{d}t}V_1(\mathbf{x}_1) = -W_1(\mathbf{x}_1) + y_1u_1 \le y_1u_1 , \qquad (1.66)$$

with the positive semidefinite function  $W_1(\mathbf{x}_1)$ . For the following, the strictly positive real controller is described by the following minimal realization

$$\frac{\mathrm{d}}{\mathrm{d}t}\mathbf{x}_2 = \mathbf{A}\mathbf{x}_2 + \mathbf{b}u_2$$

$$y_2 = \mathbf{c}^{\mathrm{T}}\mathbf{x}_2 + du_2.$$
(1.67)

Due to the KYP Lemma according to Theorem 1.5 one finds for the system (1.67) scalars w and  $\varepsilon > 0$ , a vector m, and a positive definite matrix P such that (1.64) is fulfilled.

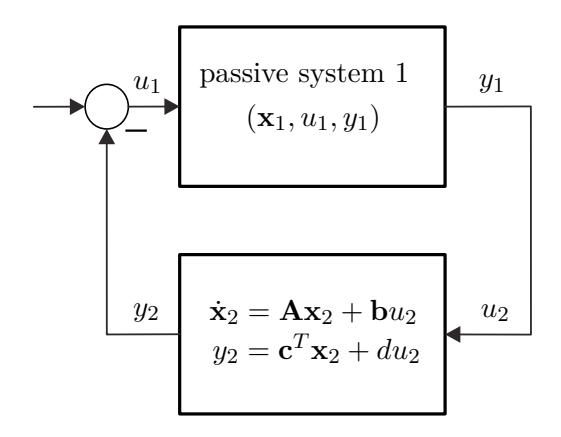


Figure 1.5: Passive system with linear controller.

This results in the Lyapunov function of the closed-loop system

$$V_e(\mathbf{x}_1, \mathbf{x}_2) = V_1(\mathbf{x}_1) + \frac{1}{2}\mathbf{x}_2^{\mathrm{T}}\mathbf{P}\mathbf{x}_2 . \qquad (1.68)$$

Then, we calculate the time derivative of (1.68) along the solution curve and considers the interconnection condition  $u_1 = -y_2$  and  $u_2 = y_1$  together with (1.64) and (1.66)

$$\frac{\mathrm{d}}{\mathrm{d}t}V_{e}(\mathbf{x}_{1},\mathbf{x}_{2}) = -W_{1}(\mathbf{x}_{1}) + y_{1}u_{1} + \frac{1}{2}\underbrace{\dot{\mathbf{x}}_{2}^{\mathrm{T}}\mathbf{P}\mathbf{x}_{2}}_{(\mathbf{x}_{2}^{\mathrm{T}}\mathbf{A}^{\mathrm{T}} + u_{2}\mathbf{b}^{\mathrm{T}})\mathbf{P}\mathbf{x}_{2}} + \frac{1}{2}\underbrace{\dot{\mathbf{x}}_{2}^{\mathrm{T}}\mathbf{P}\dot{\mathbf{x}}_{2}}_{\mathbf{x}_{2}^{\mathrm{T}}\mathbf{P}(\mathbf{A}\mathbf{x}_{2} + \mathbf{b}u_{2})}$$

$$= -W_{1}(\mathbf{x}_{1}) + y_{1}u_{1} + \frac{1}{2}\mathbf{x}_{2}^{\mathrm{T}}\underbrace{\left(\mathbf{A}^{\mathrm{T}}\mathbf{P} + \mathbf{P}\mathbf{A}\right)}_{-\mathbf{mm}^{\mathrm{T}}-\varepsilon\mathbf{P}}\mathbf{x}_{2} + \mathbf{x}_{2}^{\mathrm{T}}\underbrace{\mathbf{P}\mathbf{b}}_{\mathbf{c}-\mathbf{m}w}u_{2}$$

$$= -W_{1}(\mathbf{x}_{1}) - \underbrace{y_{1}\mathbf{c}^{\mathrm{T}}\mathbf{x}_{2}}_{=} - dy_{1}^{2} - \frac{1}{2}\mathbf{x}_{2}^{\mathrm{T}}\mathbf{m}\mathbf{m}^{\mathrm{T}}\mathbf{x}_{2} - \frac{1}{2}\varepsilon\mathbf{x}_{2}^{\mathrm{T}}\mathbf{P}\mathbf{x}_{2} + \underbrace{\mathbf{x}_{2}^{\mathrm{T}}\mathbf{c}y_{1}}_{=} - \mathbf{x}_{2}^{\mathrm{T}}\mathbf{m}wy_{1}$$

$$= -W_{1}(\mathbf{x}_{1}) - \frac{1}{2}\varepsilon\mathbf{x}_{2}^{\mathrm{T}}\mathbf{P}\mathbf{x}_{2} - \frac{1}{2}y_{1}^{2}\underbrace{\left(2d\right)}_{w^{2}} - \frac{1}{2}\mathbf{x}_{2}^{\mathrm{T}}\mathbf{m}\mathbf{m}^{\mathrm{T}}\mathbf{x}_{2} - \mathbf{x}_{2}^{\mathrm{T}}\mathbf{m}wy_{1}$$

$$= -W_{1}(\mathbf{x}_{1}) - \frac{1}{2}\varepsilon\mathbf{x}_{2}^{\mathrm{T}}\mathbf{P}\mathbf{x}_{2} - \frac{1}{2}\left(\mathbf{m}^{\mathrm{T}}\mathbf{x}_{2} + wy_{1}\right)^{\mathrm{T}}\left(\mathbf{m}^{\mathrm{T}}\mathbf{x}_{2} + wy_{1}\right) \leq 0.$$
(1.69)

This directly shows the stability of the closed-loop system of Figure 1.5.

# 1.6 Canonical Form of Passive Systems

Before a canonical form for passive systems is presented, it will be shown that the well-known Euler-Lagrange equations are passive.

### 1.6.1 Hamiltonian Systems

Consider a finite-dimensional Lagrangian system with n degrees of freedom and the generalized coordinates  $\mathbf{q} \in \mathbb{R}^n$ , then the equations of motion are known to follow from

the Euler-Lagrange equations in the form

$$\frac{\mathrm{d}}{\mathrm{d}t} \left( \frac{\partial L}{\partial v_k} \right) - \frac{\partial L}{\partial q_k} = \tau_k \;, \quad k = 1, \dots, n \tag{1.70}$$

with the Lagrangian  $L(\mathbf{q}, \mathbf{v})$ , the generalized velocities  $\frac{d}{dt}\mathbf{q} = \mathbf{v}$ , and the generalized forces  $\tau_k$ , k = 1, ..., n. For simple Lagrangian systems, the Lagrangian corresponds to the difference between kinetic and potential energy

$$L(\mathbf{q}, \mathbf{v}) = T(\mathbf{q}, \mathbf{v}) - V(\mathbf{q}) . \tag{1.71}$$

It is assumed that the generalized forces  $\boldsymbol{\tau}$  are composed of external forces  $\boldsymbol{\tau}_e$  (control and disturbance inputs) and dissipative forces  $\boldsymbol{\tau}_d^{\mathrm{T}} = -\left(\frac{\partial}{\partial \mathbf{v}}R\right)(\mathbf{v})$  with the Rayleigh dissipation function  $R(\mathbf{v})$  and

$$\left(\frac{\partial}{\partial \mathbf{v}}R\right)(\mathbf{v})\mathbf{v} \ge 0. \tag{1.72}$$

This gives

$$\frac{\mathrm{d}}{\mathrm{d}t} \left( \frac{\partial L}{\partial v_k} \right) - \frac{\partial L}{\partial q_k} + \frac{\partial}{\partial v_k} R = \tau_{e,k} , \quad k = 1, \dots, n .$$
(1.73)

**Definition 1.4.** The Lagrangian system (1.73) is called *fully damped*, if the Rayleigh dissipation function  $R(\mathbf{v})$  satisfies the following inequality condition

$$\left(\frac{\partial}{\partial \mathbf{v}}R\right)(\mathbf{v})\mathbf{v} \ge \sum_{k=1}^{n} \beta_k v_k^2, \quad \beta_k > 0, \quad k = 1, \dots, n$$
 (1.74)

If  $\beta_k = 0$  for at least one k, then the Lagranian system is not fully damped.

Using the generalized momentum coordinates

$$p_k = \frac{\partial L}{\partial v_k}, \quad k = 1, \dots, n$$
 (1.75)

and the Legendre transformation  $(q_k, v_k) \to (q_k, p_k)$ , we obtain directly from the Euler-Lagrange equations (1.70) the equivalent Hamiltonian equations

$$\frac{\mathrm{d}}{\mathrm{d}t}q_k = \frac{\partial H}{\partial p_k} 
\frac{\mathrm{d}}{\mathrm{d}t}p_k = -\frac{\partial H}{\partial q_k} + \tau_k, \quad k = 1, \dots, n$$
(1.76)

with the Hamiltonian

$$H(\mathbf{q}, \mathbf{p}) = \sum_{k=1}^{n} p_k v_k - L(\mathbf{q}, \mathbf{v}) . \qquad (1.77)$$

The implicit function theorem states that the generalized velocities  $v_k$  from (1.75) can be calculated locally if and only if the matrix  $\left[\frac{\partial^2}{\partial v_i \partial v_j} L\right]$  is non-singular. Then, L is said to be a nondegenerate Lagrangian.

*Proof.* To prove this, consider the derivatives

$$\frac{\partial H}{\partial p_k} = v_k + \sum_{j=1}^n \left( p_j \frac{\partial v_j}{\partial p_k} - \underbrace{\frac{\partial L}{\partial v_j}}_{=p_j} \frac{\partial v_j}{\partial p_k} \right) = v_k = \frac{\mathrm{d}}{\mathrm{d}t} q_k \tag{1.78}$$

and

$$\frac{\partial H}{\partial q_k} = \sum_{j=1}^n \left( p_j \frac{\partial v_j}{\partial q_k} - \underbrace{\frac{\partial L}{\partial v_j}}_{=p_j} \frac{\partial v_j}{\partial q_k} \right) - \frac{\partial L}{\partial q_k} = \tau_k - \frac{\mathrm{d}}{\mathrm{d}t} \left( \frac{\partial L}{\partial v_k} \right) = \tau_k - \frac{\mathrm{d}}{\mathrm{d}t} p_k \ . \tag{1.79}$$

If the kinetic energy  $T(\mathbf{q}, \mathbf{v})$  in (1.71) has the form

$$T(\mathbf{q}, \mathbf{v}) = \frac{1}{2} \mathbf{v}^{\mathrm{T}} \mathbf{D}(\mathbf{q}) \mathbf{v}$$
 (1.80)

with the positive definite mass matrix  $\mathbf{D}(\mathbf{q})$ , then the Hamiltonian corresponds to the energy stored in the system

$$H(\mathbf{q}, \mathbf{p}) = \sum_{k=1}^{n} p_k v_k - \frac{1}{2} \mathbf{v}^{\mathrm{T}} \mathbf{D}(\mathbf{q}) \mathbf{v} + V(\mathbf{q}) = \frac{1}{2} \mathbf{v}^{\mathrm{T}} \mathbf{D}(\mathbf{q}) \mathbf{v} + V(\mathbf{q}).$$
(1.81)

Calculating the time change of the Hamiltonian (1.81)

$$\frac{\mathrm{d}}{\mathrm{d}t}H(\mathbf{q},\mathbf{p}) = \sum_{k=1}^{n} \left[ \frac{\partial H}{\partial q_k} \frac{\partial H}{\partial p_k} + \underbrace{\frac{\partial H}{\partial p_k}}_{v_k} \left( -\frac{\partial H}{\partial q_k} - \frac{\partial}{\partial v_k} R + \tau_{e,k} \right) \right] \le \sum_{k=1}^{n} v_k \tau_{e,k}, \tag{1.82}$$

we see that the Lagrangian system according to Definition 1.2 is passive with the input variable  $\tau_e$ , the output variable  $\mathbf{v} = \frac{\mathrm{d}}{\mathrm{d}t}\mathbf{q}$ , and the storage function  $H(\mathbf{q}, \mathbf{p})$ . If in addition the Lagrangian system according to Definition 1.4 is fully damped, then the Lagrangian system due to (1.74) is even  $\beta$ -output passive with  $\beta = \min_k(\beta_k), k = 1, \ldots, n$ 

$$\frac{\mathrm{d}}{\mathrm{d}t}H(\mathbf{q},\mathbf{p}) \le \sum_{k=1}^{n} v_k \tau_{e,k} - \sum_{k=1}^{n} \beta_k v_k^2 \le \sum_{k=1}^{n} v_k \tau_{e,k} - \min_{k}(\beta_k) \|\mathbf{v}\|_2^2.$$
 (1.83)

One then also says that  $v_k$  is the *collocated output* to the generalized force  $\tau_{e,k}$ . I.e., the pairing  $(\tau_{e,k}, v_k)$  describes an energy input into the system, such as corresponding currents and voltages, forces and velocities, or moments and angular velocities. In network theory, such pairings of current and voltage that form an energy input are also called a port. The generalization of the Hamiltonian equations (1.76) in combination with the port concept leads directly to the class of Port-Hamiltonian systems.

### 1.6.2 Port-Hamiltonian Systems

A finite-dimensional Port-Hamiltonian system can be written in the form

$$\frac{\mathrm{d}}{\mathrm{d}t}\mathbf{x} = (\mathbf{J}(\mathbf{x}) - \mathbf{S}(\mathbf{x})) \left(\frac{\partial V}{\partial \mathbf{x}}\right)^{\mathrm{T}} + \mathbf{G}_{u}(\mathbf{x})\mathbf{u}$$
(1.84)

with the state  $\mathbf{x} \in \mathcal{X} \subset \mathbb{R}^n$  and the input  $\mathbf{u} \in \mathcal{U} \subset \mathbb{R}^m$ . Here,  $V(\mathbf{x})$ ,  $V(\mathbf{0}) = 0$ , denotes a continuously differentiable positive definite storage function, and the entries of the matrices  $\mathbf{G}_u(\mathbf{x})$ ,  $\mathbf{J}(\mathbf{x}) = -\mathbf{J}^{\mathrm{T}}(\mathbf{x})$  and  $\mathbf{S}(\mathbf{x}) = \mathbf{S}^{\mathrm{T}}(\mathbf{x}) \geq \mathbf{0}$  are smooth functions in  $\mathbf{x}$ . Choose the output  $\mathbf{y} \in \mathcal{Y} \subset \mathbb{R}^m$  as the *collocated output* 

$$\mathbf{y} = \mathbf{G}_u^{\mathrm{T}}(\mathbf{x}) \left(\frac{\partial V}{\partial \mathbf{x}}\right)^{\mathrm{T}},\tag{1.85}$$

then we immediately see from the differential passivity inequality

$$\frac{\mathrm{d}}{\mathrm{d}t}V = \mathbf{y}^{\mathrm{T}}\mathbf{u} - \left(\frac{\partial V}{\partial \mathbf{x}}\right)\mathbf{S}(\mathbf{x})\left(\frac{\partial V}{\partial \mathbf{x}}\right)^{\mathrm{T}} \le \mathbf{y}^{\mathrm{T}}\mathbf{u},\tag{1.86}$$

that the system (1.84) is passive with the storage function  $V(\mathbf{x})$ . The representation in the form of (1.84) provides more than a simple determination of passivity - if the storage function  $V(\mathbf{x})$  corresponds to the total energy stored in the system, it offers a deeper insight into the internal energy flows of the system and its interaction with the environment. The skew-symmetric matrix  $\mathbf{J}(\mathbf{x})$  is connected to the energy flows within the system, the symmetric, positive semidefinite matrix  $\mathbf{S}(\mathbf{x})$  encompasses the behavior of the dissipative effects, and  $\mathbf{G}_u(\mathbf{x})$  describes the energy exchange of the system with the system environment through the system ports. If (1.84) contains no dissipative elements, i.e.,  $\mathbf{S}(\mathbf{x}) = \mathbf{0}$ , then the system is lossless with respect to the supply rate  $\mathbf{y}^T\mathbf{u}$ . Perfect actuator/sensor collocation has the advantage that a simple (state-dependent) feedback of the collocated output (1.85) of the form

$$\mathbf{u} = -\mathbf{K}(\mathbf{x})\mathbf{y} = -\mathbf{K}(\mathbf{x})\mathbf{G}_{u}^{\mathrm{T}}(\mathbf{x}) \left(\frac{\partial V}{\partial \mathbf{x}}\right)^{\mathrm{T}}, \qquad (1.87)$$

with the positive definite matrix  $\mathbf{K}(\mathbf{x}) > 0$  for all  $\mathbf{x} \in \mathcal{X}$  for stable plants preserves stability in the closed-loop system

$$\frac{\mathrm{d}}{\mathrm{d}t}V = -\left(\frac{\partial V}{\partial \mathbf{x}}\right) \left(\mathbf{S}(\mathbf{x}) + \mathbf{G}_u(\mathbf{x})\mathbf{K}(\mathbf{x})\mathbf{G}_u^{\mathrm{T}}(\mathbf{x})\right) \left(\frac{\partial V}{\partial \mathbf{x}}\right)^{\mathrm{T}} \le 0.$$
 (1.88)

In the literature, this type of feedback (1.87) in connection with Port-Hamiltonian systems is called *damping injection* or for general nonlinear systems with affine input as *Jurdjevic-Quinn feedback*.

Example 1.1 (Port-Hamiltonian representation of the solenoid valve (1.14)). To bring the mathematical model of the solenoid valve (1.14) into Port-Hamiltonian form (1.84), we introduce the new state variables  $\mathbf{x}^{\mathrm{T}} = [z, p = mv, \psi_L = L(z)i_L]$ . The energy stored in the solenoid valve according to (1.15) formulated in the new state

$$[z, p, \psi_L]$$

$$V = \frac{1}{2} \left( \frac{1}{L(z)} \psi_L^2 + \frac{1}{m} p^2 + cz^2 \right)$$
(1.89)

is used as the storage function in the following. With

$$\frac{\partial V}{\partial \mathbf{x}} = \left[ cz - \frac{1}{2} \frac{\partial L(z)}{\partial z} \frac{\psi_L^2}{L^2(z)} \quad \frac{p}{m} \quad \frac{\psi_L}{L(z)} \right] \tag{1.90}$$

and the system equations (1.14) in the transformed state

$$\frac{\mathrm{d}}{\mathrm{d}t}z = \frac{p}{m}$$

$$\frac{\mathrm{d}}{\mathrm{d}t}p = \left(\frac{1}{2}\frac{\partial L(z)}{\partial z}\frac{\psi_L^2}{L^2(z)} - cz - d\frac{p}{m} + F_{ext}\right)$$

$$\frac{\mathrm{d}}{\mathrm{d}t}\psi_L = U_0 - R\frac{\psi_L}{L(z)},$$
(1.91)

we directly obtain the Port-Hamiltonian representation (1.84)

$$\frac{\mathrm{d}}{\mathrm{d}t} \begin{bmatrix} z \\ p \\ \psi_L \end{bmatrix} = \left( \underbrace{\begin{bmatrix} 0 & 1 & 0 \\ -1 & 0 & 0 \\ 0 & 0 & 0 \end{bmatrix}}_{\mathbf{J}(\mathbf{x})} - \underbrace{\begin{bmatrix} 0 & 0 & 0 \\ 0 & d & 0 \\ 0 & 0 & R \end{bmatrix}}_{\mathbf{S}(\mathbf{x})} \right) \left( \frac{\partial V}{\partial \mathbf{x}} \right)^{\mathrm{T}} + \underbrace{\begin{bmatrix} 0 & 0 \\ 0 & 1 \\ 1 & 0 \end{bmatrix}}_{\mathbf{G}_{u}(\mathbf{x})} \underbrace{\begin{bmatrix} U_{0} \\ F_{ext} \end{bmatrix}}_{\mathbf{u}} . \tag{1.92}$$

The corresponding collocated output according to (1.85) is

$$\mathbf{y} = \mathbf{G}_{u}^{\mathrm{T}}(\mathbf{x}) \left(\frac{\partial V}{\partial \mathbf{x}}\right)^{\mathrm{T}} = \begin{bmatrix} \frac{\psi_{L}}{L(z)} \\ \frac{p}{m} \end{bmatrix} = \begin{bmatrix} i_{L} \\ v \end{bmatrix}. \tag{1.93}$$

*Exercise* 1.15. Represent the mathematical models of the beam with rolling ball and the crane with a swing arm from the lecture notes VO Nonlinear Dynamic Systems and Control [1.1] as Port-Hamiltonian systems.

*Exercise* 1.16. Represent the different DC machines from Section 1.7 of the lecture notes VO Regelungssysteme 2 [1.1] as Port-Hamiltonian systems.

# 1.7 Passivity-Based Controller Design

A controller design method directly related to the Port-Hamiltonian structure (1.84) is the so-called *IDA-PBC* (Interconnection and Damping Assignment Passivity-Based Control). To this end, the following theorem is formulated:

**Theorem 1.6** (IDA-PBC). Given is the nonlinear system

$$\frac{\mathrm{d}}{\mathrm{d}t}\mathbf{x} = \mathbf{f}(\mathbf{x}) + \mathbf{G}_u(\mathbf{x})\mathbf{u} \tag{1.94}$$

with the state  $\mathbf{x} \in \mathcal{X} \subset \mathbb{R}^n$  and the input  $\mathbf{u} \in \mathcal{U} \subset \mathbb{R}^m$  with m < n. It is assumed that the matrix  $\mathbf{G}_u(\mathbf{x})$  is column regular for all  $\mathbf{x} \in \mathcal{X}$ , i.e.,  $\operatorname{rang}(\mathbf{G}_u(\mathbf{x})) = m$ . Furthermore, let  $\mathbf{G}_u^{\perp}(\mathbf{x})$  denote the left annihilator of  $\mathbf{G}_u(\mathbf{x})$ , i.e.,  $\mathbf{G}_u^{\perp}(\mathbf{x})\mathbf{G}_u(\mathbf{x}) = \mathbf{0}$ , and  $V_d(\mathbf{x})$  be the storage function of the closed-loop system and have a strict minimum at the desired equilibrium  $\mathbf{x} = \mathbf{x}_d$ 

$$V_d(\mathbf{x}) > V_d(\mathbf{x}_d)$$
 for all  $\mathbf{x} \neq \mathbf{x}_d$ ,  $\left(\frac{\partial V_d}{\partial \mathbf{x}}\right)(\mathbf{x}_d) = \mathbf{0}$  and  $\left(\frac{\partial^2 V_d}{\partial \mathbf{x}^2}\right)(\mathbf{x}_d) > 0$ . (1.95)

Thus,  $V_d(\mathbf{x}) - V_d(\mathbf{x}_d)$  is positive definite and suitable as a Lyapunov function for the closed-loop system. Assume the matrices  $\mathbf{J}_d(\mathbf{x}) = -\mathbf{J}_d^{\mathrm{T}}(\mathbf{x})$ ,  $\mathbf{S}_d(\mathbf{x}) = \mathbf{S}_d^{\mathrm{T}}(\mathbf{x}) \geq 0$ , the left annihilator  $\mathbf{G}_u^{\perp}(\mathbf{x})$  and the storage function  $V_d(\mathbf{x})$  satisfy the condition (PBC matching equation)

$$\mathbf{G}_{u}^{\perp}(\mathbf{x})\mathbf{f}(\mathbf{x}) = \mathbf{G}_{u}^{\perp}(\mathbf{x})(\mathbf{J}_{d}(\mathbf{x}) - \mathbf{S}_{d}(\mathbf{x})) \left(\frac{\partial V_{d}}{\partial \mathbf{x}}\right)^{\mathrm{T}},\tag{1.96}$$

then with the state feedback

$$\mathbf{u} = \boldsymbol{\beta}(\mathbf{x}) = \left(\mathbf{G}_u^{\mathrm{T}}(\mathbf{x})\mathbf{G}_u(\mathbf{x})\right)^{-1}\mathbf{G}_u^{\mathrm{T}}(\mathbf{x})\left\{\left(\mathbf{J}_d(\mathbf{x}) - \mathbf{S}_d(\mathbf{x})\right)\left(\frac{\partial V_d}{\partial \mathbf{x}}\right)^{\mathrm{T}} - \mathbf{f}(\mathbf{x})\right\}$$
(1.97)

inserted into (1.94), a closed-loop system in Port-Hamiltonian form is obtained

$$\frac{\mathrm{d}}{\mathrm{d}t}\mathbf{x} = (\mathbf{J}_d(\mathbf{x}) - \mathbf{S}_d(\mathbf{x})) \left(\frac{\partial V_d}{\partial \mathbf{x}}\right)^{\mathrm{T}}$$
(1.98)

with the stable desired equilibrium  $\mathbf{x} = \mathbf{x}_d$ . If the set  $\{\mathbf{x}_d\}$  is the largest positive invariant set of

$$\left\{ \mathbf{x} \in \mathbb{R}^n \middle| \left( \frac{\partial V_d}{\partial \mathbf{x}} \right) \mathbf{S}_d(\mathbf{x}) \left( \frac{\partial V_d}{\partial \mathbf{x}} \right)^{\mathrm{T}} = 0 \right\}, \tag{1.99}$$

then  $\mathbf{x} = \mathbf{x}_d$  is asymptotically stable.

*Proof.* Setting the right-hand sides of (1.98) and (1.94) equal to (1.97)

$$\mathbf{f}(\mathbf{x}) + \mathbf{G}_u(\mathbf{x})\boldsymbol{\beta}(\mathbf{x}) = (\mathbf{J}_d(\mathbf{x}) - \mathbf{S}_d(\mathbf{x})) \left(\frac{\partial V_d}{\partial \mathbf{x}}\right)^{\mathrm{T}}$$
(1.100)

and multiplying from the left by  $\mathbf{G}_{u}^{\perp}(\mathbf{x})$ , we immediately obtain the PBC matching equation (1.96). The state feedback (1.97) follows directly from (1.100) by multiplying

from the left by the pseudoinverse  $(\mathbf{G}_u^{\mathrm{T}}(\mathbf{x})\mathbf{G}_u(\mathbf{x}))^{-1}\mathbf{G}_u^{\mathrm{T}}(\mathbf{x})$ . Note that the previously assumed column regularity of  $\mathbf{G}_u(\mathbf{x})$  guarantees the regularity of the pseudoinverse. The next step is to show that (1.94) with (1.97) actually corresponds to (1.98)

$$\Psi = \mathbf{f}(\mathbf{x}) + \mathbf{G}_{u}(\mathbf{x}) \left(\mathbf{G}_{u}^{\mathrm{T}}(\mathbf{x}) \mathbf{G}_{u}(\mathbf{x})\right)^{-1} \mathbf{G}_{u}^{\mathrm{T}}(\mathbf{x}) \left\{ (\mathbf{J}_{d}(\mathbf{x}) - \mathbf{S}_{d}(\mathbf{x})) \left(\frac{\partial V_{d}}{\partial \mathbf{x}}\right)^{\mathrm{T}} - \mathbf{f}(\mathbf{x}) \right\} - (\mathbf{J}_{d}(\mathbf{x}) - \mathbf{S}_{d}(\mathbf{x})) \left(\frac{\partial V_{d}}{\partial \mathbf{x}}\right)^{\mathrm{T}} = \mathbf{0} .$$
(1.101)

To do this, multiply (1.101) by the non-singular matrix

$$\mathbf{T}(\mathbf{x}) = \begin{bmatrix} \mathbf{G}_u^{\mathrm{T}}(\mathbf{x}) \\ \mathbf{G}_u^{\perp}(\mathbf{x}) \end{bmatrix}$$
 (1.102)

and due to the PBC matching condition (1.96), it follows  $\mathbf{T}(\mathbf{x})\Psi = \mathbf{0}$  and thus  $\Psi = \mathbf{0}$ .

The difficulty of this controller design method is obviously to solve the PBC matching equation (1.96), which represents a *system of partial differential equations*. To this end, it should be mentioned that

- the matrices  $\mathbf{J}_d(\mathbf{x}) = -\mathbf{J}_d^{\mathrm{T}}(\mathbf{x})$  and  $\mathbf{S}_d(\mathbf{x}) = \mathbf{S}_d^{\mathrm{T}}(\mathbf{x}) \geq 0$  are free to choose,
- the storage function of the closed -loop system  $V_d(\mathbf{x})$  apart from the condition (1.95) can also be chosen freely,
- and the left annihilator  $\mathbf{G}_{u}^{\perp}(\mathbf{x})$  can be multiplied from the left by any non-singular  $(n-m)\times(n-m)$  matrix  $\mathbf{\Lambda}(\mathbf{x})$ , i.e.,  $\tilde{\mathbf{G}}_{u}^{\perp}(\mathbf{x})=\mathbf{\Lambda}(\mathbf{x})\mathbf{G}_{u}^{\perp}(\mathbf{x})$ , without changing the PBC matching equation (1.96). The matrix  $\mathbf{\Lambda}(\mathbf{x})$  thus represents a further degree of freedom in the design.

In recent years, the following variants of the IDA-PBC design method have essentially prevailed:

- Non-Parametrized IDA-PBC: In this case, the structure of the interconnection in the form of the matrices  $\mathbf{J}_d(\mathbf{x}) = -\mathbf{J}_d^{\mathrm{T}}(\mathbf{x})$  and  $\mathbf{S}_d(\mathbf{x}) = \mathbf{S}_d^{\mathrm{T}}(\mathbf{x}) \geq 0$  is given. With known  $\mathbf{G}_u^{\perp}(\mathbf{x})$ , the PBC matching equation (1.96) results in a partial differential equation for the storage function  $V_d(\mathbf{x})$ . From the family of all solutions, those must then be extracted that satisfy the condition (1.95). In the literature, see for example [1.2], one can also find conditions for the existence of a solution to the underlying partial differential equation (1.96).
- Algebraic IDA-PBC: In this case, the storage function  $V_d(\mathbf{x})$  is fixed under the condition (1.95), and the PBC matching equation (1.96) degenerates to an algebraic equation for the determination of the matrices  $\mathbf{J}_d(\mathbf{x}) = -\mathbf{J}_d^{\mathrm{T}}(\mathbf{x})$  and  $\mathbf{S}_d(\mathbf{x}) = \mathbf{S}_d^{\mathrm{T}}(\mathbf{x}) \geq 0$ .

• Parametrized IDA-PBC: Here, the storage function  $V_d(\mathbf{x})$  is restricted to a certain class, for example, the desired potential energy only depends on the generalized position coordinates and the desired kinetic energy is a quadratic form in the generalized velocities. This special form of  $V_d(\mathbf{x})$  implies a new PBC matching equation with restrictions regarding the choice of  $\mathbf{J}_d(\mathbf{x}) = -\mathbf{J}_d^{\mathrm{T}}(\mathbf{x})$  and  $\mathbf{S}_d(\mathbf{x}) = \mathbf{S}_d^{\mathrm{T}}(\mathbf{x}) \geq 0$ .

Example 1.2. As an application example, consider a permanently excited synchronous machine in dq-representation

$$L_{d} \frac{\mathrm{d}}{\mathrm{d}t} i_{d} = -R_{s} i_{d} + \omega L_{q} i_{q} + u_{d}$$

$$L_{q} \frac{\mathrm{d}}{\mathrm{d}t} i_{q} = -R_{s} i_{q} - \omega (L_{d} i_{d} + \Phi) + u_{q}$$

$$J \frac{\mathrm{d}}{\mathrm{d}t} \omega = p((L_{d} - L_{q}) i_{d} i_{q} + \Phi i_{q}) - \tau_{l}$$

$$(1.103)$$

with the stator currents  $i_d$  and  $i_q$  as well as the rotor speed  $\omega$  as state variables, the stator voltages  $u_d$  and  $u_q$  as control variables, and the load torque  $\tau_l$ . Furthermore, J denotes the moment of inertia,  $R_s$  the stator winding resistance,  $L_d$  and  $L_q$  the stator inductances, p the number of pole pairs, and  $\Phi$  the flux of the permanent magnet in the rotor. It should be mentioned at this point that for the case of a uniform air gap, we have  $L_d = L_q = L$ , and the mathematical model (1.103) simplifies accordingly. Now choose the state variables  $\mathbf{x}^{\mathrm{T}} = [x_1, x_2, x_3] = [L_d i_d, L_q i_q, J\omega/p]$ , then (1.103) can be written in the form of a Port-Hamiltonian system

$$\frac{\mathrm{d}}{\mathrm{d}t}\mathbf{x} = (\mathbf{J}(\mathbf{x}) - \mathbf{S}) \left(\frac{\partial V}{\partial \mathbf{x}}\right)^{\mathrm{T}} + \mathbf{G}_{u}\mathbf{u} + \mathbf{g}_{d}\tau_{l}$$
(1.104)

with the energy function as the storage function

$$V(\mathbf{x}) = \frac{1}{2L_d}x_1^2 + \frac{1}{2L_q}x_2^2 + \frac{p}{2J}x_3^2$$
 (1.105)

and

$$\mathbf{J}(\mathbf{x}) = \begin{bmatrix} 0 & 0 & x_2 \\ 0 & 0 & -(x_1 + \Phi) \\ -x_2 & x_1 + \Phi & 0 \end{bmatrix}, \qquad \mathbf{S} = \begin{bmatrix} R_s & 0 & 0 \\ 0 & R_s & 0 \\ 0 & 0 & 0 \end{bmatrix}$$
(1.106)

as well as

$$\mathbf{G}_{u} = \begin{bmatrix} 1 & 0 \\ 0 & 1 \\ 0 & 0 \end{bmatrix}, \quad \mathbf{g}_{d} = \begin{bmatrix} 0 \\ 0 \\ -1/p \end{bmatrix}, \quad \text{and} \quad \mathbf{u} = \begin{bmatrix} u_{d} \\ u_{q} \end{bmatrix}. \tag{1.107}$$

Exercise 1.17. Show the validity of (1.104).

Now, using Non-Parametrized IDA-PBC, a state feedback according to Theorem 1.6 should be designed so that the stationary operating point

$$\mathbf{x}_{d}^{\mathrm{T}} = [0, x_{2,d}, x_{3,d}] \quad \text{with} \quad x_{2,d} = \frac{\bar{\tau}_{l} L_{q}}{\Phi p}$$
 (1.108)

for a constant torque  $\bar{\tau}_l$  and a desired speed  $\omega_d = x_{3,d}p/J$  is stabilized. The structure of the closed-loop system  $\mathbf{J}_d(\mathbf{x})$  and  $\mathbf{S}_d$  is now chosen according to a machine with uniform air gap, i.e., we have  $L_d = L_q = L$ .

*Exercise* 1.18. Show that for  $L_d = L_q = L$ , the matrices  $\mathbf{J}_d(\mathbf{x})$  and  $\mathbf{S}_d$  of the Port-Hamiltonian system associated with (1.103) have the following structure

$$\mathbf{J}_d(\mathbf{x}) = \begin{bmatrix} 0 & \frac{Lp}{J}x_3 & 0\\ -\frac{Lp}{J}x_3 & 0 & -\Phi\\ 0 & \Phi & 0 \end{bmatrix} \quad \text{and} \quad \mathbf{S}_d = \mathbf{S} \ . \tag{1.109}$$

The PBC matching equation (1.96) is then

$$(\mathbf{J}(\mathbf{x}) - \mathbf{S}) \left( \frac{\partial V}{\partial \mathbf{x}} \right)^{\mathrm{T}} + \mathbf{G}_{u} \boldsymbol{\beta}(\mathbf{x}) + \mathbf{g}_{d} \bar{\tau}_{l} = (\mathbf{J}_{d}(\mathbf{x}) - \mathbf{S}_{d}) \left( \frac{\partial V_{d}}{\partial \mathbf{x}} \right)^{\mathrm{T}}, \tag{1.110}$$

or with the left annihilator of  $\mathbf{G}_{u}$ 

$$\mathbf{G}_{u}^{\perp} = [0, 0, 1] \tag{1.111}$$

and the quantities  $V_a(\mathbf{x}) = V_d(\mathbf{x}) - V(\mathbf{x})$  and

$$\mathbf{J}_{a}(\mathbf{x}) = \mathbf{J}_{d}(\mathbf{x}) - \mathbf{J}(\mathbf{x}) = \begin{bmatrix} 0 & \frac{Lp}{J}x_{3} & -x_{2} \\ -\frac{Lp}{J}x_{3} & 0 & x_{1} \\ x_{2} & -x_{1} & 0 \end{bmatrix},$$
(1.112)

we obtain

$$\mathbf{G}_{u}^{\perp}(\mathbf{J}(\mathbf{x}) - \mathbf{S}) \left(\frac{\partial V}{\partial \mathbf{x}}\right)^{\mathrm{T}} + \mathbf{G}_{u}^{\perp} \mathbf{g}_{d} \bar{\tau}_{l} = \mathbf{G}_{u}^{\perp}(\mathbf{J}(\mathbf{x}) + \mathbf{J}_{a}(\mathbf{x}) - \mathbf{S}) \left(\left(\frac{\partial V_{a}}{\partial \mathbf{x}}\right)^{\mathrm{T}} + \left(\frac{\partial V}{\partial \mathbf{x}}\right)^{\mathrm{T}}\right)$$
(1.113)

or

$$-\mathbf{G}_{u}^{\perp}\mathbf{J}_{a}(\mathbf{x})\left(\frac{\partial V}{\partial \mathbf{x}}\right)^{\mathrm{T}} + \mathbf{G}_{u}^{\perp}\mathbf{g}_{d}\bar{\tau}_{l} = \mathbf{G}_{u}^{\perp}(\mathbf{J}_{d}(\mathbf{x}) - \mathbf{S})\left(\frac{\partial V_{a}}{\partial \mathbf{x}}\right)^{\mathrm{T}}.$$
 (1.114)

Evaluating (1.114) results in the following partial differential equation

$$-\frac{x_2 x_1}{L_d} + \frac{x_2 x_1}{L_q} - \frac{1}{p} \bar{\tau}_l = \Phi \frac{\partial V_a}{\partial x_2} , \qquad (1.115)$$

whose general solution can be written as

$$V_a(x_1, x_2, x_3) = \alpha_1 \left( \frac{1}{2} x_2^2 x_1 \left( \frac{L_d - L_q}{L_d L_q \Phi} \right) - \frac{x_2}{\Phi p} \bar{\tau}_l \right) + \psi(x_1, x_3)$$
 (1.116)

with the positive parameter  $\alpha_1$  and a function  $\psi(x_1, x_3)$  still to be chosen. Thus, the storage function of the closed-loop system  $V_d = V + V_a$  has the following structure

$$V_d = \frac{1}{2L_d}x_1^2 + \frac{1}{2L_q}x_2^2 + \frac{p}{2J}x_3^2 + \frac{1}{2}\alpha_1 x_2^2 x_1 \left(\frac{L_d - L_q}{L_d L_q \Phi}\right) - \alpha_1 \frac{x_2}{\Phi p} \bar{\tau}_l + \psi(x_1, x_3) . \quad (1.117)$$

The task is to determine the function  $\psi(x_1, x_3)$  such that the conditions (1.95) are fulfilled. It can be easily verified that the ansatz

$$\psi(x_1, x_3) = -\frac{1}{2}\alpha_1 \left(\frac{L_d - L_q}{L_d L_q \Phi}\right) x_1 x_{2,d}^2 + \frac{\alpha_2}{2} x_1^2 - \frac{p}{2J} x_3^2 + \frac{\alpha_3}{2} (x_3 - x_{3,d})^2 - \frac{1}{2L_q} x_{2,d}^2$$
(1.118)

with the positive design parameters  $\alpha_1$ ,  $\alpha_2$ , and  $\alpha_3$  satisfies these conditions. To do this, calculate for

$$V_d = \left(\frac{1}{2L_d} + \frac{\alpha_2}{2}\right) x_1^2 + \left(\frac{1}{2L_q} + \frac{\alpha_1}{2} x_1 \left(\frac{L_d - L_q}{L_d L_q \Phi}\right)\right) \left(x_2^2 - x_{2,d}^2\right) - \frac{\alpha_1}{L_q} x_2 x_{2,d} + \frac{\alpha_3}{2} (x_3 - x_{3,d})^2$$

$$(1.119)$$

first the gradient and evaluate it at the point  $\mathbf{x} = \mathbf{x}_d$  (see (1.108))

$$\left(\frac{\partial}{\partial \mathbf{x}} V_d\right)^{\mathrm{T}}(\mathbf{x}_d) = \begin{bmatrix} \left(\frac{1}{L_d} + \alpha_2\right) x_{1,d} \\ \left(\frac{1}{L_q} + \alpha_1 x_{1,d} \left(\frac{L_d - L_q}{L_d L_q \Phi}\right)\right) x_{2,d} - \frac{\alpha_1}{L_q} x_{2,d} \\ 0 \end{bmatrix}.$$
(1.120)

Obviously for  $\alpha_1 = 1$ , the requirement  $\left(\frac{\partial}{\partial \mathbf{x}} V_d\right)^{\mathrm{T}}(\mathbf{x}_d) = \mathbf{0}$  is fulfilled. To ensure that  $\mathbf{x}_d$  is a strict local minimum of  $V_d$ , we must further ensure that

$$\left(\frac{\partial^2}{\partial \mathbf{x}^2} V_d\right) (\mathbf{x}_d) = \begin{bmatrix} \frac{1}{L_d} + \alpha_2 & \left(\frac{L_d - L_q}{L_d L_q \Phi}\right) x_{2,d} & 0\\ \left(\frac{L_d - L_q}{L_d L_q \Phi}\right) x_{2,d} & \frac{1}{L_q} & 0\\ 0 & 0 & \alpha_3 \end{bmatrix}$$
(1.121)

is positive definite, which can be guaranteed by a suitable choice of the parameters  $\alpha_2 > 0$  and  $\alpha_3 > 0$  with

$$\frac{1}{L_d} + \alpha_2 > 0 \quad \text{und} \quad \left(\frac{1}{L_d} + \alpha_2\right) \frac{1}{L_q} - \left(\frac{L_d - L_q}{L_d L_q \Phi}\right)^2 x_{2,d}^2 > 0.$$
(1.122)

The state feedback is then calculated according to (1.97) in the form

$$\boldsymbol{\beta}(\mathbf{x}) = \begin{bmatrix} 1 & 0 & 0 \\ 0 & 1 & 0 \end{bmatrix} \left\{ (\mathbf{J}_d(\mathbf{x}) - \mathbf{S}_d) \left( \frac{\partial V_d}{\partial \mathbf{x}} \right)^{\mathrm{T}} - (\mathbf{J}(\mathbf{x}) - \mathbf{S}) \left( \frac{\partial V}{\partial \mathbf{x}} \right)^{\mathrm{T}} - \mathbf{g}_d \Phi p x_{2,d} \right\}.$$
(1.123)

Exercise 1.19. Determine the explicit expressions of the state control law (1.123).

1.8 References Page 25

### 1.8 References

[1.1] A. Kugi, Skriptum zur VO Regelungssysteme 2 (SS 2019), Institut für Automatisierungs- und Regelungstechnik, TU Wien, 2019. [Online]. Available: https://www.acin.tuwien.ac.at/master/regelungssysteme-2/.

- [1.2] P. Tabuada and G. Pappas, "From Nonlinear to Hamiltonian via Feedback," *IEEE Transactions on Automatic Control*, vol. 48, no. 8, pp. 1439–1442, 2003.
- [1.3] O. Föllinger, Nichtlineare Regelung I + II. München: Oldenbourg, 1993.
- [1.4] H. K. Khalil, Nonlinear Systems (3rd Edition). New Jersey: Prentice Hall, 2002.
- [1.5] A. Kugi, Non-linear Control Based on Physical Models (Lecture Notes in Control and Information Sciences 260). London: Springer, 2001.
- [1.6] A. Kugi and K. Schlacher, "Analyse und Synthese nichtlinearer dissipativer Systeme: Ein Überblick (Teil 1)," at Automatisierungstechnik, vol. 50, pp. 63–69, 2002.
- [1.7] A. Kugi and K. Schlacher, "Analyse und Synthese nichtlinearer dissipativer Systeme: Ein Überblick (Teil 2)," at Automatisierungstechnik, vol. 50, pp. 103–111, 2002.
- [1.8] R. Lozano, B. Brogliato, O. Egeland, and B. Maschke, *Dissipative Systems Analysis and Control*. London: Springer, 2000.
- [1.9] R. Ortega and E. García-Canseco, "Interconnection and Damping Assignment Pasivity-Based Control: A Survey," *European Journal of Control*, vol. 10, pp. 432–450, 2004.
- [1.10] R. Ortega, A. van der Schaft, F. Castaños, and A. Astolfi, "Control by Interconnection and Standard Passivity-Based Control of Port-Hamiltonian Systems," *IEEE Transactions on Automatic Control*, vol. 53, no. 11, pp. 2527–2542, 2008.
- [1.11] V. Petrović, R. Ortega, and A. Stanković, "Interconnection and Damping Assignment Approach to Control of PM Synchronous Motors," *IEEE Transactions on Control Systems Technology*, vol. 9, no. 6, pp. 811–820, 2001.
- [1.12] R. Sepulchre, M. Janković, and P. Kokotović, *Constructive Nonlinear Control*. London: Springer, 1997.
- [1.13] E. Slotine and W. Li, Applied Nonlinear Control. New Jersey: Prentice Hall, 1991.
- [1.14] M. Vidyasagar, Nonlinear Systems Analysis. New Jersey: Prentice Hall, 1993.

# 2 Iterative learning control

A large number of physical or industrial processes operate in an repetitive fashion, whereby the same task is performed over and over again under identical or at least very similar conditions. *Iterative learning control* (ILC) is based on the notion that the performance of such repetitive processes can be improved by learning from previous trials (i.e., iterations). Typical application examples include various robotic pick-and-place tasks, switched operation of electronic or optical systems or batched manifacturing processes.

Learning on observed information from previous trials is a very general idea and holds true for many every-day activities. For example, a basketball player throwing a ball repeatedly towards the hoop from a fixed position can improve his or her success rate over time. By observing the trajectories of the ball, the player obtains information on how to subsequently modify the throwing motion such that the future outcome improves. Iterative learning strategies can thus be seen as an adaptive open-loop control scheme that refines its input signals during operation through repetition and learning. This way, iterative learning strategies achieve high control performance in the presence of large uncertainty - either due to any inevitable model-plant mismatch or under the effect of external disturbances - as long as its effect is (almost) identical in each trial. Conversely, a non-learning controller is not able to leverage this additional information and thus reproduces the same residual control error in each subsequent iteration.

While learning can be applied to a large variety of problems, ILC specifically considers tracking problems, i.e., a system **G** is operated in a repetitive fashion whereby the input  $\mathbf{u}_{j}(t) \in \mathcal{U}$  during the j-th iteration yields the corresponding output  $\mathbf{y}_{j}(t) \in \mathcal{Y}$  as

$$\mathbf{y}_{i}(t) = \mathbf{G}[\mathbf{x}_{i}(0), \mathbf{u}_{i}(t)]. \tag{2.1}$$

Within such a setting, ILC methods typically assume that:

- (i.) every iteration ends within an identical time interval  $t \in [0, t_f]$ ,
- (ii.) every iteration starts from an (almost) identical initial state  $\mathbf{x}_i(0) \approx \mathbf{x}(0)$ ,
- (iii.) there exists a unique input  $\mathbf{u}_d(t)$  that yields the desired output  $\mathbf{y}_d(t)$ .

The main goal is now to design an operator  $\Psi : \mathcal{U} \times \mathcal{Y} \to \mathcal{U}$  that produces an updated input

$$\mathbf{u}_{i+1}(t) = \mathbf{\Psi}(\mathbf{u}_i(t), \mathbf{e}_i(t)) \tag{2.2}$$

based on the previous input and the resulting tracking error  $\mathbf{e}_j(t) = \mathbf{y}_d(t) - \mathbf{y}_j(t)$  such that the output sequence asymptotically converges to the desired output  $\mathbf{y}_d(t)$ , i.e.,

$$\lim_{j \to \infty} \mathbf{G}[\mathbf{x}(0), \mathbf{u}_j(t)] = \mathbf{y}_d(t). \tag{2.3}$$

This iterative learning process is illustrated in Fig. 2.1. In some sense, ILC can be seen as a method to increase the robustness of feedforward control against model uncertainties and repetitive disturbances by determining it online through a fixed-point iteration (2.2), whose properties depend on the chosen operator  $\Psi$ . For simplicity, we will restrict ourselves to linear operators  $\Psi$ , wherefore the learning law (2.2) can be written as

$$\mathbf{u}_{j+1}(t) = \mathbf{L}_u \mathbf{u}_j(t) + \mathbf{L}_e \mathbf{e}_j(t) = \mathbf{Q}(\mathbf{u}_j(t) + \mathbf{L}\mathbf{e}_j(t))$$
(2.4)

with the linear operators  $\mathbf{L}_u$ ,  $\mathbf{L}_e$ ,  $\mathbf{Q}$ , and  $\mathbf{L}$ , respectively. Correspondingly, we will mainly restrict ourselves to linear, time-invariant systems of the form

$$\dot{\mathbf{x}}_j(t) = \mathbf{A}\mathbf{x}_j(t) + \mathbf{B}\mathbf{u}_j(t) \tag{2.5}$$

$$\mathbf{y}_j(t) = \mathbf{C}\mathbf{x}_j(t) + \mathbf{D}\mathbf{u}_j(t) \tag{2.6}$$

with the state vector  $\mathbf{x}_j^{\mathrm{T}}(t) \in \mathbb{R}^n$ , the input vector  $\mathbf{u}_j^{\mathrm{T}}(t) \in \mathbb{R}^l$  and the output vector  $\mathbf{y}_j^{\mathrm{T}}(t) \in \mathbb{R}^m$ .

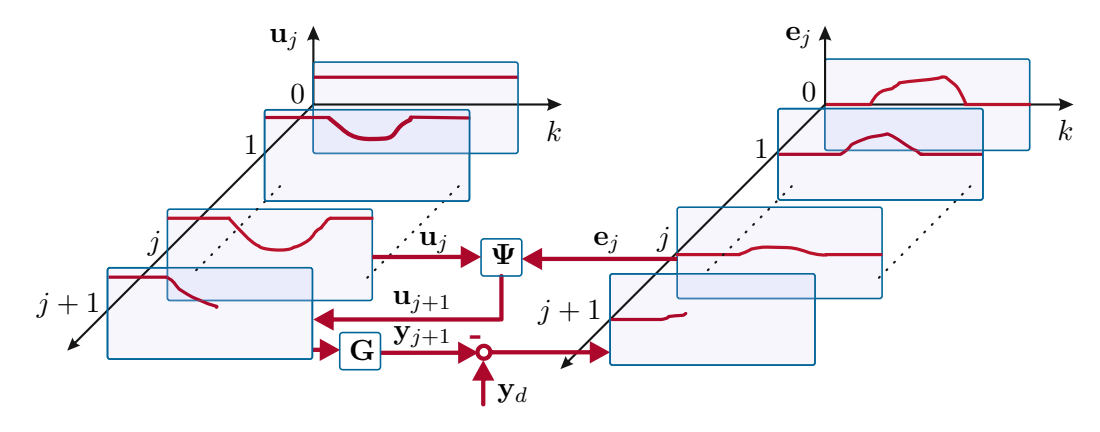


Figure 2.1: Graphical illustration of iterative learning control (ILC).

There are a number of different concepts in control theory that aim to include some element of learning. Most notably, adaptive control is using information from the past to increase the performance of the closed-loop system by continuously modifying model or (feedback) control parameters. All uncertainty is thus represented in a parametric form. Conversely, ILC modifies the feedforward inputs applied to the system and is thus not limited to parametric uncertainties. However, this entails that the learned input signal is specific to the desired output  $\mathbf{y}_d(t)$ . One property that is used to distinguish ILC [2.1–2.5] from other learning concepts [2.6] is the so-called identical initialization condition, i.e., that every iteration starts from the exact same initial state  $\mathbf{x}_j(0) = \mathbf{x}(0)$ . In a more relaxed formulation,  $\mathbf{x}_j(0)$  may be a stochastic quantity, but at least is independent of previous iterations. Repetitive control on the other hand assumes that the initial state of the current iteration is given by the terminal state of the previous one such that the sequence of all iterations can be seen as a continuously operated system.

# 2.1 Fixed-point iterations

Calculating zeros of a function

$$\gamma(\mathbf{z}) = \mathbf{0} \tag{2.7}$$

with  $\gamma(\mathbf{z}): \mathbb{R}^N \to \mathbb{R}^N$  and  $\mathbf{z}^T = \begin{bmatrix} z_1 & \dots & z_N \end{bmatrix}$  can always be recast as a fixed-point problem

$$\psi(\mathbf{z}) = \mathbf{z}.\tag{2.8}$$

A fixed-point iteration is a sequence  $\mathbf{z}_0, \mathbf{z}_1, \dots$  given by

$$\mathbf{z}_{j+1} = \psi(\mathbf{z}_j) , \quad j = 0, 1, 2, \dots$$
 (2.9)

that converges to a solution  $\mathbf{z}_{\infty}$  of (2.8) depending on the chosen function  $\psi$ . Note that there is no unique fixed-point formulation for a given zero-point problem, i.e., the choices

- $\psi(\mathbf{z}) = \mathbf{z} \gamma(\mathbf{z})$
- $\psi(\mathbf{z}) = \mathbf{z} + 2\gamma(\mathbf{z})$
- $\psi(\mathbf{z}) = \mathbf{z} \left(\frac{\partial}{\partial \mathbf{z}} \boldsymbol{\gamma}\right)^{-1}(\mathbf{z}) \boldsymbol{\gamma}(\mathbf{z})$

are equally valid. However, the choice of  $\psi$  crucially determines the convergence properties of the fixed-point iteration. Therefore, we define:

### **Definition 2.1** (Convergence). The iteration (2.9) is

- locally convergent (LC) to  $\mathbf{z}_{\infty}$  if there exists a  $\delta > 0$  such that the iteration (2.9) exists and converges to  $\mathbf{z}_{\infty}$  for all starting points  $\|\mathbf{z}_0 \mathbf{z}_{\infty}\| < \delta$ ,
- globally convergent (GC) if the iteration (2.9) converges to  $\mathbf{z}_{\infty}$  for all  $\mathbf{z}_{0}$ .

### **Definition 2.2** (Stability). A fixed-point $\mathbf{z}_{\infty}$ is

- stable (S) (in a Lyapunov sense), if for every  $\varepsilon > 0$  there exists a  $\delta > 0$  such that if  $\|\mathbf{z}_0 \mathbf{z}_\infty\| < \delta$ , the sequence  $\{\mathbf{z}_j\}$  exists and  $\|\mathbf{z}_j \mathbf{z}_\infty\| < \varepsilon$  for all  $j \geq 1$ ,
- attractive (A), if there exists a  $\delta > 0$  such that  $\|\mathbf{z}_0 \mathbf{z}_{\infty}\| < \delta$  implies that  $\{\mathbf{z}_j\}$  exists and  $\lim_{j\to\infty} \mathbf{z}_j = \mathbf{z}_{\infty}$ ,
- globally attractive (GA) if  $\delta = \infty$  above,
- asymptotically stable (AS), if stable and attractive and globally asymptotically stable (GAS), if stable and globally attractive.

Attractivity and convergence are equivalent concepts, whereby the following relations [2.7] hold true

$$GAS \Longrightarrow GA \Longleftrightarrow GC \Longrightarrow A \Longleftarrow AS$$
. (2.10)

In the following we will consider the special case of linear fixed-point iterations

$$\mathbf{z}_{i+1} = \Psi \mathbf{z}_i , \quad j = 0, 1, 2, \dots$$
 (2.11)

**Definition 2.3** (Stability and asymptotic stability of linear fixed-point iterations). A linear iteration (2.11) is stable, if

$$\sup_{j>1} \|\mathbf{\Psi}^j\| < \infty , \qquad (2.12)$$

and asymptotically stable if

$$\lim_{j \to \infty} \|\mathbf{\Psi}^j\| = 0 \ . \tag{2.13}$$

**Definition 2.4** (Spectral radius). The spectrum of a matrix  $\Gamma$  denotes the set of all its eigenvalues, i.e.,

$$\sigma(\mathbf{\Gamma}) = \{ \lambda \in \mathbb{C} \mid \det(\lambda \mathbf{I} - \mathbf{\Gamma}) = 0 \}$$
 (2.14)

and

$$\rho(\Gamma) = \max_{\lambda \in \sigma(\Gamma)} |\lambda| \tag{2.15}$$

denotes the spectral radius of  $\Gamma$ .

**Theorem 2.1.** A linear iteration (2.11) is stable iff  $\rho(\Psi) \leq 1$  and all eigenvalues at 1 are distinct eigenvalues, i.e., their algebraic multiplicity equals 1. The iteration is further asymptotically stable iff  $\rho(\Psi) < 1$ .

**Definition 2.5** (BIBO stability). A linear iteration

$$\mathbf{z}_{j+1} = \mathbf{\Psi} \mathbf{z}_j + \mathbf{\Lambda} \mathbf{v}_j , \quad \mathbf{z}_0 = \mathbf{0}$$
 (2.16)

is called bounded-input-bounded-output (BIBO) stable if every bounded input sequence  $\{\mathbf{v}_j\}$  results in a bounded output sequence  $\{\mathbf{z}_j\}$ .

**Theorem 2.2.** A linear iteration  $\mathbf{z}_{j+1} = \mathbf{\Psi}\mathbf{z}_j + \mathbf{\Lambda}\mathbf{v}_j$ ,  $\mathbf{z}_0 = \mathbf{0}$  is BIBO stable iff  $\rho(\mathbf{\Psi}) < 1$ .

**Lemma 2.1.** For a bounded sequence  $\{\mathbf{z}_i\}$  and  $\varepsilon > 0 \in \mathbb{R}$  with

$$\|\mathbf{z}_{j+1}\| \le \rho \|\mathbf{z}_j\| + \varepsilon$$
,  $0 \le \rho < 1$  (2.17)

it follows that

$$\limsup_{j \to \infty} \|\mathbf{z}_j\| \le \frac{1}{1 - \rho} \varepsilon . \tag{2.18}$$

*Proof.* Iterative application of the iteration (2.17) yields

$$\|\mathbf{z}_1\| \le \rho \|\mathbf{z}_0\| + \varepsilon$$

$$\|\mathbf{z}_2\| \le \rho^2 \|\mathbf{z}_0\| + (1+\rho)\varepsilon$$

$$\vdots$$

$$\|\mathbf{z}_{j}\| \le \rho^{j} \|\mathbf{z}_{0}\| + \sum_{j=0}^{j-1} \rho^{j} \varepsilon = \rho^{j} \|\mathbf{z}_{0}\| + \frac{1-\rho^{j}}{1-\rho} \varepsilon.$$
 (2.19)

Since 
$$0 \le \rho < 1$$
, one directly obtains (2.18) for  $j \to \infty$ .

While asymptotic stability ensures that an iteration (2.11) eventually converges, this is not necessarily happening in a monotonic way. Since the notion of iterative learning somewhat suggests that one is successively progressing towards a desired solution, i.e., that the control performance improves with every iteration, monotonicity is an important property of ILC algorithms.

**Definition 2.6** (Largest singular value). The largest singular value of a matrix  $\Psi$  is given by

$$\bar{\sigma}(\mathbf{\Psi}) = \sqrt{\rho(\mathbf{\Psi}^{\mathrm{T}}\mathbf{\Psi})} \ . \tag{2.20}$$

Our main interest in the largest singular value of a matrix stems from the fact that it is the induced norm of a matrix mapping two spaces equiped with the Euclidean norm  $||z|| = \sqrt{\mathbf{z}^T}\mathbf{z}$ , i.e.,

$$\|\mathbf{\Psi}\mathbf{z}_i\| \le \|\mathbf{\Psi}\|_{i,2} \|\mathbf{z}_i\| = \bar{\sigma}(\mathbf{\Psi}) \|\mathbf{z}_i\| . \tag{2.21}$$

The largest singular value can thus be seen as an upper bound of the gain or amplification of the mapping given by the matrix  $\Psi$ .

**Theorem 2.3** (Monotone convergence of linear iterations). A linear iteration  $\mathbf{z}_{j+1} = \Psi \mathbf{z}_{j}$  converges monotonically towards  $\mathbf{0}$  in the  $l_{2}$ -norm, i.e., it holds true that

$$\|\mathbf{z}_{j+1}\| \le \beta \|\mathbf{z}_j\| \quad and \ thus \quad \|\mathbf{z}_{j+1}\| \le \beta^j \|\mathbf{z}_0\| \tag{2.22}$$

for  $0 \le \beta < 1$ , if

$$\bar{\sigma}(\mathbf{\Psi}) < 1 . \tag{2.23}$$

Note that since  $\rho(\Psi) \leq \bar{\sigma}(\Psi)$ , monotonic convergence unsurprisingly implies convergence.

# 2.2 Signals, systems, and the frequency domain

Integral transforms are essential tools to analyze temporal signals and their interaction with dynamical systems. Here, we consider a signal as a real-valued (measureable) function that maps the real numbers  $\mathbb{R}$  to  $\mathbb{R}^n$ . The set of all signals

$$S = \{ \mathbf{f} : \mathbb{R} \to \mathbb{R}^n \} \tag{2.24}$$

can intuitively be conceived as a set that contains all signals that can possibly occur in an engineering system - and many more. Since the sum of two signals  $\mathbf{f}$  and  $\mathbf{g}$  and the product of a signal with a scalar are again contained in this set, signals form a natural linear vector space.

**Definition 2.7.** A linear vector space over a field  $\mathbb{K}$  is a set  $\mathcal{S}$  with a binary operation  $+: \mathcal{S} \times \mathcal{S} \to \mathcal{S}$  (addition) and a binary operation  $\cdot: \mathbb{K} \times \mathcal{S} \to \mathcal{S}$  (multiplication) that fulfils

- 1. The set S and the operation + are a commutative group.
- 2. Multiplication with scalars  $a, b \in \mathbb{K}$  for  $\mathbf{f}, \mathbf{g} \in \mathcal{S}$  satisfies
  - $a(\mathbf{f} + \mathbf{g}) = a\mathbf{f} + a\mathbf{g}$
  - $(a+b)\mathbf{f} = a\mathbf{f} + b\mathbf{f}$
  - $(ab)\mathbf{f} = a(b\mathbf{f})$
  - $0\mathbf{f} = \mathbf{0} \text{ and } 1\mathbf{f} = \mathbf{f}.$

To measure the size of a signal, one typically equips vector spaces with a suitable norm.

**Definition 2.8.** A normed linear vector space S is a linear vector space equipped with real-valued function  $\|\cdot\|_p: S \to \mathbb{R}$  that adheres to the following properties:

- 1.  $\|\mathbf{f}\|_{p} \geq 0$
- 2.  $\|\mathbf{f}\|_{p} = 0 \iff \mathbf{f} = 0$
- 3.  $||a\mathbf{f}||_p = |a| ||\mathbf{f}||_p$
- 4.  $\|\mathbf{f} + \mathbf{g}\|_p \le \|\mathbf{f}\|_p + \|\mathbf{g}\|_p$

Note that a vector space can be equipped with different norms. The resulting normed vector spaces are different and may contain different elements.

We will now introduce typical signal spaces that we will require to analyze ILC algorithms. Since we consider signals with values in some  $\mathbb{R}^n$ , this implicitly requires a notion of size in this underlying vector space, for which we simply use the Euclidean norm. One of the most intuitive candidates for an ILC setting is the finite-horizon 2-norm defined by

$$\|\mathbf{f}\|_{2,[0,t_f]} = \left\{ \int_0^{t_f} \|\mathbf{f}(t)\| \, \mathrm{d}t \right\}^{\frac{1}{2}} = \left\{ \int_0^{t_f} \mathbf{f}(t)^{\mathrm{T}} \mathbf{f}(t) \, \mathrm{d}t \right\}^{\frac{1}{2}}.$$
 (2.25)

The set of signals for which this norm is finite is known as the finite-horizon Lebesque 2-space

$$\mathcal{L}_2([0, t_f]; \mathbb{R}^n) = \left\{ \mathbf{f} \in \mathcal{S} : \|\mathbf{f}\|_{2, [0, t_f]} < \infty \right\}.$$
 (2.26)

For simplicity, we will simply write  $\mathcal{L}_2([0,t_f])$  in cases where the dimension of the vectorvalued signals is not important. Any signal that is continuous on  $[0,t_f]$  is bounded and thus contained in  $\mathcal{L}_2([0,t_f])$  but signals like  $\frac{1}{|2t-t_f|}$  are not. In order to address stability issues or to apply frequency-domain methods, one must consider signals over infinite time intervals. Extending the considered horizon to infinity on both sides yields the usual infinite-horizon Lebesque 2-space

$$\mathcal{L}_2(\mathbb{R}) = \{ \mathbf{f} \in \mathcal{S} : ||\mathbf{f}||_2 < \infty \}$$
 (2.27)

with the corresponding norm

$$\|\mathbf{f}\|_{2} = \left[ \int_{-\infty}^{\infty} \|\mathbf{f}(t)\| \, \mathrm{d}t \right]^{\frac{1}{2}}.$$
 (2.28)

The spaces  $\mathcal{L}_2([0,\infty))$  and  $\mathcal{L}_2((-\infty,0])$  can be defined analogously.

For convenience, we will restrict ourselves to *Hilbert spaces*, i.e., *complete* spaces whose norm is generated by an *inner product*  $\|\mathbf{f}\|_2 = \sqrt{\langle \mathbf{f}, \mathbf{f} \rangle}$ .

**Definition 2.9** (Inner product). A mapping  $S \times S \to \mathbb{K}$  that assigns a scalar to each two elements of a vector space is called an *inner product* if the conditions

- 1.  $\langle \mathbf{f} + \mathbf{g}, \mathbf{h} \rangle = \langle \mathbf{f}, \mathbf{h} \rangle + \langle \mathbf{g}, \mathbf{h} \rangle$
- 2.  $\langle \mathbf{f}, \mathbf{g} \rangle = \langle \mathbf{g}, \mathbf{f} \rangle^*$
- 3.  $\langle a\mathbf{f}, \mathbf{g} \rangle = a \langle \mathbf{f}, \mathbf{g} \rangle$
- 4.  $\langle \mathbf{f}, \mathbf{f} \rangle > 0$  and  $\langle \mathbf{f}, \mathbf{f} \rangle = 0 \iff \mathbf{f} = 0$

hold true for  $\mathbf{f}, \mathbf{g}, \mathbf{h} \in \mathcal{S}$  and  $a \in \mathbb{K}$ .

The space  $\mathcal{L}_2(\mathbb{R})$  is a Hilbert space with inner product defined by

$$\langle \mathbf{f}, \mathbf{g} \rangle = \int_{-\infty}^{\infty} \mathbf{g}(t)^{\mathrm{T}} \mathbf{f}(t) \, \mathrm{d}t.$$
 (2.29)

Two signals  $\mathbf{f}$  and  $\mathbf{g}$  are called orthogonal if  $\langle \mathbf{f}, \mathbf{g} \rangle = 0$  analogous to orthogonality in  $\mathbb{R}^n$ . The spaces  $\mathcal{L}_2([0,\infty))$ ,  $\mathcal{L}_2((-\infty,0])$ , and  $\mathcal{L}_2([0,t_f])$  are all Hilbert spaces in their own right, with the inner product integral taken over the appropriate time interval, e.g., for  $\mathcal{L}_2([0,t_f])$  we have

$$\langle \mathbf{f}, \mathbf{g} \rangle_{[0, t_f]} = \int_0^{t_f} \mathbf{g}(t)^{\mathrm{T}} \mathbf{f}(t) \, \mathrm{d}t.$$
 (2.30)

### The Fourier transform

The Fourier transform is a unique mapping of certain (real-valued) functions of time to complex-valued functions of a single real variable  $\omega$  using

$$\hat{\mathbf{f}}(j\omega) = \mathcal{F}\{\mathbf{f}\} = \int_{-\infty}^{\infty} \mathbf{f}(t) e^{-j\omega t} dt.$$
 (2.31)

Note that the Fourier transform in (2.31) is performed for each component individually and a vector-valued signal thus simply yields a vector of all transformed components. To ensure that such a function  $\hat{\mathbf{f}}(j\omega)$  exists and is reasonable well behaved, classical Fourier analysis assumes that each component of  $\mathbf{f}(t)$  is absolutely integrable over the real line

$$\int_{-\infty}^{\infty} |f_i(t)| \, \mathrm{d}t < \infty, \tag{2.32}$$

i.e., each component is a  $\mathcal{L}_1(-\infty,\infty)$  function. With some mathematical effort, the Fourier transform can be extended to  $\mathcal{L}_2(\mathbb{R})$  (and functions beyond that such as the Dirac delta function). To motivate this, one can introduce the inner product of the transformed signals

$$\langle \hat{\mathbf{f}}, \hat{\mathbf{g}} \rangle = \frac{1}{2\pi} \int_{-\infty}^{\infty} \hat{\mathbf{g}}(j\omega)^H \hat{\mathbf{f}}(j\omega) d\omega,$$
 (2.33)

which again introduces an Lebesque 2-space  $\mathcal{L}_2(\mathbb{R})$  in the frequency domain. Here,  $(\cdot)^H$  denotes the conjugate transpose or Hermitian transpose.

**Theorem 2.4** (Parseval's theorem). For 
$$\mathbf{f}, \mathbf{g} \in \mathcal{L}_2(\mathbb{R})$$
 and  $\hat{\mathbf{f}}(j\omega) = \mathcal{F}\{\mathbf{f}\}, \hat{\mathbf{g}}(j\omega) = \mathcal{F}\{\mathbf{g}\} \in \mathcal{L}_2(\mathbb{R})$  it follows that

$$\langle \mathbf{f}, \mathbf{g} \rangle = \langle \hat{\mathbf{f}}, \hat{\mathbf{g}} \rangle \tag{2.34}$$

and thus

$$\|\mathbf{f}\|_2 = \|\hat{\mathbf{f}}\|_2. \tag{2.35}$$

The Fourier transform is thus a mapping between two Lebesque 2-spaces that preserves the inner product and the norm, i.e., a Hilbert space *isomorphism*. Finally, the inverse transform is given by

$$\mathbf{f}(t) = \mathcal{F}^{-1}\{\hat{\mathbf{f}}\} = \frac{1}{2\pi} \int_{-\infty}^{\infty} \hat{\mathbf{f}}(j\omega) \,\mathrm{e}^{j\omega t} \,\mathrm{d}\omega. \tag{2.36}$$

### The bilateral Laplace transform

For reasons that are quite obvious to a control engineer, one is interested to extend the Fourier transform from the imaginary axis  $j\omega$  to the complex plane  $s = \sigma + j\omega$ , which directly yields the bilateral Laplace transform

$$\hat{\mathbf{f}}(s) = \mathcal{B}\{\mathbf{f}\} = \int_{-\infty}^{\infty} \mathbf{f}(t) e^{-st} dt$$
 (2.37)

that is equivalent to the Fourier transform for  $\sigma = 0$ . In general, the Laplace transform will not converge for arbitrary values of s. From

$$\hat{\mathbf{f}}(\sigma + j\omega) = \int_{-\infty}^{\infty} \mathbf{f}(t) e^{-\sigma t} e^{-j\omega t} dt$$
 (2.38)

we see that the region of convergence (ROC) of the Laplace transform is directly linked to the convergence of  $\mathbf{f}(t)e^{-\sigma t}$ .

**Theorem 2.5.** The ROC of a signal has the following properties:

- 1. The ROC consists of strips parallel to the  $j\omega$ -axis in the s-plane.
- 2. If  $\mathbf{f}(t)$  is of finite duration and is absolutely integrable, then the ROC is the entre s-plane.
- 3. If  $\mathbf{f}(t)$  is right-sided (i.e.,  $\mathbf{f}(t) = 0$  for  $t < \overline{t}$ ) and if the line  $\operatorname{Re}\{s\} = \sigma_0$  is in the ROC, then all values of s with  $\operatorname{Re}\{s\} > \sigma_0$  are also included in the ROC.
- 4. If  $\mathbf{f}(t)$  is left-sided (i.e.,  $\mathbf{f}(t) = 0$  for  $t > \overline{t}$ ) and if the line  $\operatorname{Re}\{s\} = \sigma_0$  is in the ROC, then all values of s with  $\operatorname{Re}\{s\} < \sigma_0$  are also included in the ROC.
- 5. If the Laplace transform  $\hat{\mathbf{f}}(s)$  is rational, then its ROC is bounded by poles or extends to infinity. No poles are contained in the ROC.

In particular, a signal that is contained in  $\mathcal{L}_2([0,\infty))$  (and assuming that it is absolutely integrable for simplicity) is thus bounded and analytic (i.e., holomorphic) for  $\operatorname{Re}\{s\} > 0$ , which is the definition of the Hardy 2-space  $\mathcal{H}_2$ . Conversely, a signal that is contained in  $\mathcal{L}_2((-\infty,0])$  is bounded and analytic for  $\operatorname{Re}\{s\} < 0$ , which is the definition of the complementary Hardy 2-space  $\mathcal{H}_2^{\perp}$ . Since for every  $\hat{\mathbf{f}} \in \mathcal{H}_2$  it follows that  $\lim_{\sigma \to +0} \hat{\mathbf{f}} \in \mathcal{L}_2(\mathbb{R})$  and analogous  $\hat{\mathbf{f}} \in \mathcal{H}_2^{\perp}$  implies that  $\lim_{\sigma \to -0} \hat{\mathbf{f}} \in \mathcal{L}_2(\mathbb{R})$ , we regard  $\mathcal{H}_2$  and  $\mathcal{H}_2^{\perp}$  closed subspaces of the frequency-domain  $\mathcal{L}_2(\mathbb{R})$ . Since any time signal can be decomposed as

$$\mathbf{f}(t) = \mathbf{f}_1(t) + \mathbf{f}_2(t) \quad \text{with} \quad \mathbf{f}_1 \in \mathcal{L}_2([0,\infty)), \mathbf{f}_2 \in \mathcal{L}_2((-\infty,0])$$
 (2.39)

and  $\langle \mathbf{f}_1, \mathbf{f}_2 \rangle = 0$ , one can see from  $\mathcal{L}_2(\mathbb{R}) = \mathcal{H}_2 \cup \mathcal{H}_2^{\perp}$  and Parseval's theorem that

$$\langle \hat{\mathbf{f}}_1, \hat{\mathbf{f}}_2 \rangle = 0 \quad \text{and} \quad \mathcal{H}_2 \cap \mathcal{H}_2^{\perp} = 0,$$
 (2.40)

which justifies the already used nomenclature  $\mathcal{H}_2$  and  $\mathcal{H}_2^{\perp}$ , respectively. A graphical illustrations of these connections is given in Fig. 2.2. Finally, the inverse transformation to 2.37 is given by the contour integral

$$\mathbf{f}(t) = \mathcal{B}^{-1} \left\{ \hat{\mathbf{f}} \right\} = \frac{1}{2\pi i} \int_{\sigma - i\infty}^{\sigma + j\infty} \hat{\mathbf{f}}(s) \, e^{st} \, ds \tag{2.41}$$

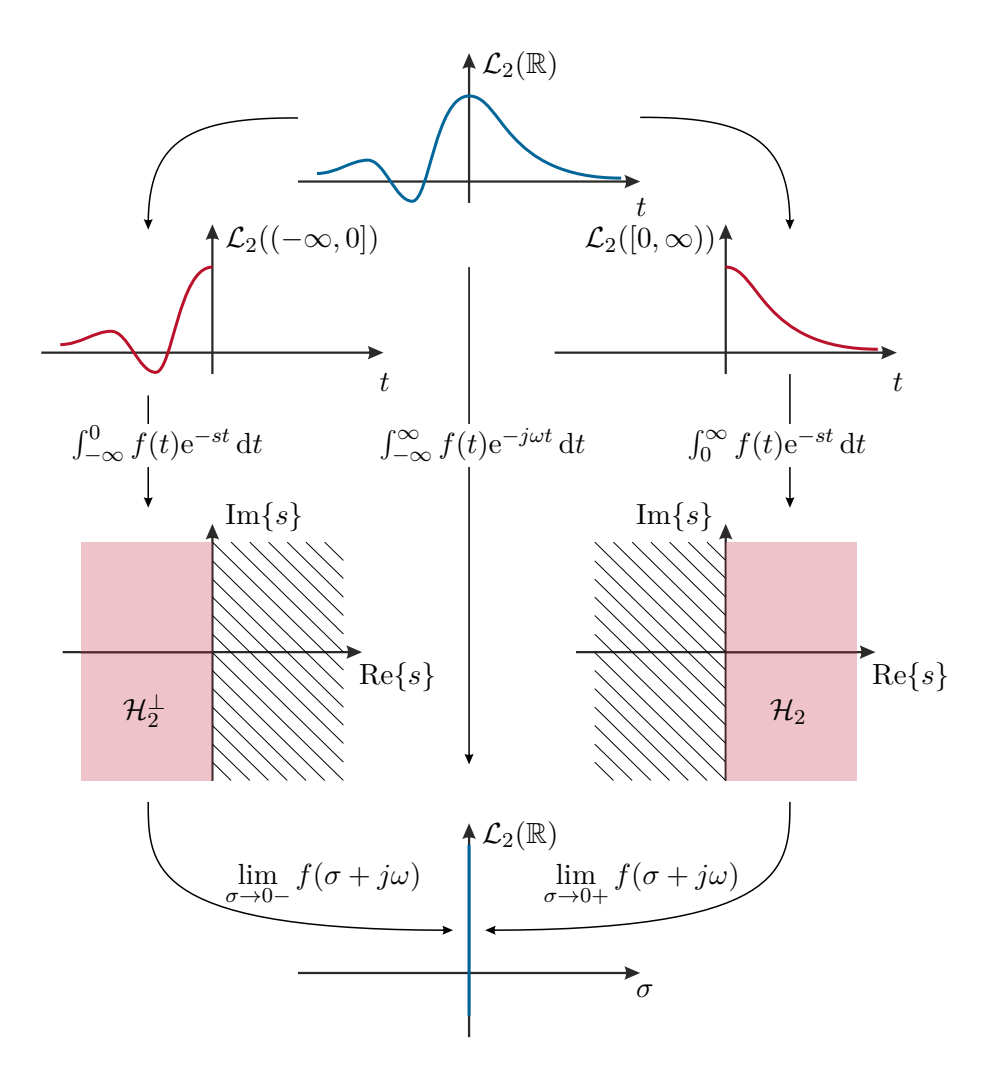


Figure 2.2: On  $\mathcal{L}_2((-\infty,0])$ ,  $\mathcal{L}_2([0,\infty))$ ,  $\mathcal{H}_2$ , and  $\mathcal{H}_2^{\perp}$ .

where the line of integration  $Re\{s\} = \sigma$  is within the corresponding ROC of  $\hat{\mathbf{f}}(s)$ .

By definition, the bilateral Laplace transform shares most of its properties with the unilateral Laplace transform. For convenience, the most common properties are summarized in Table 2.1. Selected pairs of (scalar) time-domain signals f(t) and their corresponding frequency-domain functions  $\hat{f}(s)$  are listed in Table 2.2. In the following, we will not make a notational distinction between time-domain signals and their frequency-domain representations and drop the hat notation unless it is necessary to avoid confusion. In general, the argument or the context sufficiently determines whether one is dealing with a time-domain or frequency-domain signal, which are anyhow isomorphic under the used integral transformations.

Property	Expression	ROC
Linearity	$\mathcal{B}\{af(t) + bg(t)\} = a\hat{f}(s) + b\hat{g}(s)$	s) Intersection of ROCs
Time Shifting	$\mathcal{B}\lbrace f(t-t_0)\rbrace = e^{-st_0}\hat{f}(s)$	Same as $\hat{f}(s)$
Frequency Shifting	$\mathcal{B}\{e^{at}f(t)\} = F(s-a)$	Re(s) shifted by $a$
Time Reversal	$\mathcal{B}\{f(-t)\} = F(-s)$	Reflect ROC about $Re(s)$
Differentiation (in $t$ )	$\mathcal{B}\{f'(t)\} = s\hat{f}(s)$	Same as $\hat{f}(s)$
Differentiation (in $s$ )	$\mathcal{B}^{-1}\left\{-\frac{d}{ds}\hat{f}(s)\right\} = tf(t)$	Same as $\hat{f}(s)$
Integration	$\mathcal{B}\left\{\int_{-\infty}^{t} f(\tau)  d\tau\right\} = \frac{1}{s} \hat{f}(s)$	ROC extends to include $s = 0$
Convolution	$\mathcal{B}\{f(t) * g(t)\} = \hat{f}(s)\hat{g}(s)$	Intersection of ROCs

Table 2.1: Selected properties of the bilateral Laplace transform.

Signal $f(t)$	Bilateral Laplace Transform $\hat{f}(s)$	ROC
$\delta(t)$	1	all $s$
h(t)	$\frac{1}{s}$	$\operatorname{Re}(s) > 0$
-h(-t)	$\frac{1}{s}$	$\operatorname{Re}(s) < 0$
$\tfrac{t^{n+1}}{(n-1)!}h(t)$	$\frac{1}{s^n}$	$\operatorname{Re}(s) > 0$
$-\tfrac{t^{n+1}}{(n-1)!}h(-t)$	$\frac{1}{s^n}$	$\operatorname{Re}(s) < 0$
$e^{-at}h(t)$	$\frac{1}{s+a}$	$\operatorname{Re}(s) > -a$
$-e^{-at}h(-t)$	$\frac{1}{s+a}$	$\operatorname{Re}(s) < -a$
$\frac{t^{n+1}}{(n-1)!}e^{-at}h(t)$	$\frac{1}{(s+a)^n}$	$\operatorname{Re}(s) > -a$
$-\frac{t^{n+1}}{(n-1)!}e^{-at}h(-t)$	$\frac{1}{(s+a)^n}$	$\operatorname{Re}(s) < -a$
$e^{-at}\sin(bt)h(t)$	$\frac{b}{(s+a)^2+b^2}$	$\operatorname{Re}(s) > -a$
$e^{-at}\cos(bt)h(t)$	$\frac{s+a}{(s+a)^2+b^2}$	$\operatorname{Re}(s) > -a$
$e^{-a t }$	$\frac{2a}{a^2 - s^2}$	$-a < \operatorname{Re}(s) < -a$
$e^{-a^2t^2}$	$\frac{\sqrt{\pi}}{a}e^{\frac{s^2}{4a^2}}$	all $s$

Table 2.2: Selected transform pairs of the bilateral Laplace transform and their associated ROC with the Dirac delta function  $\delta(t)$  and the Heaviside step function h(t).

## Input-output representation of linear systems

The input-output behavior of a dynamical system can be seen as a mapping from one signal space, the input space  $\mathcal{U}$ , to another space, the output space  $\mathcal{Y}$ :

$$\mathbf{G}: \mathbf{u} \in \mathcal{U} \mapsto \mathbf{y} = \mathbf{G}\mathbf{u} \in \mathcal{Y} \tag{2.42}$$

For the case  $\mathcal{U} = \mathcal{L}_2(\mathbb{R}; \mathbb{R}^l)$  and  $\mathcal{Y} = \mathcal{L}_2(\mathbb{R}; \mathbb{R}^m)$ , the input-output behavior of any linear system can be represented by the integral operator

$$\mathbf{y}(t) = \int_{-\infty}^{\infty} \mathbf{G}(t, \tau) \mathbf{u}(t) \, d\tau \tag{2.43}$$

with the kernel function  $\mathbf{G}(t,\tau) \in \mathbb{R}^{m \times l}$  that is usually referred to as the systems impulse response matrix. The system is said to be causal iff  $\mathbf{G}(t,\tau) = 0$  for all  $\tau > t$  and time-invariant if  $\mathbf{G}(t,\tau) = \mathbf{G}(t-\tau,0)$  for all  $t,\tau$ . Linear time-invariant (LTI) systems are thus represented by a convolution-type integral

$$\mathbf{y}(t) = \int_{-\infty}^{\infty} \mathbf{G}(t - \tau)\mathbf{u}(t) d\tau$$
 (2.44)

where  $\mathbf{G}(t-\tau,0)$  is denoted as  $\mathbf{G}(t-\tau)$  for simplicity. A system is called *causal* if  $\mathbf{G}(t)=0$  for t<0 and *anticausal* if  $\mathbf{G}(t)=0$  for t>0. If a system is neither causal nor anticausal, it is called *non-causal* or *acausal*. By applying the Laplace transform (2.37) to (2.44), one obtains

$$\mathbf{y}(s) = \mathbf{G}(s)\mathbf{u}(s) \tag{2.45}$$

with the transfer function matrix

$$\mathbf{G}(s) = \int_{-\infty}^{\infty} \mathbf{G}(t) \,\mathrm{e}^{-st} \,\mathrm{d}t. \tag{2.46}$$

The following properties of a dynamic system are directly related to the ROC of the transfer function matrix:

**Theorem 2.6** (Causality and stability). For an LTI system G(s) with corresponding ROC it holds true that:

- 1. If it is causal then its ROC is a right-half plane. If G(s) is rational, then causality is equivalent to the ROC being the right-half plane to the right of the rightmost pole.
- 2. If it is anticausal then its ROC is a left-half plane. If G(s) is rational, then anticausality is equivalent to the ROC being the left-half plane to the left of the leftmost pole.
- 3. It is stable iff the ROC includes  $Re\{s\} = 0$ .

Note that if one assumes a system to be rational and causal, then this is equivalent to the usual stability criterion that all poles have negative real part, i.e., they lie in the left-half of the s-plane. Unlike feedback control, ILC methods do not need to be causal

in time. In fact, strictly causal ILC algorithms are known to be inferior to noncausal algorithms since they lack the ability to *plan ahead*. This ability is closely linked to so-called *adjoint systems* that regularly appear in (optimation-based) feedforward control methods.

Exercise 2.1. Show that the system

$$G(s) = \frac{\exp(s)}{s+1} \quad \text{with Re}\{s\} > -1 \tag{2.47}$$

is not causal although the ROC is right to the rightmost pole.

Exercise 2.2. Specify all possible ROCs for the system

$$G(s) = \frac{s-1}{(s+1)(s-2)}$$
 (2.48)

and determine the corresponding impulse response functions.

# The $\mathcal{L}_{\infty}$ norm

That a linear time-invariant system indeed maps some  $\mathcal{L}_2(\mathbb{R}; \mathbb{R}^l)$  to  $\mathcal{L}_2(\mathbb{R}; \mathbb{R}^m)$  is only true if  $\mathbf{G}\mathbf{u} \in \mathcal{L}_2(\mathbb{R}; \mathbb{R}^m)$  for any  $\mathbf{u} \in \mathcal{L}_2(\mathbb{R}; \mathbb{R}^l)$ . Due to Parseval's theorem 2.4, one can evaluate the norm of a signal either in the time or frequency domain. The 2-norm of the output is thus

$$\|\mathbf{G}\mathbf{u}\|_{2}^{2} = \langle \mathbf{G}\mathbf{u}, \mathbf{G}\mathbf{u} \rangle = \frac{1}{2\pi} \int_{-\infty}^{\infty} \|\mathbf{G}(j\omega)\mathbf{u}(j\omega)\| \,d\omega$$

$$\leq \frac{1}{2\pi} \int_{-\infty}^{\infty} \bar{\sigma}(\mathbf{G}(j\omega))^{2} \|\mathbf{u}(j\omega)\| \,d\omega$$

$$\leq \sup_{\omega} \bar{\sigma}(\mathbf{G}(j\omega))^{2} \frac{1}{2\pi} \int_{-\infty}^{\infty} \|\mathbf{u}(j\omega)\| \,d\omega. \tag{2.49}$$

Using the definition of the supremum norm or  $\mathcal{L}_{\infty}$ -norm

$$\|\mathbf{G}\|_{\infty} = \sup_{\sigma} \bar{\sigma}(\mathbf{G}(j\omega)) \tag{2.50}$$

yields

$$\|\mathbf{G}\mathbf{u}\|_2 \le \|\mathbf{G}\|_{\infty} \|\mathbf{u}\|_2,\tag{2.51}$$

i.e., the  $\mathcal{L}_{\infty}$ -norm is the induced operator norm of a mapping between two  $\mathcal{L}_2$ -spaces. Consequently, a sufficient condition for  $\mathbf{G}\mathbf{u} \in \mathcal{L}_2(\mathbb{R};\mathbb{R}^m)$  is  $\sup_{\omega} \bar{\sigma}(\mathbf{G}(j\omega)) < \infty$ . Note that if  $\mathbf{G}(s)$  is a rational transfer matrix, this is true if and only if  $\mathbf{G}(s)$  has no poles on the imaginary axis.

# Systems in state-space representation

For a given state-space representation of a LTI system with measurement noise

$$\dot{\mathbf{x}}(t) = \mathbf{A}\mathbf{x}(t) + \mathbf{B}\mathbf{u}(t) , \quad \mathbf{x}(0) = \mathbf{x}_0$$
 (2.52a)

$$\mathbf{y}(t) = \mathbf{C}\mathbf{x}(t) + \mathbf{D}\mathbf{u}(t) + \mathbf{w}(t), \tag{2.52b}$$

which is the main type of system we will investigate in this chapter, one obtains a corresponding input-output representation (2.1) as

$$\mathbf{y}(t) = \mathbf{C}\mathbf{\Phi}(t)\mathbf{x}_0 + \mathbf{D}\mathbf{u}(t) + \int_0^t \mathbf{C}\mathbf{\Phi}(t-\tau)\mathbf{B}\mathbf{u}(\tau)\,\mathrm{d}\tau + \mathbf{w}(t)$$
 (2.53)

with  $\Phi(t) = \exp(\mathbf{A}t)$ . If  $\mathbf{x}_0 = 0$ , the system is said to be relaxed at t = 0. It is often convenient to assume that the system is relaxed in the infinitely remote past, wherefore  $\mathbf{C}\Phi(t)\mathbf{x}_0$  vanishes and (2.53) can be extended to an infinite time horizon

$$\mathbf{y} = \mathbf{G}\mathbf{u} + \mathbf{w} \tag{2.54}$$

and  $\mathbf{G}(t) = \mathcal{B}^{-1}\{\mathbf{G}(s)\} = \mathbf{C}\Phi(t-\tau)\mathbf{B} + \mathbf{D}\delta(t)$  using the Dirac-delta function  $\delta(t)$ . Note that (2.54) is more general than (2.52), since it can describe dynamic systems that do not have a state-space representation or whose state-space is infinite-dimensional, i.e., distributed-parameter systems described by partial differential equations. Further, the noise term  $\mathbf{w}$  can be arbitrary and may thus be used to also include process noise which is not present in (2.52).

# Adjoint systems

For a given system  $\mathbf{G}: \mathcal{L}_2(\mathbb{R}; \mathbb{R}^l) \to \mathcal{L}_2(\mathbb{R}; \mathbb{R}^m)$ , the *adjoint system* is defined as the linear system  $\mathbf{G}^{\dagger}: \mathcal{L}_2(\mathbb{R}; \mathbb{R}^m) \to \mathcal{L}_2(\mathbb{R}; \mathbb{R}^l)$  such that

$$\langle \mathbf{G}\mathbf{w}, \mathbf{y} \rangle = \langle \mathbf{w}, \mathbf{G}^{\dagger} \mathbf{y} \rangle.$$
 (2.55)

It is easy to show that this uniquely defines  $\mathbf{G}^{\dagger}$  and that  $(\mathbf{G}^{\dagger})^{\dagger} = \mathbf{G}$ . Furthermore, if a real-valued  $\mathbf{G}$  has a state-space representation  $(\mathbf{A}, \mathbf{B}, \mathbf{C}, \mathbf{D})$ , then  $\mathbf{G}^{\dagger}$  has a realization  $(-\mathbf{A}^{\mathrm{T}}, -\mathbf{C}^{\mathrm{T}}, \mathbf{B}^{\mathrm{T}}, \mathbf{D}^{\mathrm{T}})$  and the transfer matrix

$$\mathbf{G}^{\dagger}(s) = \mathbf{G}^{\mathrm{T}}(-s). \tag{2.56}$$

Exercise 2.3. Determine the adjoint  $\mathbf{G}^{\dagger}$  in the Hilbert space  $\mathcal{L}_2([0,t_f])$  using (2.55).

# 2.3 Frequency-domain ILC methods on infinite time horizons

Following the previous section, we consider a linear LTI system that is relaxed in the infinitely remote past and performs the same task over and over again. Each iteration is then described by

$$\mathbf{y}_j = \mathbf{G}\mathbf{u}_j + \mathbf{w}_j \tag{2.57}$$

with the input and output quantities  $\mathbf{y}_j(t) \in \mathbb{R}^l$  and  $\mathbf{u}_j(t) \in \mathbb{R}^m$ , respectively, as well as a exogenous disturbance  $\mathbf{w}_j(t) \in \mathbb{R}^l$ . We assume that the system  $\mathbf{G}$  is inherently BIBO-stable and thus  $\mathbf{G}(j\omega) < \infty$  for all  $\omega$ . Since ILC can be seen as an adaptive open-loop control strategy, this assumption is quite natural. Unstable plants thus have to be stabilized before applying ILC methods. By using a linear ILC law (2.4) on an infinite time horizon, i.e.,

$$\mathbf{u}_{j+1} = \mathbf{Q}(\mathbf{u}_j + \mathbf{L}\mathbf{e}_j) \tag{2.58}$$

with

$$\mathbf{Q}\mathbf{u} = \int_{-\infty}^{\infty} \mathbf{Q}(t-\tau)\mathbf{u}(\tau) d\tau \quad \text{and} \quad \mathbf{L}\mathbf{u} = \int_{-\infty}^{\infty} \mathbf{L}(t-\tau)\mathbf{u}(\tau) d\tau, \tag{2.59}$$

we want to iteratively track a desired output  $\mathbf{y}_d$  that exists and is uniquely defined by  $\mathbf{y}_d = \mathbf{G}\mathbf{u}_d$ . Following a signal processing nomenclature,  $\mathbf{Q}$  and  $\mathbf{L}$  are usually referred to as Q-filter and L-filter or learning filter, respectively.

# 2.3.1 Analysis of ILC laws

To analyze stability and convergence of the learning law (2.58), we assume a deterministic input-output behavior with  $\mathbf{w}_j = 0$ . Using the output error  $\mathbf{e}_j = \mathbf{y}_d - \mathbf{y}_j$  and the learning law (2.58) yields

$$\mathbf{u}_{j+1} = \mathbf{\Psi} \mathbf{u}_j + \mathbf{\Lambda} \mathbf{y}_d , \qquad (2.60)$$

with  $\Psi = \mathbf{Q}(\mathbf{I} - \mathbf{L}\mathbf{G})$  and  $\Lambda = \mathbf{Q}\mathbf{L}$ . The asymptotic input  $\mathbf{u}_{j+1} = \mathbf{u}_j = \mathbf{u}_{\infty}$  of the input iteration (2.60) is given by

$$\mathbf{u}_{\infty} = (\mathbf{I} - \mathbf{\Psi})^{-1} \mathbf{\Lambda} \mathbf{y}_d . \tag{2.61}$$

By introducing the input error  $\bar{\mathbf{u}}_j = \mathbf{u}_j - \mathbf{u}_{\infty}$ , one obtains the input error iteration

$$\bar{\mathbf{u}}_{j+1} = \mathbf{\Psi}\bar{\mathbf{u}}_j \ , \tag{2.62}$$

for which the follow theorem assures stability:

**Theorem 2.7** (Asymptotic stability of the ILC law). The input error iteration (2.62) of the ILC law (2.58) is asymptotically stable if

$$\sup_{\omega} \rho \Big( \mathbf{Q}(j\omega) \big( \mathbf{I} - \mathbf{L}(j\omega) \mathbf{G}(j\omega) \big) \Big) < 1$$
 (2.63)

and  $\mathbf{u}_i$  converges to  $\mathbf{u}_{\infty}$ .

For practical reasons, we are usually much more interested in making stability assertions for the output error  $\mathbf{e}_j$ . Assuming that there exists a formal inverse  $\mathbf{G}^{-1}$ , we can rewrite the input-output behavior as  $\mathbf{u}_j = \mathbf{G}^{-1}(\mathbf{y}_d - \mathbf{e}_j)$  which yields the output iteration

$$\mathbf{e}_{j+1} = \mathbf{G} \mathbf{\Psi} \mathbf{G}^{-1} \mathbf{e}_j + (\mathbf{I} - \mathbf{G} \mathbf{Q} \mathbf{G}^{-1}) \mathbf{y}_d . \tag{2.64}$$

It is immediately clear from this equation that perfect tracking, i.e., a vanishing asymptotic output error  $\mathbf{e}_{\infty} = \mathbf{0}$ , is only possible for  $\mathbf{Q} = \mathbf{I}$  and one may be inclined to question other choices for  $\mathbf{Q}$ . We will get back to this issue later. The asymptotic output error  $\mathbf{e}_{\infty}$  is given by

$$\mathbf{e}_{\infty} = \mathbf{y}_d - \mathbf{G}\mathbf{u}_{\infty}$$

$$= \left(\mathbf{I} - \mathbf{G}(\mathbf{I} - \mathbf{\Psi})^{-1}\mathbf{\Lambda}\right)\mathbf{y}_d.$$
(2.65)

Using  $\bar{\mathbf{e}}_j = \mathbf{e}_j - \mathbf{e}_{\infty}$  yields

$$\bar{\mathbf{e}}_{j+1} = \mathbf{G} \mathbf{\Psi} \mathbf{G}^{-1} \bar{\mathbf{e}}_j \ . \tag{2.66}$$

Since

$$\rho(\mathbf{G}\mathbf{\Psi}\mathbf{G}^{-1}) = \rho(\mathbf{\Psi}), \tag{2.67}$$

it follows that:

**Theorem 2.8** (Asymptotic stability of the output iteration). The output iteration (2.64) of the ILC law (2.58) is asymptotically stable iff the input iteration is stable, i.e.,

$$\sup_{\omega} \rho \Big( \mathbf{Q}(j\omega) \big( \mathbf{I} - \mathbf{L}(j\omega) \mathbf{G}(j\omega) \big) \Big) < 1$$
 (2.68)

and  $\mathbf{e}_j$  then converges to the asymptotic tracking error

$$\mathbf{e}_{\infty} = \left(\mathbf{I} - \mathbf{G}(\mathbf{I} - \mathbf{\Psi})^{-1} \mathbf{\Lambda}\right) \mathbf{y}_{d} = \left(\mathbf{I} - \mathbf{G} \mathbf{\Psi} \mathbf{G}^{-1}\right)^{-1} \left(\mathbf{I} - \mathbf{G} \mathbf{Q} \mathbf{G}^{-1}\right) \mathbf{y}_{d} . \tag{2.69}$$

Exercise 2.4. Show the equivalence of both expressions in (2.69).

If one wants to avoid (potentially) large transient errors during the learning process, monotonic convergence of the learning law has to be ensured.

**Theorem 2.9** (Monotonic convergence of the input iteration). The input iteration (2.60) of the ILC law (2.58) converges monotonically to  $\mathbf{u}_{\infty}$ , i.e., it holds that

$$\|\mathbf{u}_{j+1} - \mathbf{u}_{\infty}\|_{2} \le \alpha \|\mathbf{u}_{j} - \mathbf{u}_{\infty}\|_{2} \tag{2.70}$$

for  $0 < \alpha < 1$  if

$$\|\mathbf{\Psi}\|_{\infty} = \sup_{\omega} \bar{\sigma} \Big( \mathbf{Q}(j\omega) \big( \mathbf{I} - \mathbf{L}(j\omega) \mathbf{G}(j\omega) \big) \Big) = \alpha < 1 .$$
 (2.71)

**Theorem 2.10** (Monotonic convergence of the output iteration). The output iteration (2.64) of the ILC law (2.58) converges monotonically to  $\mathbf{e}_{\infty}$ , i.e., it holds that

$$\|\mathbf{e}_{i+1} - \mathbf{e}_{\infty}\|_{2} \le \beta \|\mathbf{e}_{i} - \mathbf{e}_{\infty}\|_{2} \tag{2.72}$$

for 
$$0 \le \alpha < 1$$
 if
$$\|\mathbf{G}\mathbf{\Psi}\mathbf{G}^{-1}\|_{\infty} = \sup_{\omega} \bar{\sigma}\Big(\mathbf{G}(j\omega)\mathbf{Q}(j\omega)\big(\mathbf{I} - \mathbf{L}(j\omega)\mathbf{G}(j\omega)\big)\mathbf{G}^{-1}(j\omega)\Big) = \beta < 1. \quad (2.73)$$

Note that monotonic convergence of the input iteration *does not* imply monotonic convergence of the output iteration and vice versa.

# 2.3.2 Deterministic design methods

All types of ILC algorithms try to perform some kind of approximate inversion of the input-output behavior of the system. Since this inversion has to be performed online based on measurements, it is inherently constrained by the presence of disturbances and measurement noise. Ideally, an ILC algorithm is able to iteratively separate repeating disturbances and effects of a model-plant mismatch from non-repeating disturbances and measurement noise. Nevertheless, most ILC designs are developed within a deterministic framework with  $\mathbf{w} = \mathbf{0}$  which we will adopt in this section. Note that we introduce ILC as a pure open-loop control strategy here, henceforth ILC algorithms are not able to respond to non-repeating (and unanticipated) disturbances. For the performance of the complete control concept, it is thus advisable to incorporate feedback control methods. For simplicity, we thus assume that the system  $\mathbf{G}$  already incorporates a suitable feedback control strategy and thus  $\mathbf{G}$  is BIBO-stable.

We know from the previous section that  $\mathbf{Q} = \mathbf{I}$  is a necessary condition to achieve perfect tracking. One thus only wants do deviate from this ideal if necessary to achieve a stable ILC algorithm that is sufficiently robust to model variations. We will thus start with three typical design strategies to obtain suitable learning operators before considering the relation between Q-filtering and robustness. As we will see later, good learning filters usually avoid to learn at high frequencies due to the presence of measurement noise. By assuming  $\mathbf{Q} = \mathbf{I}$ , however,  $\mathbf{I} - \mathbf{L}(j\omega)\mathbf{G}(j\omega) \to \mathbf{I}$  for  $\omega \to \infty$ , which would always violate the stability condition in Theorem 2.7. We will therefore consider a finite frequency range up to some  $\bar{\omega}$  and assume  $\mathbf{Q} = \mathbf{0}$  above, which is always possible.

## PD-type ILC laws

As the name implies, PD-type learning laws combine proportional and derivative action, i.e,

$$\mathbf{L}\mathbf{e}_{j} = \mathbf{K}_{p}\mathbf{e}_{j}(t) + \mathbf{K}_{d}\frac{\mathrm{d}\mathbf{e}_{j}(t)}{\mathrm{d}t}$$
(2.74)

with the proportional and derivative gain matrices  $\mathbf{K}_p$  and  $\mathbf{K}_d$ , respectively, that are tunable parameters that have to be chosen such that a desired performance is reached. These heuristic designs are arguably the most widely used ILC laws in the literature since they do not require an accurate model but rely on intensive tuning of the gain matrices. Since this can be a quite tedious task for MIMO systems, PD-type ILC laws are typically used for SISO systems only, which yields the learning filter

$$\mathbf{L}(s) = k_p + k_d s \tag{2.75}$$

in the frequency domain. While there are no tuning guidelines, it is usually suggested to start with small gain values and increase them until a growth of (usually) high-frequency components indicate that the learning law left the stable parameter regime [2.8].

The fact that such simple ILC laws perform quite well for a large class of systems is somewhat surprising. However, this can be explained by observing that a PD-type laws (2.74) is the exact inverse of a first-order lag (i.e., P-T<sub>1</sub>) element. Since most technical systems exhibit some kind of low-pass behavior, PD-type laws can be seen as an approximate inverse of their behavior. Note that the learning filter (2.75) yields infinite gains for  $\omega \to \infty$ , which is problematic in the presence of measurement noise.

Example 2.1. Consider a system described by the scalar transfer function

$$G(s) = \frac{s+1/2}{s^2+s+3} \tag{2.76}$$

together with the PD-type law (2.75). To evaluate stability for different parameter choices of  $k_p$  and  $k_d$ , the absolute value of  $I - L(j\omega)G(j\omega)$  is plotted in Fig. 2.3 together with the resulting convergence behavior of the ILC law. Note that the ILC law ultimately reaches the precision of the numerical simulation. Observing that the inverse of the system's transfer function is

$$G^{-1}(s) = 1/2 + s + \frac{11}{2(2s+1)},$$
 (2.77)

one could try to use  $k_p = 1/2$  and  $k_d = 1$ , which is in fact unstable according to Theorem 2.7.

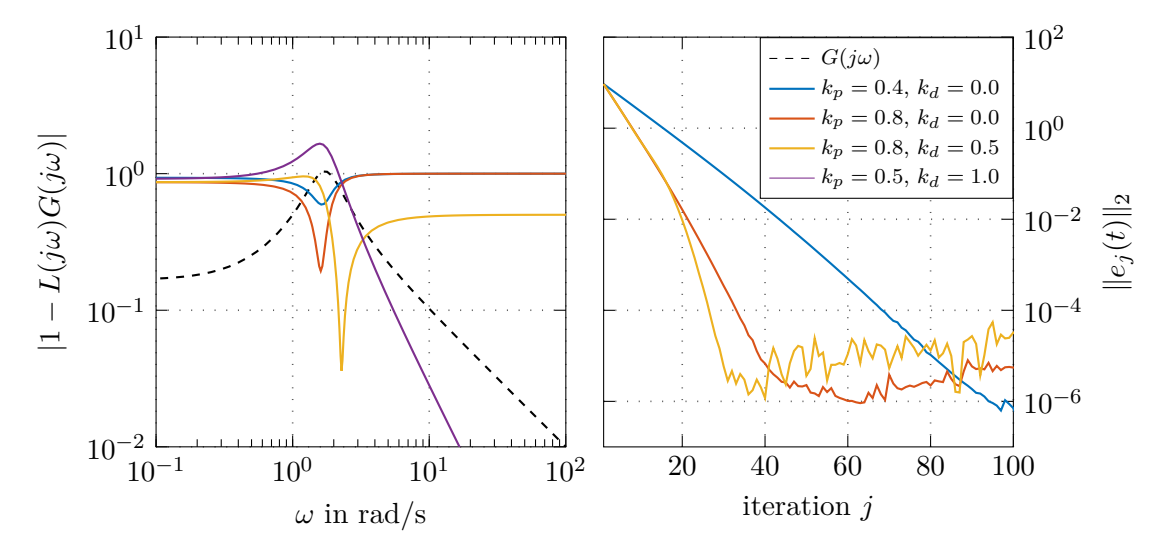


Figure 2.3: Stability and convergence behavior of a PD-type learning law for different parameters  $k_p$  and  $k_d$ .

#### Inversion-based ILC law

A particularly intuitive choice is to use  $\mathbf{L} = \mathbf{G}^{-1}$ , which yields

$$\mathbf{u}_{j+1} = \mathbf{Q}\left(\mathbf{u}_j + \mathbf{G}^{-1}\mathbf{e}_j\right) = \mathbf{Q}\left(\mathbf{u}_j + \mathbf{G}^{-1}(\mathbf{y}_d - \mathbf{G}\mathbf{u}_j)\right) = \mathbf{Q}\left(\mathbf{G}^{-1}\mathbf{y}_d\right). \tag{2.78}$$

The input  $\mathbf{u}_j$  thus remains unchanged after the first iteration (dead-beat behavior) with a resulting output error

$$\mathbf{e}_{j+1} = \mathbf{e}_{\infty} = \mathbf{y}_d - \mathbf{G}\mathbf{Q}(\mathbf{G}^{-1}(\mathbf{y}_d - \mathbf{y}_0)). \tag{2.79}$$

Using  $\mathbf{Q} = \mathbf{I}$  further implies  $\mathbf{e}_{\infty} = \mathbf{0}$ . There are several caveats to this result: First of all,  $\mathbf{G}$  is never known exactly which limits the usability of inversion-based ILC laws and mandates an additional  $\mathbf{Q}$ -filter. Further,  $\mathbf{G}(s)$  is strictly proper for any physical process, wherefore its inverse  $\mathbf{G}^{-1}(s)$  is unbound for  $s = j\omega \to \infty$  and thus  $\mathbf{e}_{\infty}$  is undefined for arbitrary  $\mathbf{y}_d - \mathbf{y}_0 \in \mathcal{L}_2(\mathbb{R})$ . Finally,  $\mathbf{G}^{-1}$  is unstable for non-minimum phase systems although this can be alleviated by (non-causal) stable-inversion methods [2.9].

#### Pseudo-Inversion-based ILC law

Using an inversion-based ILC law is essentially determining an exact feedforward input signal from output data. Unlike for feedforward purposes, however, we cannot demand certain levels of regularity of the output signals due to the presence of stochastic disturbances and measurement noise. The obvious solution is to regularize the system inversion by using a pseudo-inverse learning filter [2.10], i.e.,

$$\mathbf{L}(s) = \left(\alpha \mathbf{I} + \mathbf{G}^{\dagger}(s)\mathbf{G}(s)\right)^{-1}\mathbf{G}^{\dagger}(s) \tag{2.80}$$

with the regularization parameter  $\alpha > 0$  and the transfer matrix of the adjoint system  $\mathbf{G}^{\dagger}(s)$ . The regularization parameter separates regions where the learning law is approaching an inversion-based law (i.e.,  $\mathbf{L}(s) \approx \mathbf{G}^{-1}(s)$ ) from regions where learning is almost prohibited (i.e.,  $\mathbf{L}(s) \approx \mathbf{0}$ ) depending on whether  $\|\mathbf{G}^{\dagger}(s)\mathbf{G}(s)\|$  is much larger or smaller than  $\alpha$ , respectively. For systems with low-pass behavior where  $\mathbf{G}(s)$  is strictly proper, the learning filter (2.80) thus naturally avoids learning in the high-frequency region, i.e.,  $\lim_{s \to \infty} \mathbf{L}(s) = \mathbf{0}$ . It still remains to be shown that (2.80) results in a stable learning iteration. Using

$$\mathbf{I} - \mathbf{L}\mathbf{G} = \mathbf{I} - \left(\alpha \mathbf{I} + \mathbf{G}^{\dagger} \mathbf{G}\right)^{-1} \mathbf{G}^{\dagger} \mathbf{G} = \left(\mathbf{I} + \frac{1}{\alpha} \mathbf{G}^{\dagger} \mathbf{G}\right)^{-1}$$
(2.81)

it follows with the definition of the adjoint system that

$$\rho(\mathbf{I} - \mathbf{L}(j\omega)\mathbf{G}(j\omega)) = \rho\left(\left(\mathbf{I} + \frac{1}{\alpha}(\mathbf{G}(-j\omega))^T\mathbf{G}(j\omega)\right)^{-1}\right)$$
(2.82)

$$= \rho \left( \left( \mathbf{I} + \frac{1}{\alpha} (\mathbf{G}(j\omega))^H \mathbf{G}(j\omega) \right)^{-1} \right). \tag{2.83}$$

Assuming that  $\mathbf{G}(j\omega)\mathbf{u} \neq \mathbf{0}$  for any  $\mathbf{u} \neq \mathbf{0}$ , the matrix  $\frac{1}{\alpha}(\mathbf{G}(j\omega))^H \mathbf{G}(j\omega)$  is positive definite and thus all of its eigenvalues are strictly positive. This implies the asymptotic stability of the learning law since  $\rho(\mathbf{I} - \mathbf{L}(j\omega)\mathbf{G}(j\omega)) < 1$  for all  $\omega$ .

Example 2.2. Consider again the plant (2.76). According to Figure 2.3, the magnitude of  $G(j\omega)$  is above  $1\cdot 10^{-1}$  for the essential part of its dynamic behavior. The resulting Pseudo-Inversion-based learning filter (2.80) for different choices of the regularization parameter  $\alpha = \{1\cdot 10^{-1}, 5\cdot 10^{-2}, 1\cdot 10^{-2}, 1\cdot 10^{-3}\}$  is illustrated in Figure 2.4. As one can see, the learning filter (2.80) is an approximation of the exact inverse  $G^{-1}(j\omega)$ . While  $L(j\omega)$  deviates (significantly) over the whole frequency range for high values of  $\alpha$ , small values of  $\alpha$  only introduce a roll-off for high-frequency components. Since asymptotic convergence is equivalent to monotonic convergence for SISO plants according to Theorem 2.7 and Theorem 2.9, the learning law (2.80) always converges exponentially. Note that this holds only true for infinite time horizons and that the convergence rate in Theorem (2.9) is in general not equivalent (but determined by) the regularization parameter  $\alpha$ .

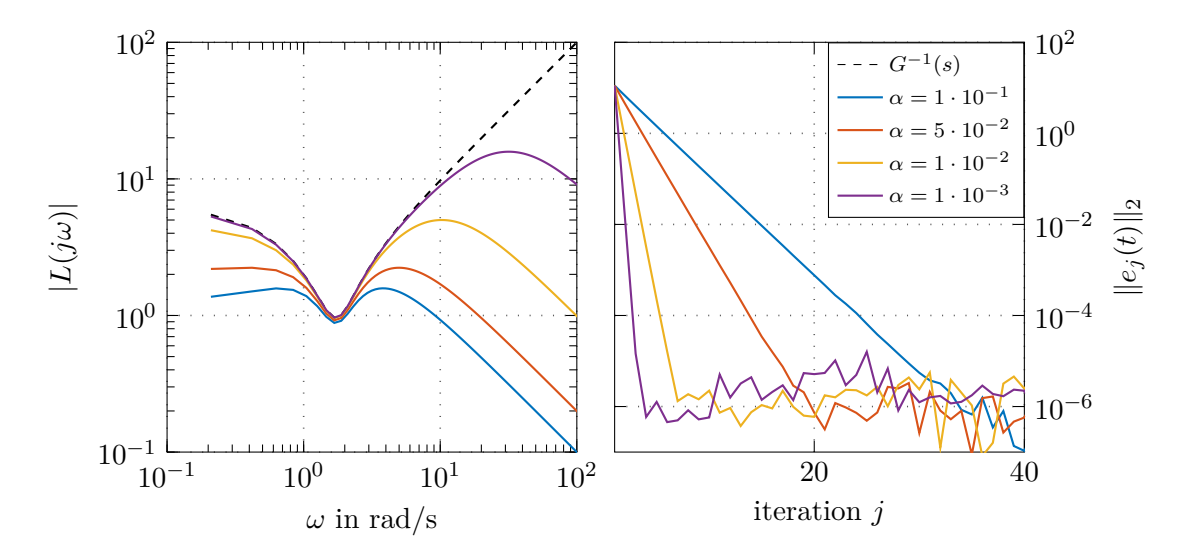


Figure 2.4: Learning filter and convergence behavior of the Pseudo-Inversion-based learning filter (2.80) for different regularization parameters  $\alpha$ .

## 2.3.3 Stochastically optimal learning laws

We already mentioned in the previous section that the approximate inversion due to the learning filter **L** is inherently constrained by the presence of stochastic quantities, namely (non-repeating) process disturbances and measurement noise  $\mathbf{w}_i(t) \in \mathbb{R}^l$  in

$$\mathbf{y}_{i}(t) = \mathbf{G}\mathbf{u}_{i}(t) + \mathbf{w}_{i}(t) \tag{2.84}$$

that is given by a zero-mean wide-sense stationary (WSS) process with identical stochastic properties in each iteration. To analyze this problem in a stochastic framework, we

introduce the following notation: For two vector-valued stochastic signals  $\mathbf{a}_k(t)$  and  $\mathbf{b}_l(t)$  with the iteration indices k and l, their cross-correlation function is given by  $\mathbf{R}^{a_k b_l}(\tau) = \mathbf{E}\left\{\mathbf{a}_k(t+\tau)(\mathbf{b}_l(t))^{\mathrm{T}}\right\}$  where  $\mathbf{E}\{\cdot\}$  denotes the expectation operator. The corresponding power spectral density (PSD) reads as  $\mathbf{S}^{a_k b_l}(s) = \mathcal{B}\left\{\mathbf{R}^{a_k b_l}(\tau)\right\}$ . In case k=l, the common index is written as subscript, i.e.,  $\mathbf{R}_k^{ab}(\tau) = \mathbf{R}^{a_k b_k}(\tau)$  and  $\mathbf{S}_k^{ab}(s) = \mathbf{S}^{a_k b_k}(s)$ .

For generality, we use a *iteration-varying* learning law (again without **Q**-filter)

$$\mathbf{u}_{j+1}(t) = \mathbf{u}_j(t) + \mathbf{L}_j \mathbf{e}_j(t). \tag{2.85}$$

Our goal now is to design a learning filter  $\mathbf{L}_j$  in a stochastically optimal way, i.e.  $\mathbf{u}_{j+1}(t)$  should be determined such that it minimizes the expected value of the mean-square output error  $\mathbf{E}\{(\mathbf{e}_{j+1}(t))^{\mathrm{T}}\mathbf{e}_{j+1}(t)\}$ . Following section 2.3.1, the output error  $\mathbf{e}_j(t) = \mathbf{y}_d(t) - \mathbf{y}_j(t)$  of the iteration j is given by

$$\mathbf{e}_{j}(t) = \mathbf{G}\boldsymbol{\nu}_{j}(t) - \mathbf{w}_{j}(t) \tag{2.86}$$

using the input error  $\nu_j(t) = \mathbf{u}_d(t) - \mathbf{u}_j(t)$ . Together with the learning law, the evolution of the input error is described by

$$\boldsymbol{\nu}_{j+1}(t) = \boldsymbol{\nu}_j(t) - \mathbf{L}_j \mathbf{e}_j(t) \tag{2.87}$$

and the output error of the iteration j + 1 yields

$$\mathbf{e}_{j+1}(t) = (\mathbf{I} - \mathbf{GL}_j)\mathbf{e}_j(t) + \mathbf{w}_j(t) - \mathbf{w}_{j+1}(t). \tag{2.88}$$

The problem of learning in a stochastically optimal sense can be written as the optimization problem

$$\min_{\mathbf{L}_{j}(t)} \mathrm{E}\left\{ (\mathbf{e}_{j+1}(t))^{\mathrm{T}} \mathbf{e}_{j+1}(t) \right\}. \tag{2.89}$$

Since we only consider LTI systems and the stochastic disturbance  $\mathbf{w}_j$  is WSS, the optimization problem (2.89) can be treated in the Laplace domain by applying the bilateral Laplace transform, which yields

$$\min_{\mathbf{L}_{j}(t)} \mathrm{E}\left\{\left(\mathbf{e}_{j+1}(t)\right)^{\mathrm{T}} \mathbf{e}_{j+1}(t)\right\} = \min_{\mathbf{L}_{j}(t)} \mathrm{Tr}\left\{\mathbf{R}_{j+1}^{ee}(0)\right\}$$

$$= \min_{\mathbf{L}_{j}(s)} \frac{1}{j2\pi} \mathrm{Tr}\left\{\int_{-\infty}^{\infty} \mathbf{S}_{j+1}^{ee}(j\omega) d\omega\right\}, \tag{2.90}$$

where Tr  $\{\cdot\}$  denotes the trace operator. To obtain the output error PSD  $\mathbf{S}_{j+1}^{ee}(s)$ , one can use (2.88) together with (2.86), which yields

$$\mathbf{e}_{i+1}(t) = (\mathbf{G} - \mathbf{G}\mathbf{L}_i\mathbf{G})\boldsymbol{\nu}_i(t) + \mathbf{G}\mathbf{L}_i\mathbf{w}_i(t) - \mathbf{w}_{i+1}(t). \tag{2.91}$$

In general, the stochastic quantities  $\nu_j$ ,  $\mathbf{w}_j$  and  $\mathbf{w}_{j+1}$  will be correlated. We thus make the following assumptions:

- A1 different instances of the disturbance are uncorrelated, i.e.,  $\mathrm{E}\left\{\mathbf{w}_i(t+\tau)(\mathbf{w}_j(t))^{\mathrm{T}}\right\} = \mathbf{0}$  for  $i \neq j$
- A2 the input error  $\nu_j$  is uncorrelated with the exogenous disturbance of the current and the following iteration, i.e.,  $\mathrm{E}\Big\{\nu_j(t+\tau)(\mathbf{w}_i(t))^\mathrm{T}\Big\} = \mathbf{0}$  for  $i \in \{j,j+1\}$ . Together with A1, this is equivalent to  $\mathrm{E}\Big\{\nu_0(t+\tau)(\mathbf{w}_j(t))^\mathrm{T}\Big\} = \mathbf{0}$
- A3 the stochastic properties of of the disturbance do not change over iterations, i.e.,  $\mathrm{E}\left\{\mathbf{w}_{j}(t+\tau)(\mathbf{w}_{j}(t))^{\mathrm{T}}\right\} = \mathbf{S}^{ww}$ .

Using these assumption, we obtain

$$\mathbf{S}_{i+1}^{ee} = (\mathbf{G} - \mathbf{G}\mathbf{L}_{i}\mathbf{G})\mathbf{S}_{i}^{\nu\nu}(\mathbf{G} - \mathbf{G}\mathbf{L}_{i}\mathbf{G})^{\dagger} + \mathbf{G}\mathbf{L}_{i}\mathbf{S}^{ww}(\mathbf{L}_{i})^{\dagger}\mathbf{G}^{\dagger} + \mathbf{S}^{ww}$$
(2.92)

The optimization problem (2.90) can be solved by variational calculus. The resulting learning filter

$$\mathbf{L}_{k}(s) = \mathbf{S}_{j}^{\nu\nu}(s)\mathbf{G}^{\dagger}(s)\left[\mathbf{G}(s)\mathbf{S}_{j}^{\nu\nu}(s)\mathbf{G}^{\dagger}(s) + \mathbf{S}^{ww}(s)\right]^{-1}$$
(2.93)

is an iterative version of the well-known (non-causal) Wiener filter, which is used to estimate the input deviation that optimally explains the measured output error. A common problem of Wiener-filter-based approaches is that the optimal solution (2.93) requires knowledge of the input error PSD  $\mathbf{S}_{j}^{\nu\nu}(s)$ , which is typically handled using a-priori knowledge of the problem.

Due to the learning process, the measured output error  $\mathbf{e}_{j}(t)$  will be increasingly dominated by stochastic disturbances. A stochastically optimal learning law will therefore reduce its learning action with increasing iterations. Such a behavior is intrinsic to (2.93) due to the decreasing input error PSD  $\mathbf{S}_{j}^{\nu\nu}(s)$ . From (2.86), (2.87) and (2.93) we obtain the iterative relation

$$\mathbf{S}_{j+1}^{\nu\nu}(s) = (\mathbf{I} - \mathbf{L}_j(s)\mathbf{G}(s))\mathbf{S}_j^{\nu\nu}(s). \tag{2.94}$$

By starting from an initial PSD  $\mathbf{S}_0^{\nu\nu}(s)$  and the corresponding learning filter (2.93), one can iterate forward in time to obtain a stochastically optimal ILC method.

**Theorem 2.11** (Stochastically optimal learning). If  $\mathbf{S}^{ww}(s)$  and the initial input error PSD  $\mathbf{S}_0^{\nu\nu}(s)$  are positive definite and the system's transfer matrix  $\mathbf{G}(s)$  does not exhibit transmission zeros on the imaginary axis, the learning filter (2.93) together with (2.94) yields a stable learning law that ensures convergence to the optimal error PSDs

$$\mathbf{S}_{\infty}^{\nu\nu}(s) = \mathbf{0}, \quad \mathbf{S}_{\infty}^{\eta\eta}(s) = \mathbf{S}^{ww}(s). \tag{2.95}$$

The fact that one can iteratively construct a noise-less representation of the unknown desired input  $\mathbf{u}_{\infty}$  from noisy output measurements and an output error containing only noise sounds like a very attractive solution. However, there is a severe limitation to this seemingly nice result: By design, the learning filter is asymptotically vanishing and thus the learning process comes to a halt. Since the forward iteration (2.94) is independent

of actual measurements, this is the case even if some unforeseen disturbance (i.e., not represented in the stochastic model) is causing large output errors.

Since iteration-varying learning laws furthermore increase the effort of implementation, one may thus prefer to accept sub-optimal performance by using a fixed input error PSD  $\mathbf{S}_{i}^{\nu\nu}(s) = \mathbf{S}^{\nu\nu}(s)$ .

**Theorem 2.12** (Stochastically sub-optimal learning). If  $\mathbf{S}^{ww}(s)$  and the chosen input error PSD  $\mathbf{S}^{\nu\nu}(s)$  are positive definite and the system's transfer matrix  $\mathbf{G}(s)$  does not exhibit transmission zeros on the imaginary axis, the iteration-invariant learning filter

$$\mathbf{L}(s) = \mathbf{S}^{\nu\nu}(s)\mathbf{G}^{\dagger}(s)\left[\mathbf{G}(s)\mathbf{S}^{\nu\nu}(s)\mathbf{G}^{\dagger}(s) + \mathbf{S}^{ww}(s)\right]^{-1}$$
(2.96)

yields a stable learning law that converges to a positive definite asymptotic output error PSD  $\mathbf{S}^{ee}_{\infty}(s)$  given by the solution of

$$(\mathbf{I} - \mathbf{G}(s)\mathbf{L}(s))\mathbf{S}_{\infty}^{ee}(s)(\mathbf{I} - \mathbf{G}(s)\mathbf{L}(s))^{\dagger} - \mathbf{S}_{\infty}^{ee}(s) + \mathbf{GL}(s)\mathbf{S}^{ww}(s) + \mathbf{S}^{ww}(s)\mathbf{L}^{\dagger}(s)\mathbf{G}^{\dagger}(s) = \mathbf{0}.$$
(2.97)

This sub-optimal learning law is structurally similar to pseudo-inversion-based learning laws. For the special case of  $\mathbf{S}^{\nu\nu}(s) = \sigma_{\nu}\mathbf{I}$  and  $\mathbf{S}^{ww}(s) = \sigma_{w}\mathbf{I}$ , it is easy to show that (2.96) is identical to (2.80) with  $\alpha = \frac{\sigma_{w}}{\sigma_{\nu}}$ . Stochastically optimal learning filters thus regularize the system inversion according to the expected signal-to-noise ratio.

# 2.3.4 Q-filtering and robustness

One of the main advantages of ILC over other control approaches is its ability to achieve (almost) perfect tracking in the presence of external disturbances and model-plant mismatch. While we have investigated external disturbances in the previous section, we may now shift our attention to an inevitable model-plant mismatch. Assuming that the plant can be described by  $\mathbf{G}(s) = \mathbf{G}_0(s)\Delta\mathbf{G}(s)$  with the nominal (design) model  $\mathbf{G}_0(s)$  and the unknown deviation  $\Delta\mathbf{G}(s)$ , it is expected that  $\rho(\mathbf{I} - \mathbf{L}(j\omega)\mathbf{G}_0(s)\Delta\mathbf{G}(s))$  will in general be larger than one for some  $\omega$  since we designed the learning filter  $\mathbf{L}(s)$  such that  $\rho(\mathbf{I} - \mathbf{L}(j\omega)\mathbf{G}_0(s)) < 1$ . However, it is clear that the asymptotic stability criterion

$$\sup_{\omega} \rho \Big( \mathbf{Q}(j\omega) \big( \mathbf{I} - \mathbf{L}(j\omega) \mathbf{G}(j\omega) \big) \Big) < 1$$
 (2.98)

can always be met by choosing  $\mathbf{Q}(s)$  sufficiently small. For example, for a known  $\Delta \mathbf{G}(s)$  one could always use  $\mathbf{Q}(s) = \kappa \mathbf{I}$  with  $\kappa > 1/\sup_{\omega} \rho(\mathbf{I} - \mathbf{L}(j\omega)\mathbf{G}_0(j\omega)\Delta\mathbf{G}(j\omega))$ .

Using a spectrally uniform  $\mathbf{Q}$ -filter is usually not recommended, since  $\Delta \mathbf{G}(s)$  is typically small in those parts of the frequency range within which we want to learn. To avoid unnecessary large asymptotic tracking errors, a spectrally selective  $\mathbf{Q}$ -filter is thus usually advisable. The most common case in practice is that the (identified) nominal model fits quite accurately up to a certain frequency  $\omega_c$  and starts to deteriorate beyond that frequency, which motivates the use of low-pass filters.

Example 2.3. Consider the plant (2.76) again with an additional model-plant mismatch given by

$$G_0(s) = \frac{s+1/2}{s^2+s+3}$$
 and  $\Delta G(s) = \frac{1}{1+s/30+(s/15)^2}$  (2.99)

and a pseudo-inverse learning law L(s) with  $\alpha=1\cdot 10^{-2}$  for the nominal model  $G_0(s)$ . Simulation scenarios for different choices of Q(s) are illustrated in Figure 2.5. For Q(s)=1, we can see that  $|1-L(j\omega)G(j\omega)|>1$  for  $\omega>10$ , which leads to high-frequency oscillations that build up over time. Note that the error seems to converge initially but diverges after 20 iterations. Using a simple first-order low-pass filter

$$Q(s) = \frac{10}{s+10} \tag{2.100}$$

stabilizes the learning iteration, but at the cost of a significantly higher asymptotic output error. Interestingly, for the more aggressive choice (see left-hand side of Figure 2.5)

$$Q(s) = \frac{10^2}{(s+10)(-s+10)},$$
(2.101)

the asymptotic output error is vastly improved. The main reason for this is that simple first-order low-pass filter introduces a phase shift to the learned signal, which in turn results in a slight temporal mismatch between  $y_d(t)$  and  $y_{\infty}(t)$  that dominates all other error sources. The latter choice of Q(s) is a so-called zero-phase filter.

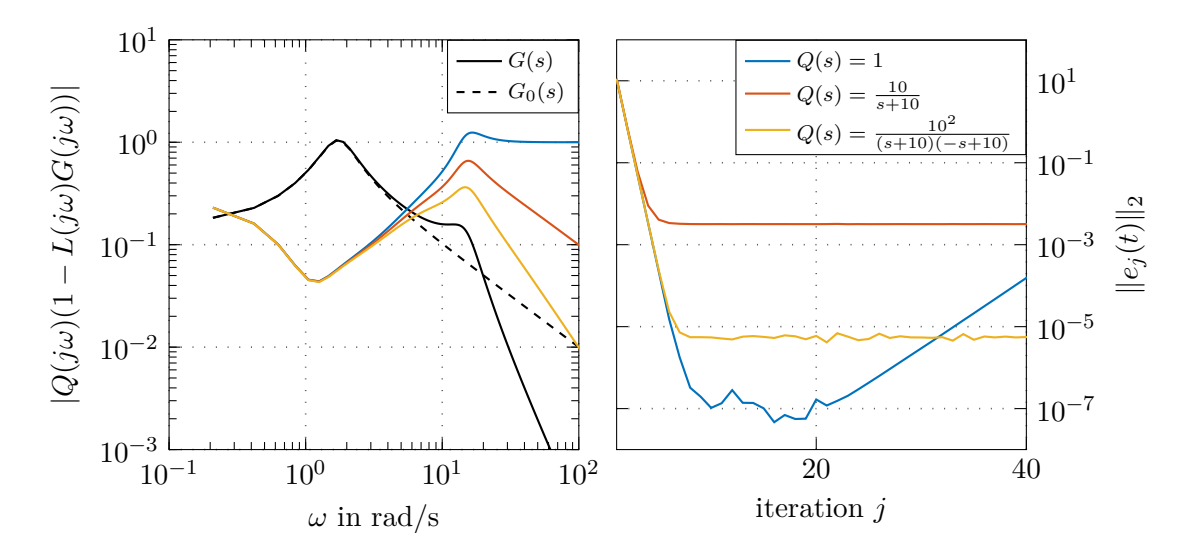


Figure 2.5: Robustness to model-plant mismatch by using a **Q**-filter.

Since there is no systematic design for  $\mathbf{Q}$  in the MIMO case, we will restrict ourselves to the SISO case in the following. In line with Example 2.3, it is generally recommended

to use zero-phase filters for Q(s), i.e.,

$$\operatorname{Im}\{Q(j\omega)\} = 0. \tag{2.102}$$

*Exercise* 2.5. Show that a zero-phase filter  $\mathbf{Q}(s)$  that is not a constant gain matrix is necessarily noncausal.

#### Gaussian filter

A particularly simple type of zero-phase filter is the Gaussian filter given by the impulse response

$$Q(t) = \frac{1}{\sigma_q \sqrt{2\pi}} \exp\left(-\frac{t^2}{2\sigma_q^2}\right) \tag{2.103}$$

with the standard deviation  $\sigma_q$  that is related to the 3-dB bandwidth  $f_c$ 

$$\sigma_q = \frac{\sqrt{\ln(2)}}{2\pi f_c} \tag{2.104}$$

of the corresponding frequency-domain representation

$$Q(j\omega) = \exp\left(-\frac{\sigma_q^2 \omega^2}{2}\right). \tag{2.105}$$

#### Forward-Backward-Filtering

A popular alternative with arbitrary spectral behavior is to use

$$Q(s) = Q_f^{\dagger}(s)Q_f(s) \tag{2.106}$$

where  $Q_f(s)$  is stable and causal. As a result, Q(s) can be easily implemented by integrating the realization of  $Q_f(s)$  forward and  $Q_f^{\dagger}(s)$  backward in time (see MATLAB command filtfilt). This procedure was used in Example 2.3 to implement the zero-phase Q-filter.

#### Time delay

One particular type of model-plant mismatch in ILC applications is a temporal delay by time T, i.e.,

$$\Delta G(s) = \exp(-sT). \tag{2.107}$$

Using a pseudo-inversion-based learning law, it follows that

$$|1 - L(j\omega)G(j\omega)| = |1 - L(j\omega)G_0(j\omega)\exp(-j\omega T)|$$

$$= \left|1 - \frac{|G_0(j\omega)|^2}{\alpha + |G_0(j\omega)|^2}\exp(-j\omega T)\right|.$$
(2.108)

As one can see, the resulting ILC law is always unstable in the absence of a Q-filter for sufficiently high frequencies  $\omega$ . Any predictable time-delay should thus be compensated by shifting the time axis respectively.

# 2.3.5 Implementation aspects

After having designed a suitable learning filter  $\mathbf{L}(s)$ , there are still some open questions on how to implement the resulting learning law for a practical problem that is typically defined on a finite time horizon  $t \in [0, t_f]$ .

## **Spectral factorization**

A direct method to achieve this is to use spectral factorization methods to decompose the learning filter into the product of two parts: one that is causal (i.e., its impulse response matrix is in  $\mathcal{H}_2$ ), and one that is anti-causal (i.e., its impulse response matrix is in  $\mathcal{H}_2^{\perp}$ ). Since the anti-causal part can also be written as the adjoint of a causal system, one obtains the factorization

$$\mathbf{L}(s) = \mathbf{L}_{b}^{\dagger}(s)\mathbf{L}_{f}(s) \tag{2.109}$$

As a result, the learning filter  $\mathbf{L}(s)$  can be implemented by finding a state-space representation of  $\mathbf{L}_{b}(s)$  that is solved forward in time and a state-space representation of  $\mathbf{L}_{b}^{\dagger}(s)$  that is solved backwards in time. Note that this solution procedure requires corresponding initial and terminal conditions for the state-space representations that are not determined from the infinite time-horizon design.

# FIR-filter approximation

Finding a factorization (2.109) can be quite tedious except for SISO systems. An alternative solution is to determine the impulse response matrix  $\mathbf{L}(t)$  directly. Since  $\mathbf{L}(t)$  is in general not of finite support, it has to be truncated in time to a finite-impulse response (FIR) approximation to implement the convolution (2.59). Along this line,  $\mathbf{L}(t)$  can either be transformed back analytically using the inverse bilateral Laplace transform and truncated afterwards or one chooses to use numerical methods. By assumption, the system's transfer matrix  $\mathbf{G}(s)$  has no poles on the imaginary axis  $s = j\omega$ , wherefore  $\mathbf{L}(s)$  has a ROC around the imaginary axis where  $\mathbf{L}(t)$  is given by

$$\mathbf{L}(t) = \mathcal{F}^{-1}\{\mathbf{L}(j\omega)\}. \tag{2.110}$$

A convolution with  $\mathbf{L}(t)$  is therefore equivalent to a forward and backward integration of the spectral factorization (2.109). The continuous Fourier transform can be approximately computed using the discrete Fourier transform (DFT) on a sampled temporal and spectral grid. By assuming that  $\mathbf{L}(j\omega) = \mathbf{0}$  outside the finite interval  $\left[-\frac{\omega_s}{2}, \frac{\omega_s}{2}\right]$ , we can approximate the inverse Fourier transform for  $t \in \left[-\frac{t_s}{2}, \frac{t_s}{2}\right]$  on the discrete grids  $t_n = (n - N/2)\frac{t_s}{N}$  and

$$\omega_m = (m - N/2) \frac{\omega_s}{N}$$
 with  $0 \le n, m < N$  by

$$\mathbf{L}(t_n) = \frac{1}{2\pi} \int_{-\omega_s/2}^{\omega_s/2} \mathbf{L}(j\omega) \exp[j\omega t_n] d\omega$$

$$\approx \frac{\omega_s}{2\pi N} \sum_{m=0}^{N-1} \mathbf{L}(j\omega_m) \exp\left[j\frac{t_s\omega_s}{N^2} \left(n - \frac{N}{2}\right) \left(m - \frac{N}{2}\right)\right]$$

$$= \frac{\omega_s}{2\pi N} \exp\left[-j\frac{t_s\omega_s}{2N} \left(n - \frac{N}{2}\right)\right] \sum_{m=0}^{N-1} \mathbf{L}(j\omega_m) \exp\left[-j\frac{t_s\omega_s}{2N} m\right] \exp\left[j\frac{t_s\omega_s}{N^2} mn\right]$$
(2.111)

Calculating the right-hand side of (2.111) can be computationally quite expensive. For the case  $\omega_s t_s = 2\pi N$ , however, this can be reformulated as<sup>1</sup>

$$\mathbf{L}(t_n) \approx \frac{\omega_s}{2\pi N} \exp\left[-j\pi \left(n - \frac{N}{2}\right)\right] \sum_{m=0}^{N-1} \mathbf{L}(j\omega_m) \exp[-j\pi m] \exp\left[j\frac{2\pi}{N}mn\right]$$

$$= \frac{\omega_s}{2\pi N} \exp\left[-j\pi \left(n - \frac{N}{2}\right)\right] \text{DFT}\{\mathbf{L}(j\omega_m) \exp[-j\pi m]\}$$
(2.112)

which is computationally very efficient by using FFT algorithms to compute the DFT for N chosen as a power of 2. Note that this method does not require  $\mathbf{L}(s)$  to be a rational transfer matrix, see Example 2.4.

## **Boundary effects**

Finally, to implement such learning laws requires information that is not provided by the infinite time horizon design. This lack was already quite explicit when factorizing the learning law and finding state-space representations for forward and backward integration, where suitable boundary conditions at t = 0 and  $t = t_f$  are required. Using the convolutional representation (2.59) with a FIR filter of length  $t_s$ , i.e.,  $\mathbf{L}(t) \neq \mathbf{0}$  only if  $t \in [-t_s/2, t_s/2]$ , yields

$$(\mathbf{L}\mathbf{e}_j)(t) = \int_{-t_s}^{t_f + t_s} \mathbf{L}(t - \tau)\mathbf{e}_j(\tau) d\tau \quad \text{for} \quad t \in [0, t_f].$$
 (2.113)

Rather than additional boundary values, the convolutional representation requires values of  $\mathbf{e}_j(t)$  for  $t \in [-t_s, t_f + t_s]$ , which extends beyond the available measurements. Since we assumed that the system is correctly (and identically) initialized,  $\mathbf{e}_j(0) = \mathbf{0}$  and thus  $\mathbf{e}_j(t) = \mathbf{0}$  for  $t \in [-t_s, 0]$  is a obvious choice. For  $t = t_f$ , the two most widely used options are:

1. 
$$\mathbf{e}(t) = 0 \text{ for } t \in [t_f, t_f + t_s]$$
 (truncation)

2. 
$$\mathbf{e}(t) = \mathbf{e}(t_f)$$
 for  $t \in [t_f, t_f + t_s]$  (extension)

<sup>&</sup>lt;sup>1</sup>This links the temporal resolution  $t_s/N$  with the spectral resolution  $\omega_s/N$ , which can be problematic for some applications with large bandwidths where a sufficient temporal resolution requires a very high number of discretization points.

Note that this choice will impact the stability of the learning law in general [2.11]. However, if an infinite time horizon convolution operator  $\Psi$  according to

$$\Psi \mathbf{e} = \int_{-\infty}^{\infty} \Psi(t - \tau) \mathbf{e}(\tau) \, d\tau, \qquad (2.114)$$

with  $\mathbf{e} \in \mathcal{L}_2(-\infty, \infty)$  is a contraction mapping, i.e.,  $\|\mathbf{\Psi}\mathbf{e}\|_2 < \|\mathbf{e}\|_2$ , then its truncated version

$$\mathbf{\Psi}_T \mathbf{e}' = \int_0^{t_f} \mathbf{\Psi}(t - \tau) \mathbf{e}'(\tau) \,d\tau \tag{2.115}$$

is a contraction mapping on the truncated space  $\mathbf{e}' \in \mathcal{L}_2([0,t_f])$ , too. This can be seen by using the standard truncation operator

since

$$\|\mathbf{\Psi}_T \mathbf{e}'\|_{2,[0,T]} = \|\mathbf{T}\mathbf{\Psi}\mathbf{T}\mathbf{e}\|_2 \le \|\mathbf{\Psi}\mathbf{T}\mathbf{e}\|_2 \le \|\mathbf{\Psi}\|_{\infty} \|\mathbf{T}\mathbf{e}\|_2 = \|\mathbf{\Psi}\|_{\infty} \|\mathbf{e}'\|_{2,[0,T]}$$
(2.117)

using the identity  $\Psi_T = \mathbf{T}\Psi\mathbf{T}$  and the fact that the induced norm  $\|\mathcal{T}\|_{\infty} = 1$ .

Example 2.4. Consider the coupled system of parabolic PDEs

$$\frac{\partial \mathbf{x}}{\partial t}(z,t) = \underbrace{\begin{bmatrix} \lambda_1 & 0 \\ 0 & \lambda_2 \end{bmatrix}}_{=\mathbf{A}} \frac{\partial^2}{\partial z^2} \mathbf{x}(z,t) + \underbrace{\begin{bmatrix} 0 & \sigma_{12} \\ \sigma_{21} & 0 \end{bmatrix}}_{=\mathbf{\Sigma}} \mathbf{x}(z,t)$$
(2.118a)

defined on the spatial domain  $z \in [0,1]$ , with the initial condition  $\mathbf{x}(z,0) = \mathbf{0}$ , the boundary conditions

$$\mathbf{x}(0,t) = \mathbf{u}(t) \qquad \frac{\partial \mathbf{x}}{\partial z}(1,t) = \underbrace{\begin{bmatrix} \Gamma_{11} & \Gamma_{12} \\ \Gamma_{21} & \Gamma_{22} \end{bmatrix}}_{\mathbf{R}} \mathbf{x}(1,t), \tag{2.118b}$$

and the output equation

$$\mathbf{y}(t) = \mathbf{x}(1, t). \tag{2.118c}$$

To obtain a transfer function description of the system (2.118), we apply the bilateral Laplace transform to (2.118a). This gives the spatial ODE

$$\frac{\partial^2}{\partial z^2} \mathbf{x}(z, s) = \underbrace{\mathbf{\Lambda}^{-1}(s\mathbf{I} - \mathbf{\Sigma})}_{=\mathbf{H}(s)} \mathbf{x}(z, s). \tag{2.119}$$

The dependence of  $\mathbf{H}(s)$  on the Laplace variable s will be omitted for the following calculations. The matrix  $\mathbf{H}$  can be diagonalized by using the state transform  $\mathbf{x}(z,s) =$ 

 $\mathbf{P}\chi(z,s)$ , which yields

$$\frac{\partial^2}{\partial z^2} \chi(z, s) = \tilde{\mathbf{H}}^2 \chi(z, s), \tag{2.120}$$

with the diagonal matrix  $\tilde{\mathbf{H}} = \sqrt{\mathbf{P}^{-1}\mathbf{H}\mathbf{P}}$  and the corresponding boundary conditions

$$\chi(0,s) = \mathbf{P}^{-1}\mathbf{u}(s), \qquad \frac{\partial \chi}{\partial z}(1,s) = \tilde{\mathbf{\Gamma}}\chi(1,s)$$
(2.121)

with  $\tilde{\Gamma} = \mathbf{P}^{-1} \mathbf{\Gamma} \mathbf{P}$ . Applying the ansatz

$$\chi(z,s) = \cosh\left(\tilde{\mathbf{H}}z\right) \begin{bmatrix} c_{11} \\ c_{21} \end{bmatrix} + \sinh\left(\tilde{\mathbf{H}}z\right) \begin{bmatrix} c_{12} \\ c_{22} \end{bmatrix}$$
(2.122)

to (2.120), (2.121) yields the solution

$$\mathbf{x}(z,s) = \mathbf{P} \Big[ \cosh \Big( \tilde{\mathbf{H}} z \Big) - \sinh \Big( \tilde{\mathbf{H}} z \Big) \mathbf{\Xi} \Big] \mathbf{P}^{-1} \mathbf{u}(s), \tag{2.123}$$

with

$$\mathbf{\Xi} = \left[\tilde{\mathbf{H}}\cosh\left(\tilde{\mathbf{H}}\right) - \tilde{\mathbf{\Gamma}}\sinh\left(\tilde{\mathbf{H}}\right)\right]^{-1} \left[\tilde{\mathbf{H}}\sinh\left(\tilde{\mathbf{H}}\right) - \tilde{\mathbf{\Gamma}}\cosh\left(\tilde{\mathbf{H}}\right)\right]. \tag{2.124}$$

Finally, with (2.118c) the transfer matrix is given by

$$\mathbf{G}_{u} = \mathbf{P} \Big[ \cosh \Big( \tilde{\mathbf{H}} \Big) - \sinh \Big( \tilde{\mathbf{H}} \Big) \mathbf{\Xi} \Big] \mathbf{P}^{-1}. \tag{2.125}$$

In the absence of stochastic disturbances, a simple pseudo-inversion-based law (2.80) with  $\alpha = 1 \cdot 10^{-3}$  is chosen. Using the parameter values  $\lambda_1 = \lambda_2 = 1$ ,  $\sigma_{12} = \frac{1}{2}$ ,  $\sigma_{21} = -1$ ,  $\Gamma_{11} = 0$ ,  $\Gamma_{12} = \frac{1}{2}$ ,  $\Gamma_{21} = 1$ , and  $\Gamma_{22} = \frac{1}{10}$ , one obtains a numerical solution of the impulse response matrix  $\mathbf{L}(t)$  using (2.112) as shown in Figure 2.6.

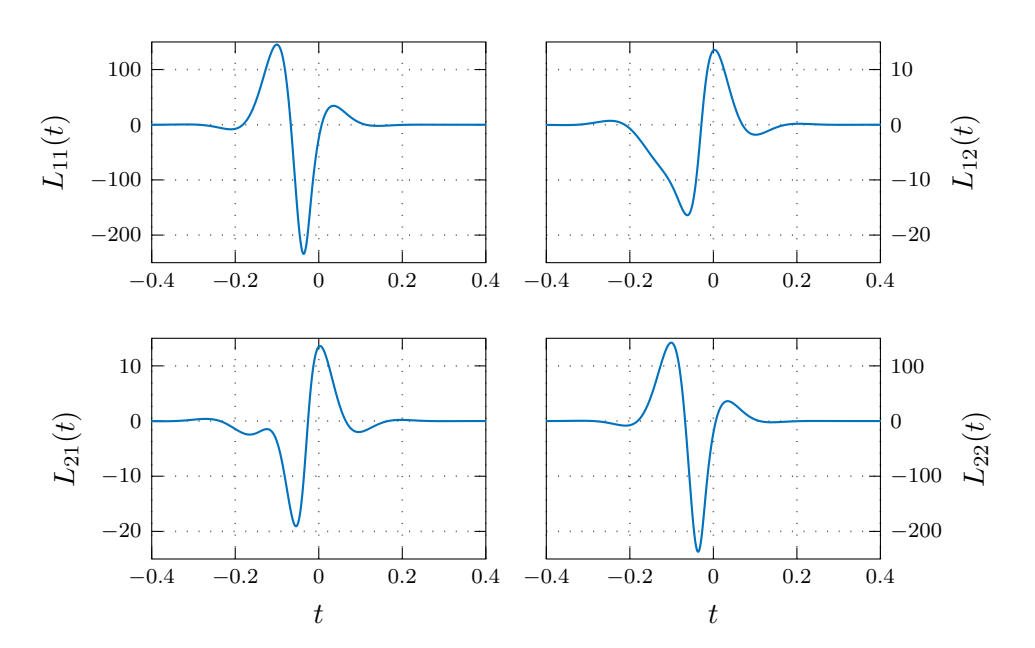


Figure 2.6: Entries of the (non-causal) learning kernel  $\mathbf{L}(t)$  calculated as a FIR-approximation using the FFT.

Using the calculated learning kernel to track a desired output trajectory  $\mathbf{y}^d(t) = [y_1^d(t), y_2^d(t)]^T$ ,  $t \in [0, 10]$  given by

$$y_1^d(t) = \Theta_5(t - 2.5), \quad y_2^d(t) = 3\frac{\mathrm{d}}{\mathrm{d}t}(\Theta_5(t) + \Theta_5(t - 5))$$
 (2.126)

with the smoothed step function

$$\Theta_T(t) = \begin{cases}
0 & t \le 0 \\
1 & t \ge T \\
\frac{\int_0^t \theta_T(\tau) d\tau}{\int_0^T \theta_T(\tau) d\tau} & t \in (0, T),
\end{cases}$$
(2.127)

whereby

$$\theta_T(t) = \begin{cases} 0 & t \notin (0, T) \\ \exp\left[-\left((1 - t/T)t/T\right)^{-1.5}\right] & t \in (0, T), \end{cases}$$
 (2.128)

the system (2.118) converges up to numeric precision of the solver after the first iteration with the resulting state profile  $\mathbf{x}_1(z,t)$  shown in (2.7). Using higher values for  $\alpha$  reduces the learning rate as expected.

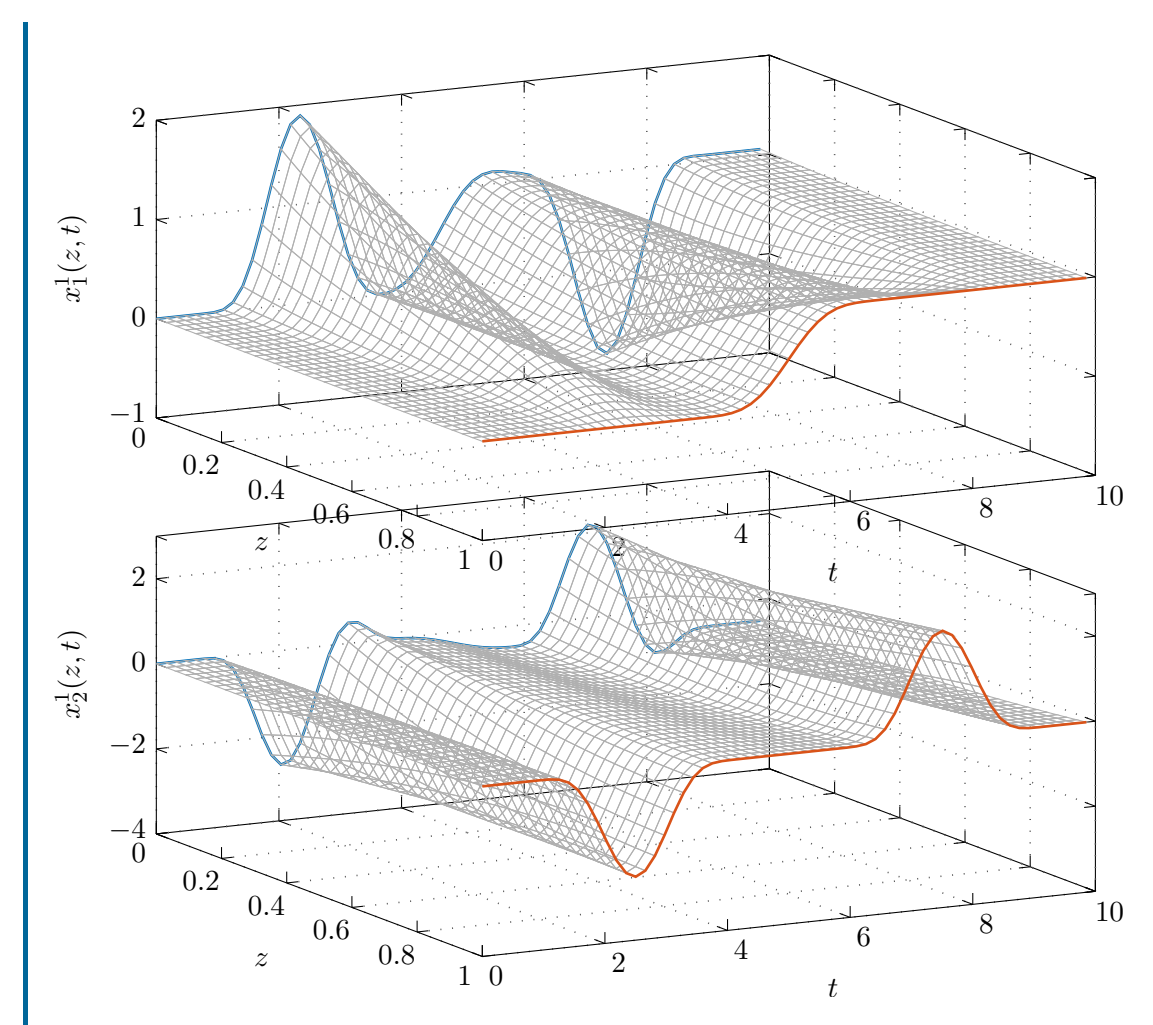


Figure 2.7: State  $\mathbf{x}_1(z,t)$  of the PDE system (2.118) with the input  $\mathbf{u}_1(t) = \mathbf{x}_1(0,t)$  (blue) that yields  $\mathbf{y}_1(t) = \mathbf{x}_1(1,t) \approx \mathbf{y}^d(t)$  (red) after the first iteration.

# 2.4 Discrete-time systems on finite time horizons

Frequency-domain methods are a very valuable tool to gain insight and intuition, but they are limited to infinite time horizons by design. For the finite time horizon, one has to either analyze the input-output behavior using the (linear) integral operator of the convolution in time-domain or to revert to state-space methods. For discrete-time systems, however, there exist an alternative approach: since the signal spaces of the system input and output are reduced to finite dimensions, every linear mapping between these spaces can be represented as a matrix. This is the basis of the so-called *lifted system representation*, which is commonly used to analyze ILC schemes.

# 2.4.1 Lifted system respresentation

In this section, we restrict the general state-space description (2.52) to the SISO case without measurement noise, i.e.,

$$\dot{\mathbf{x}}_{i}(t) = \mathbf{A}\mathbf{x}_{i}(t) + \mathbf{b}u_{i}(t) , \quad \mathbf{x}_{i}(0) = \mathbf{x}_{0}$$
 (2.129a)

$$y_i(t) = \mathbf{c}^{\mathrm{T}} \mathbf{x}_i(t) + du_i(t), \tag{2.129b}$$

Note that the lifted-system representation is in principle open to time-varying and MIMO systems. Using a zero-order hold (ZOH) model with a sampling time  $T_a$ , we obtain the discrete time system

$$\mathbf{x}_{j}[k+1] = \mathbf{\Phi}\mathbf{x}_{j}[k] + \mathbf{\Gamma}u_{j}[k] , \quad \mathbf{x}_{j}[0] = \mathbf{x}_{0}$$
 (2.130a)

$$y_j[k] = \mathbf{c}^{\mathrm{T}} \mathbf{x}_j[k] + du_j[k] \tag{2.130b}$$

with time index k = 0, 1, ... and the sampled state of the j-th iteration  $\mathbf{x}_j[k] = \mathbf{x}_j(kT_a)$ , the input  $u_j[k] = u_j(kT_a)$ , the output  $y_j[k] = y_j(kT_a)$ , and

$$\mathbf{\Phi} = \exp(\mathbf{A}T_a)$$
 und  $\mathbf{\Gamma} = \int_0^{T_a} \exp(\mathbf{A}\tau) d\tau \mathbf{b} = (\exp(\mathbf{A}T_a) - \mathbf{I})\mathbf{A}^{-1}\mathbf{b}$ . (2.131)

The corresponding input-output representation in discrete time reads

$$y_j[0] = \mathbf{c}^{\mathrm{T}} \mathbf{x}_0 + du_j[0] ,$$
 (2.132a)

$$y_j[k] = \mathbf{c}^{\mathrm{T}} \mathbf{\Phi}^k \mathbf{x}_0 + \mathbf{c}^{\mathrm{T}} \sum_{m=0}^{k-1} (\mathbf{\Phi}^{k-m-1} \mathbf{\Gamma} u_j[m]) + du_j[k], \quad k = 1, 2, \dots$$
 (2.132b)

that can be rewritten using

$$g[k] = \begin{cases} d & \text{for } k = 0\\ \mathbf{c}^{\mathrm{T}} \mathbf{\Phi}^{k-1} \mathbf{\Gamma} & \text{for } k = 1, 2, \dots \end{cases}$$
(2.133)

to obtain the discrete-time input-output representation

$$y_j[k] = \mathbf{c}^{\mathrm{T}} \mathbf{\Phi}^k \mathbf{x}_0 + \sum_{m=0}^k g[m] u_j[k-m] .$$
 (2.134)

This equation is the analogous result to (2.53) using the discrete convolution with the impulse response g[k], except that on a finite horizon we cannot assume that the system is relaxed initially and thus there is a remaining contribution of the initial state  $\mathbf{x}_0$ . By introducing the shift operator  $\delta : \delta(z_j[k]) = z_j[k+1]$  and assuming  $\mathbf{x}_0 = \mathbf{0}$ , one can again define the transfer operator

$$G(\delta) = \frac{y_j[k]}{u_j[k]} = d + \mathbf{c}^{\mathrm{T}} (\delta \mathbf{I} - \mathbf{\Phi})^{-1} \mathbf{\Gamma} = d + \delta^{-1} \mathbf{c}^{\mathrm{T}} (\mathbf{I} - \delta^{-1} \mathbf{\Phi})^{-1} \mathbf{\Gamma}$$

$$= d + \delta^{-1} \mathbf{c}^{\mathrm{T}} (\mathbf{I} + \delta^{-1} \mathbf{\Phi}^1 + \delta^{-2} \mathbf{\Phi}^2 + \dots) \mathbf{\Gamma} = d + \delta^{-1} \mathbf{c}^{\mathrm{T}} \sum_{k=0}^{\infty} (\delta^{-k} \mathbf{\Phi}^k) \mathbf{\Gamma}$$

$$= d + \sum_{k=1}^{\infty} \mathbf{c}^{\mathrm{T}} \mathbf{\Phi}^{k-1} \mathbf{\Gamma} \delta^{-k} = \sum_{k=0}^{\infty} g[k] \delta^{-k}.$$

$$(2.135)$$

Note 2.1. The infinite-horizon methods introduced in the previous section for continuous-time systems can be transferred to the discrete-time case directly using (2.135).

*Note* 2.2. The relative degree of a discrete-time systems is defined as follows:

Definition 2.10. A system (2.130) with d = 0 is of relative degree r if

(A) 
$$\mathbf{c}^{\mathrm{T}} \mathbf{\Phi}^k \mathbf{\Gamma} = 0$$
,  $k = 0, 1, \dots r - 2$ 

(B) 
$$\mathbf{c}^{\mathrm{T}} \mathbf{\Phi}^{r-1} \mathbf{\Gamma} \neq 0$$
.

The relative degree of a discrete-time systems thus merely corresponds to the time index k of  $y_i[k]$  at which the input  $u_i[0]$  appears for the first time, i.e.,

$$y_j[0] = \mathbf{c}^{\mathrm{T}} \mathbf{x}_0 \tag{2.136a}$$

$$y_j[1] = \mathbf{c}^{\mathrm{T}} \mathbf{\Phi} \mathbf{x}_0 + \underbrace{\mathbf{c}^{\mathrm{T}} \mathbf{\Gamma}}_{=0} u_j[0]$$
 (2.136b)

$$y_j[2] = \mathbf{c}^{\mathrm{T}} \mathbf{\Phi}^2 \mathbf{x}_0 + \underbrace{\mathbf{c}^{\mathrm{T}} \mathbf{\Phi} \mathbf{\Gamma}}_{=0} u_j[0] + \underbrace{\mathbf{c}^{\mathrm{T}} \mathbf{\Gamma}}_{=0} u_j[1]$$
 (2.136c)

:

$$y_j[r-1] = \mathbf{c}^{\mathrm{T}} \mathbf{\Phi}^{r-1} \mathbf{x}_0 + \mathbf{c}^{\mathrm{T}} \sum_{m=0}^{r-2} \mathbf{\Phi}^{r-m-1} \mathbf{\Gamma} u_j[m]$$

$$(2.136d)$$

$$y_j[r] = \mathbf{c}^{\mathrm{T}} \mathbf{\Phi}^r \mathbf{x}_0 + \mathbf{c}^{\mathrm{T}} \sum_{m=0}^{r-1} \mathbf{\Phi}^{r-m-1} \mathbf{\Gamma} u_j[m]$$

$$(2.136e)$$

The case of a discrete-time system (2.130) obtained by (ZOH-) sampling of a continuoustime system (2.129) begs the questions how the relative degrees of these two systems compare. Using a series expansion of the exponential matrix  $\exp(\mathbf{A}\tau)$  yields

$$\mathbf{c}^{\mathrm{T}}\mathbf{\Gamma} = \mathbf{c}^{\mathrm{T}} \int_{0}^{T_{a}} \sum_{m=0}^{\infty} \frac{(\mathbf{A}\tau)^{m}}{m!} \mathbf{b} \mathrm{d}\tau$$
 (2.137a)

$$= \mathbf{c}^{\mathrm{T}} \int_{0}^{T_a} \mathbf{b} + \mathbf{A} \mathbf{b} \tau + \ldots + \frac{1}{(n-1)!} \mathbf{A}^{n-1} \mathbf{b} \tau^{n-1} + \mathcal{O}(T_a^n) d\tau$$
 (2.137b)

$$= \mathbf{c}^{\mathrm{T}} \mathbf{b} T_a + \frac{1}{2!} \mathbf{c}^{\mathrm{T}} \mathbf{A} \mathbf{b} T_a^2 + \ldots + \frac{1}{n!} \mathbf{c}^{\mathrm{T}} \mathbf{A}^{n-1} \mathbf{b} T_a^n + \mathcal{O}(T_a^{n+1})$$
(2.137c)

which is always unequal to zero. A discrete-time system derived from a continuous-time system via ZOH is thus always of relative degree r=1 for d=0 (and r=0 for  $d \neq 0$ ).

Before trying to obtain a matrix representation of the system's input-output behavior (2.134), it makes sense to carefully define suitable input and output sequences that shall

be related by this mapping. Specifically, the initial input  $u_j[0]$  will only start to act on the output  $y_j[m]$  with some temporal delay m=r+w, where r is the relative degree of the system (2.130) and w is an additional delay due to sampling, conversion and processing of data that is unavoidable in real-world applications. For a finite time horizon  $t \in [0, t_f]$  with  $t_f = NT_a$  we will thus consider the input and output sequences

$$u_i[k], \quad k = 0, 1, \dots, N - 1$$
 (2.138a)

$$y_i[k], \quad k = m, m+1, \dots, N+m-1$$
 (2.138b)

as well as a desired output sequence

$$y_d[k], \quad k = m, m+1, \dots, N+m-1.$$
 (2.139a)

Note that this is essentially shifting the time axis of the output sequence relative to the input sequence to compensate for the total system delay (cf. the time delay analysis in Section 2.3.4). Rewriting the corresponding input and output sequences in vector notation, i.e.,

$$\mathbf{u}_j^{\mathrm{T}} = \begin{bmatrix} u_j[0] & u_j[1] & \dots & u_j[N-1] \end{bmatrix} \in \mathbb{R}^N$$
(2.140a)

$$\mathbf{y}_j^{\mathrm{T}} = \begin{bmatrix} y_j[m] & y_j[m+1] & \dots & y_j[m+N-1] \end{bmatrix} \in \mathbb{R}^N$$
 (2.140b)

$$\mathbf{y}_d^{\mathrm{T}} = \begin{bmatrix} y_d[m] & y_d[m+1] & \dots & y_d[m+N-1] \end{bmatrix} \in \mathbb{R}^N$$
 (2.140c)

$$\mathbf{y}_0^{\mathrm{T}} = \begin{bmatrix} y_0[m] & y_0[m+1] & \dots & y_0[m+N-1] \end{bmatrix} \in \mathbb{R}^N$$
 (2.140d)

$$\mathbf{e}_{j}^{\mathrm{T}} = \mathbf{y}_{d}^{\mathrm{T}} - \mathbf{y}_{j}^{\mathrm{T}} = \begin{bmatrix} e_{j}[m] & e_{j}[m+1] & \dots & e_{j}[m+N-1] \end{bmatrix} \in \mathbb{R}^{N}$$
, (2.140e)

and using (2.134) yields the so-called lifted system representation

$$\mathbf{y}_{i} = \mathbf{y}_{0} + \mathbf{G}\mathbf{u}_{i} \tag{2.141}$$

with the matrix

$$\mathbf{G} = \begin{bmatrix} g[m] & 0 & \cdots & 0 \\ g[m+1] & g[m] & \cdots & 0 \\ \vdots & \vdots & \ddots & 0 \\ g[m+N-1] & g[m+N-2] & \cdots & g[m] \end{bmatrix} \in \mathbb{R}^{N \times N} . \tag{2.142}$$

For LTI systems this is a so-called *Toeplitz* matrix where the entries  $\mathbf{G}_{ij}$  only depend on the difference i-j. An equivalent representation for time-varying systems can be found in [2.12]. Note that since  $\mathbf{G}$  is a lower triangular matrix due to causality of the system (2.129) and we assured by definition that  $g[m] \neq 0$ ,  $\mathbf{G}$  is of full rank and thus always invertible. Analogous to (2.4), a linear ILC law for the lifted system representation is given by

$$\mathbf{u}_{j+1} = \mathbf{Q} \Big( \mathbf{u}_j + \mathbf{L} \mathbf{e}_j \Big) \tag{2.143}$$

with the **Q**-filtering matrix

$$\mathbf{Q} = \begin{bmatrix} q[0] & q[-1] & \cdots & q[-(N-1)] \\ q[1] & q[0] & \cdots & q[-(N-2)] \\ \vdots & \vdots & \ddots & \vdots \\ q[N-1] & q[N-2] & \cdots & q[0] \end{bmatrix} \in \mathbb{R}^{N \times N}$$
 (2.144)

and the learning gain matrix

$$\mathbf{L} = \begin{bmatrix} l[0] & l[-1] & \cdots & l[-(N-1)] \\ l[1] & l[0] & \cdots & l[-(N-2)] \\ \vdots & \vdots & \ddots & \vdots \\ l[N-1] & l[N-2] & \cdots & l[0] \end{bmatrix} \in \mathbb{R}^{N \times N} .$$
 (2.145)

Exercise 2.6. Reformulate a PD-type learning law analogous to (2.74) with a Gaussian Q-filter (2.103) in the lifted framework. What options do you have? What about the boundaries of the time horizon?

The system description (2.141) and the learning law (2.143) are very similar to the infinite-horizon case (2.57) and (2.58) except for the constant term  $\mathbf{y}_0$ . Defining  $\tilde{\mathbf{y}}_d = \mathbf{y}_d - \mathbf{y}_0$ , one obtains the input iteration

$$\mathbf{u}_{j+1} = \mathbf{\Psi} \mathbf{u}_j + \mathbf{\Lambda} \tilde{\mathbf{y}}_d \tag{2.146}$$

with  $\Psi = \mathbf{Q}(\mathbf{I} - \mathbf{L}\mathbf{G})$  and  $\Lambda = \mathbf{Q}\mathbf{L}$  and the corresponding iteration of the output error  $\mathbf{e}_j = \mathbf{y}_d - \mathbf{y}_j$  as

$$\mathbf{e}_{j+1} = \mathbf{G} \mathbf{\Psi} \mathbf{G}^{-1} \mathbf{e}_j + (\mathbf{I} - \mathbf{G} \mathbf{Q} \mathbf{G}^{-1}) \mathbf{y}_d. \tag{2.147}$$

Both iterations are algebraically identical to the infinite-horizon case. We can thus directly transfer stability and convergence results to the lifted system representation, which are restated in the following for completeness.

**Theorem 2.13** (Asymptotic stability of the ILC law). The input iteration (2.146) of the ILC law (2.143) is asymptotically stable if

$$\rho(\mathbf{Q}(\mathbf{I} - \mathbf{L}\mathbf{G})) < 1 \tag{2.148}$$

and  $\mathbf{u}_j$  converges to  $\mathbf{u}_{\infty}$ .

**Theorem 2.14** (Asymptotic stability of the output iteration). The output iteration (2.147) of the ILC law (2.143) is asymptotically stable iff the input iteration is stable, i.e.,

$$\rho(\mathbf{Q}(\mathbf{I} - \mathbf{L}\mathbf{G})) < 1 \tag{2.149}$$

and  $\mathbf{e}_i$  then converges to the asymptotic tracking error

$$\mathbf{e}_{\infty} = \left(\mathbf{I} - \mathbf{G}(\mathbf{I} - \mathbf{\Psi})^{-1} \mathbf{\Lambda}\right) \mathbf{y}_{d} = \left(\mathbf{I} - \mathbf{G} \mathbf{\Phi} \mathbf{G}^{-1}\right)^{-1} \left(\mathbf{I} - \mathbf{G} \mathbf{Q} \mathbf{G}^{-1}\right) \mathbf{y}_{d}. \tag{2.150}$$

**Theorem 2.15** (Monotonic convergence of the input iteration). The input iteration (2.146) of the ILC law (2.143) converges monotonically to  $\mathbf{u}_{\infty}$ , i.e., it holds that

$$\|\mathbf{u}_{j+1} - \mathbf{u}_{\infty}\| \le \alpha \|\mathbf{u}_j - \mathbf{u}_{\infty}\| \tag{2.151}$$

for  $0 \le \alpha < 1$  if

$$\|\mathbf{\Psi}\| = \bar{\sigma}(\mathbf{Q}(\mathbf{I} - \mathbf{L}\mathbf{G})) = \alpha < 1$$
. (2.152)

**Theorem 2.16** (Monotonic convergence of the output iteration). The output iteration (2.64) of the ILC law (2.58) converges monotonically to  $\mathbf{e}_{\infty}$ , i.e., it holds that

$$\|\mathbf{e}_{i+1} - \mathbf{e}_{\infty}\| \le \beta \|\mathbf{e}_i - \mathbf{e}_{\infty}\| \tag{2.153}$$

for  $0 \le \alpha < 1$  if

$$\|\mathbf{G}\mathbf{\Psi}\mathbf{G}^{-1}\| = \bar{\sigma}\left(\mathbf{G}\mathbf{Q}(\mathbf{I} - \mathbf{L}\mathbf{G})\mathbf{G}^{-1}\right) = \beta < 1.$$
 (2.154)

Note 2.3. These results are structurally very similar to the infinite time horizon case with a number of significant differences: By applying the Laplace transform on infinite time horizons, one is considering stability for every  $\omega \in \mathbb{R}$  independently. While stability can be transferred to the finite time horizon as shown in the previous section, frequency-domain criteria are rather conservative. Conversely, stability criteria using the lifted system representation are sharp by accurately accounting for boundary effects. The dimension of  $\mathbf{Q}$  and  $\mathbf{L}$  is determined by the length of the sampled time horizon N, which can be problematic for long time horizons.

## 2.4.2 ILC as an online optimization strategy

Using measurements of a system's behavior to iteratively improve its performance with respect to some cost function can also be seen as an optimization problem that is solved online. Consider the problem

$$\min_{\mathbf{u}} \frac{1}{2} \mathbf{e}^{\mathrm{T}} \mathbf{P} \mathbf{e} + \frac{1}{2} \mathbf{u}^{\mathrm{T}} \mathbf{W} \mathbf{u} + \mathbf{u}^{\mathrm{T}} \mathbf{F} \mathbf{e}$$
 (2.155a)

subject to 
$$\mathbf{e} = \mathbf{y}_d - \mathbf{G}\mathbf{u}$$
, (2.155b)

with the symmetric, positive (semi-) definite weighting matrices  $\mathbf{P}$  und  $\mathbf{W}$ . One can assume that  $\mathbf{FG}$  is a skew-symmetric matrix without loss of generality since any symmetric component could always be absorbed into  $\mathbf{W}$ . This becomes apparent when plugging

(2.155b) into (2.155a), which yields the equivalent problem

$$\min_{\mathbf{u}} J(\mathbf{u}) = \frac{1}{2} \mathbf{u}^{\mathrm{T}} \bar{\mathbf{A}} \mathbf{u} + \mathbf{u}^{\mathrm{T}} \bar{\mathbf{b}} + \bar{\mathbf{c}}$$
 (2.156)

with

$$\bar{\mathbf{A}} = \mathbf{G}^{\mathrm{T}} \mathbf{P} \mathbf{G} + \mathbf{W} \tag{2.157a}$$

$$\bar{\mathbf{b}} = \left(\mathbf{F} - \mathbf{G}^{\mathrm{T}} \mathbf{P}\right) \mathbf{y}_{d} \tag{2.157b}$$

$$\bar{\mathbf{c}} = \frac{1}{2} \mathbf{y}_d^{\mathrm{T}} \mathbf{P} \mathbf{y}_d. \tag{2.157c}$$

The quadratic expression  $\mathbf{u}^{\mathrm{T}}\mathbf{F}\mathbf{G}\mathbf{u}$  vanishes due to  $\mathbf{F}\mathbf{G}$  being skew-symmetric. Since we further assumed that  $\mathbf{P}$  and  $\mathbf{W}$  are symmetric and positive (semi-) definite matrices, the same holds true for  $\bar{\mathbf{A}}$ . In case  $\bar{\mathbf{A}}$  is indeed positive definite, the cost function  $J(\mathbf{u})$  is strictly convex and thus has a unique global minimum at  $\mathbf{u}_{\infty} = -\bar{\mathbf{A}}^{-1}\bar{\mathbf{b}}$  which is determined by the necessary and sufficient first-order condition  $\nabla J(\mathbf{u}_{\infty}) = \bar{\mathbf{A}}\mathbf{u}_{\infty} + \bar{\mathbf{b}} = \mathbf{0}$ .

Alternatively, such an optimization problem can be solved iteratively using a gradient-descent method with constant step width  $\alpha$ , e.g.,

$$\mathbf{u}_{j+1} = \mathbf{u}_j - \alpha \nabla J(\mathbf{u}_j) = (\mathbf{I} - \alpha \bar{\mathbf{A}}) \mathbf{u}_j - \alpha \bar{\mathbf{b}}, \tag{2.158}$$

where  $0 < \alpha < 2/\|\bar{\mathbf{A}}\|$  ensures (monotone) convergence, cf. Theorem 2.1.13 in [2.13]. Plugging (2.157b) into (2.158) and suppressing  $\mathbf{y}_d$  in favor of  $\mathbf{u}_j$  and  $\mathbf{e}_j$  using (2.155b) yields an ILC-like update law

$$\mathbf{u}_{j+1} = \mathbf{Q} \Big( \mathbf{u}_j + \mathbf{L} \mathbf{e}_j \Big) \tag{2.159}$$

with

$$\mathbf{Q} = \mathbf{L}_u = \mathbf{I} - \alpha(\mathbf{W} + \mathbf{FG}) \tag{2.160a}$$

$$\mathbf{QL} = \mathbf{L}_e = \alpha \Big( \mathbf{G}^{\mathrm{T}} \mathbf{P} - \mathbf{F} \Big). \tag{2.160b}$$

#### 2.4.3 Norm-optimal ILC strategies

Along the same line of thought, norm-optimal ILC methods [2.12, 2.14] avoid the explicit design of a Q-filter and learning filter by solving the optimization problem

$$\min_{\mathbf{u}_{j+1}} J(\mathbf{u}_{j+1}) = \underbrace{\frac{1}{2} \mathbf{e}_{j+1}^{\mathrm{T}} \mathbf{V} \mathbf{e}_{j+1}}_{J_1(\mathbf{u}_{j+1})} + \underbrace{\frac{1}{2} \mathbf{u}_{j+1}^{\mathrm{T}} \mathbf{S} \mathbf{u}_{j+1} + \frac{1}{2} (\mathbf{u}_{j+1} - \mathbf{u}_j)^{\mathrm{T}} \mathbf{R} (\mathbf{u}_{j+1} - \mathbf{u}_j)}_{J_2(\mathbf{u}_{j+1})}$$
u.B.v. 
$$\mathbf{e}_{j+1} = \mathbf{y}_d - \mathbf{y}_{j+1} = \mathbf{e}_j + \mathbf{G} \mathbf{u}_j - \mathbf{G} \mathbf{u}_{j+1}$$
(2.161)

for every iteration. Note that this is in contrast to the previous section, where ILC was rewritten as an *iterative solution* of a *single* optimization problem. We assume that  $\mathbf{V}$  and  $\mathbf{S}$  are symmetric, positive semidefinite matrices and  $\mathbf{R}$ ,  $\mathbf{G}^{\mathrm{T}}\mathbf{V}\mathbf{G} + \mathbf{R}$ ,  $\mathbf{G}^{\mathrm{T}}\mathbf{V}\mathbf{G} + \mathbf{S}$  are symmetric, positive definit matrices.

Plugging the constraint into the cost function of (2.161) yields

$$J_{1}(\mathbf{u}_{j+1}) = \frac{1}{2} (\mathbf{e}_{j} + \mathbf{G}\mathbf{u}_{j} - \mathbf{G}\mathbf{u}_{j+1})^{\mathrm{T}} \mathbf{V} (\mathbf{e}_{j} + \mathbf{G}\mathbf{u}_{j} - \mathbf{G}\mathbf{u}_{j+1})$$

$$= \frac{1}{2} (\mathbf{e}_{j}^{\mathrm{T}} \mathbf{V} \mathbf{e}_{j} + \mathbf{u}_{j}^{\mathrm{T}} \mathbf{G}^{\mathrm{T}} \mathbf{V} \mathbf{e}_{j} - 2\mathbf{u}_{j+1}^{\mathrm{T}} \mathbf{G}^{\mathrm{T}} \mathbf{V} \mathbf{e}_{j}$$

$$+ \mathbf{e}_{j}^{\mathrm{T}} \mathbf{V} \mathbf{G} \mathbf{u}_{j} + \mathbf{u}_{j}^{\mathrm{T}} \mathbf{G}^{\mathrm{T}} \mathbf{V} \mathbf{G} \mathbf{u}_{j} - 2\mathbf{u}_{j+1}^{\mathrm{T}} \mathbf{G}^{\mathrm{T}} \mathbf{V} \mathbf{G} \mathbf{u}_{j} + \mathbf{u}_{j+1}^{\mathrm{T}} \mathbf{G}^{\mathrm{T}} \mathbf{V} \mathbf{G} \mathbf{u}_{j+1})$$

$$(2.162)$$

and

$$J_{2}(\mathbf{u}_{j+1}) = \frac{1}{2} \mathbf{u}_{j+1}^{\mathrm{T}} \mathbf{S} \mathbf{u}_{j+1} + \frac{1}{2} (\mathbf{u}_{j+1}^{\mathrm{T}} - \mathbf{u}_{j}^{\mathrm{T}}) \mathbf{R} (\mathbf{u}_{j+1} - \mathbf{u}_{j})$$

$$= \frac{1}{2} (\mathbf{u}_{j+1}^{\mathrm{T}} \mathbf{S} \mathbf{u}_{j+1} + \mathbf{u}_{j+1}^{\mathrm{T}} \mathbf{R} \mathbf{u}_{j+1} - 2 \mathbf{u}_{j+1}^{\mathrm{T}} \mathbf{R} \mathbf{u}_{j} + \mathbf{u}_{j}^{\mathrm{T}} \mathbf{R} \mathbf{u}_{j}) .$$

$$(2.163)$$

Using the first-order optimality condition

$$\left(\frac{\partial}{\partial \mathbf{u}_{j+1}}J\right)(\mathbf{u}_{j+1}) = \mathbf{0} \tag{2.164}$$

results in input update

$$\left(\mathbf{G}^{\mathrm{T}}\mathbf{V}\mathbf{G} + \mathbf{S} + \mathbf{R}\right)\mathbf{u}_{j+1} = \left(\mathbf{G}^{\mathrm{T}}\mathbf{V}\mathbf{G} + \mathbf{R}\right)\mathbf{u}_{j} + \mathbf{G}^{\mathrm{T}}\mathbf{V}\mathbf{e}_{j}$$
(2.165)

that is equivalent to an ILC law (2.143) with Q-filtering and learning matrices

$$\mathbf{Q} = \left(\mathbf{G}^{\mathrm{T}}\mathbf{V}\mathbf{G} + \mathbf{S} + \mathbf{R}\right)^{-1} \left(\mathbf{G}^{\mathrm{T}}\mathbf{V}\mathbf{G} + \mathbf{R}\right)$$
(2.166a)

$$\mathbf{L} = \left(\mathbf{G}^{\mathrm{T}}\mathbf{V}\mathbf{G} + \mathbf{R}\right)^{-1}\mathbf{G}^{\mathrm{T}}\mathbf{V}.$$
(2.166b)

By considering

$$\mathbf{Q}(\mathbf{I} - \mathbf{L}\mathbf{G}) = (\mathbf{G}^{\mathrm{T}}\mathbf{V}\mathbf{G} + \mathbf{S} + \mathbf{R})^{-1}(\mathbf{G}^{\mathrm{T}}\mathbf{V}\mathbf{G} + \mathbf{R})(\mathbf{I} - (\mathbf{G}^{\mathrm{T}}\mathbf{V}\mathbf{G} + \mathbf{R})^{-1}\mathbf{G}^{\mathrm{T}}\mathbf{V}\mathbf{G})$$
$$= (\mathbf{G}^{\mathrm{T}}\mathbf{V}\mathbf{G} + \mathbf{S} + \mathbf{R})^{-1}\mathbf{R}. \tag{2.167}$$

one can show that the derived norm-optimal ILC scheme is asymptotically stable, i.e.,

$$\rho\left(\left(\mathbf{G}^{\mathrm{T}}\mathbf{V}\mathbf{G} + \mathbf{S} + \mathbf{R}\right)^{-1}\mathbf{R}\right) < 1. \tag{2.168}$$

The values of V, S and R are tuning parameters that are often simplified by using diagonal matrices, i.e., V = vI > 0, S = sI > 0 und R = rI > 0. It follows that:

- Large values of v increases the weighting of the output error  $\mathbf{e}_j$ , which increases the convergence rate and reduces  $\mathbf{e}_{\infty}$ . The learning gain is becoming more aggressive and the action of the  $\mathbf{Q}$ -filter is reduced. The limit  $v \to \infty$  yields  $\mathbf{L} \to \mathbf{G}^{-1}$  and  $\mathbf{Q} \to \mathbf{I}$ .
- Large values of s penalize the control input  $\mathbf{u}_j$ , which increases the asymptotic output error  $\mathbf{e}_{\infty}$ . Note that s only affects  $\mathbf{Q}$  where  $s \to 0$  yields  $\mathbf{Q} \to \mathbf{I}$ .
- Large values of r penalize changes of the control input  $\mathbf{u}_{j+1} \mathbf{u}_j$ , which decreases the convergence rate. For  $r \to 0$  it follows that  $\mathbf{L} \to \mathbf{G}^{-1}$ .

2.5 References Page 64

# 2.5 References

[2.1] Z. Bien and J.-X. Xu, Iterative learning control - analysis, design, integration and applications. London: Springer, 1998.

- [2.2] D. Owens and J. Hätönen, "Iterative learning control an optimization paradigm," *Annual Reviews in Control*, vol. 29, no. 1, pp. 57–70, 2005.
- [2.3] D. A. Bristow, M. Tharayil, and A. Alleyne, "A survey of iterative learning control," *Control Systems, IEEE*, vol. 26, no. 3, pp. 96–114, 2006.
- [2.4] H.-S. Ahn, Y.-Q. Chen, and K. Moore, "Iterative learning control: Brief survey and categorization," Systems, Man, and Cybernetics, Part C: Applications and Reviews, IEEE Transactions on, vol. 37, no. 6, pp. 1099–1121, 2007.
- [2.5] H.-S. Ahn, K. L. Moore, and Y. Chen, *Iterative learning control robustness and monotonic convergence for interval system*. London: Springer, 2007.
- [2.6] Y. Wang, F. Gao, and F. J. Doyle III, "Survey on iterative learning control, repetitive control, and run-to-run control," *Journal of Process Control*, vol. 19, no. 10, pp. 1589–1600, 2009.
- [2.7] J. M. Ortega, "Stability of difference equations and convergence of iterative processes," SIAM Journal on Numerical Analysis, vol. 10, no. 2, pp. 268–282, 1973.
- [2.8] D. A. Bristow, "Iterative learning control for precision motion of microscale and nanoscale tracking systems," Ph.D. dissertation, University of Illinois at Urban-Champaign, 2007.
- [2.9] J. Ghosh and B. Paden, "Iterative learning control for nonlinear nonminimum phase plants with input disturbances," in *Proceedings of the American Control Conference*, Jun. 1999, pp. 2584–2589. Accessed: May 24, 2016.
- [2.10] J. Ghosh and B. Paden, "A pseudoinverse-based iterative learning control," *IEEE Transactions on Automatic Control*, vol. 47, no. 5, pp. 831–837, 2002.
- [2.11] J. Wallén, S. Gunnarsson, and M. Norrlöf, "Analysis of boundary effects in iterative learning control," *International Journal of Control*, vol. 86, no. 3, pp. 410–415, 2013.
- [2.12] J. H. Lee, K. S. Lee, and W. C. Kim, "Model-based iterative learning control with a quadratic criterion for time-varying linear systems," *Automatica*, vol. 36, no. 5, pp. 641–657, 2000.
- [2.13] Y. Nesterov, Introductory lectures on convex optimization: A basic course. Dordrecht: Kluwer Academic Publishers, 2004.
- [2.14] K. Barton and A. Alleyne, "A norm optimal approach to time-varying ilc with application to a multi-axis robotic testbed," *Control Systems Technology, IEEE Transactions on*, vol. 19, no. 1, pp. 166–180, Jan. 2011.